

# Glacier variations in the Bernese Alps (Switzerland) – Reconstructions and simulations

Inauguraldissertation  
der Philosophisch–naturwissenschaftlichen Fakultät  
der Universität Bern

vorgelegt von

**Daniel Steiner**

von Signau BE

Leiter der Arbeit:  
PD Dr. Heinz J. Zumbühl  
Geographisches Institut  
Universität Bern



# Glacier variations in the Bernese Alps (Switzerland) – Reconstructions and simulations

Inauguraldissertation  
der Philosophisch–naturwissenschaftlichen Fakultät  
der Universität Bern

vorgelegt von

**Daniel Steiner**

von Signau BE

Leiter der Arbeit:  
PD Dr. Heinz J. Zumbühl  
Geographisches Institut  
Universität Bern

Von der Philosophisch–naturwissenschaftlichen Fakultät angenommen.

Bern, 17. November 2005

Der Dekan:

Prof. Dr. P. Messerli



Dedicated to Maria,  
Tabitha Maria and Raphael Mattia

The only way to have real success in science,  
the field I'm familiar with,  
is to describe the evidence very carefully  
without regard to the way you feel it should be.

If you have a theory,  
you must try to explain what's good  
and what's bad about it equally.

In science, you learn a kind of standard integrity and honesty.<sup>1</sup>

(Richard Phillips Feynman, 1918–1988, Nobelist Physicist)

---

<sup>1</sup>Feynman, Richard Phillips (1988). "What do you care what other people think?": further adventures of a curious character. W. W. Norton, New York.

# Summary

## **Two Alpine glaciers over the last two centuries: a scientific view based on pictorial sources**

Starting with the idea of an ice age hypothesis, Louis Agassiz initiated a research program on the Lower Aare Glacier, Switzerland, which marked the beginning of modern experimental glacier research. The results of this new scientific view were published in 1847, and included the first scientific maps of a glacier on a large scale. The original drawing of the panorama by Jacques Bourkhardt, which was missing for a long time and has recently been rediscovered, shows the extension of the Lower Aare Glacier in the 1840s and the extreme conditions under which the scientists and artists had been living and working. Since 1849, the material of the Lower Aare Glacier was updated with the first photographs of Swiss Alpine glaciers. Therefore, this period of the beginning of experimental glaciology on the one hand coincides with a change of glacier representation techniques from drawings/paintings and maps to photographs within 15 years. On the other hand, it is also the time when a majority of (Alpine) glaciers show their last maximum extent.

The Lower Grindelwald Glacier, Switzerland, plays a similar important role to the Lower Aare Glacier for scientific glacier research. Its well-documented record of length variations back to 1535 illustrates the Little Ice Age climate changes. Newly discovered (stereo) photographs and old topographic maps of the Lower Grindelwald Glacier also show the impressive dimension of the 1855/56 maximum extent and the rapid glacier retreat since then.

In general, this glacier maximum extent in the mid-19th century and the subsequent retreat have been extensively studied for both, the Lower Grindelwald and the Lower Aare Glacier. The quality of its documentary data allows, probably better than elsewhere in the world, the development of accurate digital elevation models (DEMs). Thus, volume and area changes of these two glaciers since their mid-19th century maximum extent were determined by DEM comparisons.

It can be shown that the Lower Grindelwald Glacier has lost 5.5 km<sup>2</sup> of area and 1.56 km<sup>3</sup> of ice and the Lower Aare Glacier 4.3 km<sup>2</sup> of area and 1.59 km<sup>3</sup> of ice since their last maximum extent. However, for the Lower Grindelwald Glacier the spatial distribution of thickness changes could possibly signify extraordinary dynamical behavior since the mid-19th century.

## **The application of a nonlinear Backpropagation Neural Network to study the mass balance of Great Aletsch Glacier, Switzerland**

Glacier mass changes are considered to represent key variables related to climate variability. We have reconstructed a proxy for annual mass balance changes in the Great Aletsch Glacier, Swiss Alps, back

to AD 1500 using a nonlinear Backpropagation Neural Network (BPN). The model skill of the BPN performs better than reconstructions using conventional stepwise multiple linear regression.

The BPN, driven by monthly instrumental series of local temperature and precipitation, provides a proxy for 20th-century mass balance. The long-term mass balance reconstruction back to AD 1500 is based on a multiproxy approach of seasonally resolved temperature and precipitation reconstructions (mean over a specific area) as input variables. The relation between the driving factors (temperature, precipitation) used and the reconstructed mass balance series is discussed. Mass changes in the Great Aletsch Glacier are shown to be mainly influenced by summer (JJA) temperatures, but winter (DJF) precipitation also seems to contribute.

Furthermore, we found a significant nonlinear part within the climate-mass balance relation of Great Aletsch Glacier.

## **Sensitivity of European Glaciers to Precipitation and Temperature – Two case studies**

A nonlinear Backpropagation Neural Network (BPN) has been trained with high-resolution multiproxy reconstructions of temperature and precipitation (input data) and glacier length variations of the Alpine Lower Grindelwald Glacier, Switzerland (output data).

The model was then forced with two regional climate scenarios of temperature and precipitation derived from a probabilistic approach: The first scenario ("no change") assumes no changes in temperature and precipitation for the 2000–2050 period compared to the 1970–2000 mean. In the second scenario ("combined forcing") linear warming rates of 0.036–0.054 °C per year and changing precipitation rates between –17% and +8% compared to the 1970–2000 mean have been used for the 2000–2050 period. In the first case the Lower Grindelwald Glacier shows a continuous retreat until the 2020s when it reaches an equilibrium followed by a minor advance. For the second scenario a strong and continuous retreat of approximately –30 meters per year since the 1990s has been modelled.

By processing the used climate parameters with a sensitivity analysis based on neural networks we investigate the relative importance of different climate configurations for the Lower Grindelwald Glacier during four well-documented historical advance (1590–1610, 1690–1720, 1760–1780, 1810–1820) and retreat periods (1640–1665, 1780–1810, 1860–1880, 1945–1970). It is shown that different combinations of seasonal temperature and precipitation have led to glacier variations.

In a similar manner, we establish the significance of precipitation and temperature for the well-known early 18th century advance and the 20th century retreat of Nigardsbreen, a glacier in western Norway. We show that the maritime Nigardsbreen Glacier is more influenced by winter and/or spring precipitation than the Lower Grindelwald Glacier.



# Zusammenfassung

Ausgangspunkt dieser Dissertation ist die in den Schweizer Alpen vorliegende einzigartige Verfügbarkeit qualitativ hochstehender Daten vergangener Gletscherveränderungen. Mit Hilfe dieser Daten lässt sich sowohl die Gletschergeschichte der letzten Jahrhunderte wie auch die Klimavariabilität innerhalb des mitteleuropäischen Raumes analysieren und quantifizieren – mit einer Präzision, welche sonst wohl in keiner anderen Gegend der Erde erreicht werden kann. Zusammen mit neueren hochauflösenden Temperatur- und Niederschlagsrekonstruktionen, welche auf verschiedenen, unabhängigen Proxy-Daten beruhen, lässt sich somit der hochkomplexe Zusammenhang zwischen Klima und Gletscher wirksamer studieren, als dies bisher der Fall war.

Die Arbeit versucht, beiden Aspekten – der Gletschergeschichte und der Analyse des Systems Klima-Gletscher – gerecht zu werden, indem die folgenden zwei Leitfragen aufgeworfen werden:

1. Wie wurden exemplarisch ausgewählte Gletscher zu Beginn/Mitte des 19. Jahrhunderts von Naturforschern und Künstlern wahrgenommen und dargestellt? Wie haben sich diese Gletscher seither verändert?
2. Inwiefern lassen sich nichtlineare neuronale Netzwerke in der Glaziologie als Alternative zu konventionellen linearen statistischen Ansätzen verwenden?

## **Bildquellen als Hilfsmittel zur Analyse von Gletscherperzeption und Gletscherfluktuationen**

Angespornt durch die Idee einer "Eiszeittheorie" und den dadurch ausgelösten kontroversen Diskussionen initiierte der Schweizer Naturforscher Louis Agassiz (1807–1873) zu Beginn der 1840er-Jahre ein interdisziplinäres Forschungsprogramm auf dem Unteraargletscher. Diese Forschungsarbeiten können mitunter als Beginn der modernen experimentellen Glaziologie betrachtet werden. Die verschiedenen Resultate dieser neuen wissenschaftlichen Betrachtungsweise von Gletschern wurden 1847 publiziert, darunter auch die ersten Gletscherkarten von wissenschaftlichem Wert. Zusätzlich zu diesen Ergebnissen sind weitere Bildquellen (Zeichnungen, Gemälde), v.a. aber auch ein kürzlich wieder aufgetauchtes herausragendes Panorama, aus derselben Zeit bekannt. Ab 1849 kamen zudem fotografische Darstellungen von Gletschern hinzu.

Damit sind wir im Fall des Unteraargletschers in der einzigartigen Situation, dass die Entwicklung eines neuen wissenschaftlichen Forschungsgebietes, nämlich die Glaziologie, mit einem Wandel der verwendeten Aufnahmetechniken von Zeichnungen/Gemälden zu Fotografien und topografischen Karten einhergeht. Diese Entwicklung, welche sich innerhalb von lediglich 15 Jahren vollzog, fand zudem unmittelbar vor den letzten alpinen Gletscherhochständen der "Kleinen Eiszeit" statt. Wir besitzen somit aus der Zeit der genannten Maximalstände eine stattliche Zahl an Bildquellen, welche

ihrerseits zu qualitativen und quantitativen Aussagen über die damalige Gletscherausdehnung herangezogen werden können.

Der Untere Grindelwaldgletscher spielt in der Geschichte der Glaziologie eine ähnlich wegweisende Rolle wie der Unteraargletscher. Die grosse Menge an qualitativ hochstehenden Bildquellen der vergangenen vier bis fünf Jahrhunderte erlaubt es, eine detailreiche Kurve der Gletscherlängenveränderungen bis 1535 zurück zu erstellen. Verschiedene Bildquellen (v.a. Fotografien) zeigen auch hier ein Bild des imposanten Gletscherhochstandes um 1855/56 und des nachfolgenden rasanten Gletscherrückzuges.

Schliesslich können aus diesen Quellen – wahrscheinlich genauer als sonstwo – hochauflösende digitale Höhenmodelle erstellt werden, die Vergleiche zwischen früheren Gletscherständen möglich machen. Demnach hat der Untere Grindelwaldgletscher seit seinem letzten Hochstand 5.5 km<sup>2</sup> an Fläche und 1.56 km<sup>3</sup> an Volumen eingebüsst. Eine Analyse der räumlichen Dickenveränderungen für die gleiche Zeitperiode könnte zudem Hinweise auf ein aussergewöhnliches gletscherdynamisches Verhalten des Gletschers liefern. Der Unteraargletscher verlor seit seinem letzten Hochstand 4.3 km<sup>2</sup> an Fläche und 1.59 km<sup>3</sup> an Volumen.

## Neuronale Netzwerke in der Glaziologie

Im Gegensatz zum Unteren Grindelwaldgletscher und Unteraargletscher, welche detaillierte Kurven von Längenveränderungen, aber kaum Massenbilanzmessungen aufweisen, besitzt der Grosse Aletschgletscher eine bis 1920 zurückreichende, auf hydrologischer Basis erstellte, Zeitreihe von jährlichen Massenbilanzen. Da die Massenbilanz von Gletschern als direktes, ungefiltertes Klimasignal interpretiert werden kann, kommt ihr in der Diskussion um Klimavariabilität und Klimaerwärmung eine entscheidende Rolle zu.

Mit einer, in der Glaziologie vermutlich zum ersten Mal angewandten, neuen Methodik, basierend auf neuronalen Netzwerken, wird eine jährlich aufgelöste Massenbilanzreihe des Grossen Aletschgletschers für die vergangenen fünf Jahrhunderte rekonstruiert. Dabei werden neue, hochauflösende, gegitterte Klimadaten (als unabhängige Grössen) mit der qualitativ hochstehenden Massenbilanzreihe des Grossen Aletschgletschers (als abhängige Grösse) verknüpft. Es zeigt sich, dass die Massenbilanz des Grossen Aletschgletschers vor allem durch die Sommertemperatur (Juni–August) bestimmt ist. Der Winterniederschlag (Dezember–Februar) spielt eine zeitlich variierende, aber tendenziell untergeordnete Rolle.

Auch im Bereich der Gletscherlängenvariationen werden neuronale Netzwerke eingesetzt. Da es sich aber bei der Gletscherlänge um ein indirektes, gefiltertes Klimasignal handelt, ist dessen Modellierung viel schwieriger. Nichtsdestotrotz werden als Modelleingänge wiederum saisonal aufgelöste, gegitterte Temperatur- und Niederschlagsrekonstruktionen verwendet. Die Zeitreihe der Längenveränderungen des Unteren Grindelwaldgletschers dient in diesem Fall als Zielgrösse.

In einer ersten Fallstudie werden die zukünftigen Gletscherlängenveränderungen des Unteren Grindelwaldgletschers simuliert, indem zwei regionale Klimaszenarien für den Alpenraum für die Periode 2000–50 angewandt werden. Das erstere, zurückhaltende Klimaszenario geht von einem kontinuierlichen Gletscherrückgang bis in die 2020er-Jahre aus, bevor der Gletscher ein neues Gleichgewicht einnimmt und anschliessend wieder leicht vorstossen könnte. Das zweite, wohl realistischere Klimaszenario mit erhöhten Temperaturen und wechselnden saisonalen Niederschlagsentwicklungen sagt einen kontinuierlichen und rasanten Gletscherrückgang voraus.

Eine zweite Fallstudie beinhaltet eine Sensitivitätsanalyse, wiederum basierend auf neuronalen Net-

zwerken, welche die wechselnden klimatischen Einflussfaktoren auf verschiedene Vorstösse und Rückzüge des Unteren Grindelwaldgletschers analysieren soll. Es kann gezeigt werden, dass verschiedene Kombinationen von saisonaler Temperatur und saisonalem Niederschlag einen Gletschervorstoss bzw. -rückzug auslösen können. In einem unabhängigen Vergleich mit einem norwegischen Gletscher (Nigardsbreen) konnte die Zweckmässigkeit der methodischen Annahmen bestätigt werden.

Somit können neuronale Netzwerke im Kontext des Systems Klima–Gletscher als erfolgsversprechende nichtlineare Methodik angesehen werden. Dem Vorteil der Nichtlinearität, die in neuronalen Netzwerken an sich gegeben ist, steht der Nachteil des reinen statistischen Modells gegenüber. Es muss auch festgehalten werden, dass die vorgeschlagenen Methoden nur dann Sinn machen, wenn eine aussergewöhnliche Qualität und Dichte der Klima- und Gletscherdaten vorliegt. Dann ist es auch möglich, vertiefte Einsichten in das hochkomplexe Klimasystem zu erlangen bzw. eine Methode auf ihre Stärken und Schwächen zu untersuchen. Um gar zu einer allgemeinen Theorie einer "Neuro–Glaziologie" zu gelangen, müssten aber noch weitere Gletscher in anderen Regionen der Erde (z.B. Himalaja, Neuseeland, Südamerika) untersucht werden.



# Contents

<b>Summary</b>	<b>i</b>
<b>Zusammenfassung</b>	<b>iii</b>
<b>Contents</b>	<b>vii</b>
<b>List of Figures</b>	<b>xi</b>
<b>List of Tables</b>	<b>xiii</b>
<b>Abbreviations</b>	<b>xv</b>
<b>1 Introduction</b>	<b>1</b>
1.1 Aims and significance of the project PALVAREX . . . . .	1
1.2 Importance of glacier variations (mass balance and length fluctuations) . . . . .	2
1.2.1 Direct measurements . . . . .	2
1.2.2 Glacier variations as climate indicators . . . . .	4
1.3 Glacier changes since the 16th century . . . . .	5
1.3.1 Jostedalbreen, western south Norway . . . . .	5
1.3.2 Bernese Alps, Switzerland . . . . .	5
1.4 Modelling and reconstructing glacier variations . . . . .	7
1.4.1 Reconstructions . . . . .	7
1.4.2 Mass balance models . . . . .	8
1.4.3 Modelling glacier length . . . . .	9
1.4.4 Multiproxy reconstructions of temperature and precipitation . . . . .	9
1.5 Structure of this thesis . . . . .	10
<b>2 Two Alpine glaciers over the last two centuries: a scientific view based on pictorial sources</b>	<b>17</b>
2.1 Introduction . . . . .	18
2.2 The area investigated . . . . .	19

2.2.1	From first observations to detailed studies . . . . .	21
2.2.2	Panorama of Jacques Bourkhardt (1842) . . . . .	22
2.2.3	First photographs of glaciers . . . . .	23
2.2.4	(First) topographic maps and digital elevation models (DEMs) . . . . .	27
2.2.5	Results . . . . .	31
2.3	Summary and conclusions . . . . .	35
2.4	Appendix 1 . . . . .	40
2.5	Appendix 2 . . . . .	41
2.6	Appendix 3 . . . . .	42
2.7	Appendix 4 . . . . .	43
2.8	Appendix 5 . . . . .	44
2.9	Appendix 6 . . . . .	45
<b>3</b>	<b>The application of a nonlinear Backpropagation Neural Network to study the mass balance of Great Aletsch Glacier, Switzerland</b>	<b>47</b>
3.1	Introduction . . . . .	48
3.2	Data and methods . . . . .	49
3.2.1	Instrumental data of the 20th century . . . . .	49
3.2.2	Multiproxy reconstructions of temperature and precipitation back to 1500 . . . . .	53
3.2.3	Backpropagation Neural networks as modelling tools . . . . .	53
3.2.4	The Backpropagation Architecture . . . . .	56
3.3	Results . . . . .	58
3.3.1	Mass Balance in the 20th century . . . . .	58
3.3.2	Proxy-based reconstructions of mass balance back to 1500 . . . . .	60
3.4	Conclusions and Outlook . . . . .	64
3.5	Appendix 1 . . . . .	70
<b>4</b>	<b>Sensitivity of European Glaciers to Precipitation and Temperature – Two case studies</b>	<b>71</b>
4.1	Introduction . . . . .	72
4.2	Data and methods . . . . .	73
4.2.1	The study sites . . . . .	73
4.2.2	Multiproxy reconstructions of temperature and precipitation back to 1500 . . . . .	76
4.2.3	Climate scenarios for the Swiss Alpine region . . . . .	77
4.2.4	Backpropagation Neural Networks as modelling and analysis tools . . . . .	77
4.3	Results . . . . .	80
4.3.1	Modelling the response of the Lower Grindelwald Glacier to climate change . . . . .	80
4.3.2	Precipitation and temperature significance for historic glacier variations – a comparison . . . . .	83

<i>Contents</i>	ix
4.4 Discussion . . . . .	85
4.4.1 Simulation of future glacier length variations . . . . .	85
4.4.2 Climate parameters and historic glacier variations . . . . .	88
4.5 Conclusions and Outlook . . . . .	91
4.6 Appendix 1 . . . . .	96
4.7 Appendix 2 . . . . .	97
4.8 Appendix 3 . . . . .	98
4.9 Appendix 4 . . . . .	100
<b>5 Concluding remarks</b>	<b>103</b>
<b>Acknowledgments</b>	<b>107</b>
<b>Curriculum Vitae</b>	<b>109</b>





# List of Figures

1.1	Cumulative length changes of Nigardsbreen, Lower Grindelwald Glacier, Lower Aare Glacier and Great Aletsch Glacier . . . . .	6
1.2	The Lower Grindelwald Glacier in 1826 (S. Birmann) . . . . .	7
2.1	The Lower Aare and the Grindelwald region . . . . .	20
2.2	Cumulative length variations of the Lower Grindelwald and the Lower Aare Glacier . . . . .	21
2.3	Panoramas of the Lower Aare Glacier in 1842 (J. Bourkhardt) and 2004 . . . . .	24
2.4	Double portrayal of Louis Agassiz and Jean Édouard Desor (F. Berthoud) . . . . .	25
2.5	The Lower Grindelwald Glacier in summer or autumn 1855/56 (Bisson Brothers) . . . . .	26
2.6	The Lower Grindelwald Glacier in 1858 (A. Braun) and 2003 . . . . .	27
2.7	Forefield of the Lower Grindelwald Glacier with the glacier extensions of 1855/56, 1860/61 and 1870 . . . . .	28
2.8	Composition of the maps "Grindelwald 1860/61" and "Jungfrau 1872" . . . . .	30
2.9	Surface profiles of the Lower Grindelwald Glacier along two flowlines . . . . .	32
2.10	Average changes of surface heights between DEM1861 and DEM2004 . . . . .	34
2.11	The Lower Aare Glacier . . . . .	40
2.12	Lithography "Carte du glacier inférieur de l'Aar" (J. Wild) . . . . .	41
2.13	Lithography "Carte Orographique du Glacier de l'Aar Montrant les détails de la Stratification et l'origine des glaciers de second ordre" (J.R. Stengel) . . . . .	41
2.14	Oil painting "Hôtel des Neuchâtelois Glacier de l'Aar" (J. Bourkhardt) . . . . .	42
2.15	The Lower Aare Glacier in 1855 (Bisson Brothers) and 2004 . . . . .	43
2.16	Distribution of the glacier surface thickness changes for the model DEM1861–DEM2004 . . . . .	44
2.17	Glacier hypsographies from DEM1861, DEM1926, DEM1993, DEM2000 and DEM2004 . . . . .	45
3.1	The Aletsch region and the used meteorological stations . . . . .	50
3.2	An example of a simplified BPN architecture . . . . .	54
3.3	Results of the Backpropagation Network (BPN) simulation and reconstruction over the 20th century . . . . .	59
3.4	Results of the Backpropagation Network (BPN) simulation and reconstruction back to 1500 . . . . .	61

3.5	Cumulative glacier mass balance changes in Great Aletsch Glacier for the 1500–1999 period . . . . .	62
3.6	Winter (DJF) precipitation anomalies for the 1500–1999 period . . . . .	63
3.7	Summer (JJA) temperature anomalies for the 1500–1999 period . . . . .	64
3.8	The Great Aletsch Glacier . . . . .	70
4.1	The topography of the Lower Grindelwald Glacier with its main branches and tributaries.	74
4.2	The location of the Nigardsbreen Glacier and its foreland with dates for the formation of some moraines. . . . .	75
4.3	An example of a simplified BPN architecture . . . . .	79
4.4	Cumulative length variations of the Lower Grindelwald Glacier from 1535 to 1983 . .	81
4.5	Cumulative glacier length variations of the Lower Grindelwald Glacier for the 1550–2050 period. For the 1976–2050 period the model was forced with two regional climate scenarios . . . . .	82
4.6	Relative importance of climate input variables to length fluctuations of the Lower Grindelwald Glacier for four advance periods . . . . .	86
4.7	Relative importance of climate input variables to length fluctuations of the Lower Grindelwald Glacier for four retreat periods . . . . .	87
4.8	RE values of the precipitation time series over selected Scandinavian regions . . . . .	88
4.9	Relative importance of climate input variables to length fluctuations of the glacier Nigardsbreen for two periods. . . . .	89
4.10	The Nigardsbreen Glacier . . . . .	96
4.11	The Lower Grindelwald Glacier . . . . .	96
4.12	Seasonal Sensitivity Characteristic (SSC) for the Lower Grindelwald Glacier. . . . .	97
4.13	Precipitation anomalies for the 1500–2000 period in the Grindelwald region. . . . .	98
4.14	Temperature anomalies for the 1500–2000 period in the Grindelwald region. . . . .	99
4.15	Precipitation anomalies for the 1500–2000 period in the Nigardsbreen region. . . . .	100
4.16	Temperature anomalies for the 1500–2000 period in the Nigardsbreen region. . . . .	101

# List of Tables

2.1	Topographical characteristics of the Lower Grindelwald Glacier . . . . .	22
2.2	The DEMs used and their sources . . . . .	29
2.3	Changes in glacier parameters of the Lower Grindelwald and the Lower Aare Glacier	33
3.1	Principal meteorological stations used in the study . . . . .	52
4.1	Topographical characteristics of the Lower Grindelwald Glacier, Switzerland, and Nigardsbreen, Norway. . . . .	76
4.2	Two regional climate scenarios for the northern part of the Swiss Alps. . . . .	78
4.3	Major advance and retreat periods of the Lower Grindelwald Glacier and the relevant combinations of seasonal temperature and precipitation . . . . .	85



# Abbreviations

## Scientific programmes and projects

PALVAREX	PALeoclimate VARIability and EXtreme Events
SOAP	Simulations, Observations And Palaeoclimate Data: Climate Variability over the last 500 Years

## Institutions

CIG	Commission Internationale des Glaciers (predecessor of ICSI)
CRU	Climate Research Unit
DWD	Deutscher Wetterdienst
ETH	Eidgenössische Technische Hochschule
IAHS	International Association of Hydrological Sciences
ICSI	International Commission on Snow and Ice
IPCC	Intergovernmental Panel on Climate Change
KLIMET	KLImatologie und METeorologie
NCCR	National Center of Competence in Research
NVE	Norwegian Water Resources and Energy Directorate
PSFG	Permanent Service on the Fluctuations of Glaciers
SAC	Swiss Alpine Club
SANW	Swiss Academy of Sciences
SBF	Staatssekretariat für Bildung und Forschung
SNSF	Swiss National Science Foundation
swisstopo	Federal Office of Topography
WGMS	World Glacier Monitoring Service

## Variables

AAR	Accumulation Area Ratio
AD	Anno Domini
AOGCM	Atmosphere Ocean Global Circulation Model
asl.	above sea level
BP	Before Present
BPN	Backpropagation Neural Network
CPU	Central Processing Unit
DEM	Digital Elevation Model
ELA	Equilibrium Line Altitude
EOF	Empirical Orthogonal Function

GCM	Global (General) Circulation Model
LIA	Little Ice Age
mwe	meter water equivalent
NAO	North Atlantic Oscillation
NN	Neural Network
NNM	Neural Network Model
MLR	Multiple Linear Regression
Prec	Precipitation
RE	Reduction of Error
SSC	Seasonal Sensitivity Characteristic
Temp	Temperature
weq	water equivalent
WP	Work Package

# Chapter 1

## Introduction

### 1.1 Aims and significance of the project PALVAREX

This PhD thesis is embedded in the research project PALEoclimate VARIability and EXtreme events (PALVAREX) within Work Package 1 (Past Climate Variability, Trends and Extreme Events) of the National Center of Competence in Research on Climate (NCCR Climate). This research program is funded by the Swiss National Science Foundation (SNSF).

The NCCR Climate is a scientific network aiming to a better understanding of the climate system by carrying out interdisciplinary research on its variability and its potential for change. Research in NCCR Climate is divided into four distinct Work Packages (WP), each addressing different fields of climate research.

Work Package 1 (WP 1) encompasses three research projects and focuses on the understanding of the processes that govern natural variability. A quantitative reconstruction is required for the times when anthropogenic influences on the climate system and its variability were either absent, different or reduced. Above all, the goal of this WP is to obtain high-resolution records for an extended period of time.

PALVAREX, one of the three research projects within WP 1, includes studies of climate dynamics and socio-economic investigations of the University of Bern, Switzerland.

The PALVAREX research project attempts to investigate the following tasks:

- To investigate the spatial characteristics, such as synoptic patterns and their behavior in the state space, spectral characteristics, and trends of seasonal to century scale climate variability in the Atlantic–European area.
- To assess the sensitivity of intermittent climate system reactions to (a) different forcing factors, (b) internal system oscillations, and determine the correlations between these two factors as well as the relevant teleconnections.
- To estimate the necessary time resolution for a precise diagnosis of extreme events in the central European and Alpine area and determine their temporal distribution.
- To determine the correlations of these extreme events with distinct climate patterns or data from natural archives.

- To assess the impact of extreme climate events on past ecosystems and societies in a natural climate (e.g. before 1900).
- To study the relationship between the most extreme events documented within the last millennium and the "one in a century events" of the 20th century.

Past climate variability can either be studied in reconstructions or in long coupled atmosphere–ocean general circulation model (AOGCM) runs. Throughout this dissertation, we exemplarily connect selected high–quality time series of glacier variations with new multiproxy reconstructions of temperature and precipitation. We want to test both, the quality and capabilities of the series of glacier variations as well as the multiproxy reconstructions. Generally, we are aiming to gain more insight into the highly complex climate–glacier relation.

Three main aims of this PhD thesis were defined:

1. To test the general capabilities of Neural Networks (NNs) in modelling and simulating glacier mass balance and glacier length fluctuations, respectively.
2. To study the climate–mass balance and climate–glacier length relation, with special consideration of multiproxy reconstructions of temperature and precipitation as climate forcing variables.
3. To analyze selected glacier advance and retreat periods, in order to gain more insight into their forcing factors and/or their perception.

## 1.2 Importance of glacier variations (mass balance and length fluctuations)

### 1.2.1 Direct measurements

Precise observations of glacier variations are already known from the beginning of the 19th century. In 1827, Franz Joseph Hugi of Solothurn, Switzerland, built a simple hut on the central moraine of the Lower Aare Glacier, Switzerland. He pounded in a series of stakes and chiselled marks onto the rocks, becoming the first to measure glacial movement (Hugi, 1830). It was an important consequence, confirming what mountain dwellers already knew, that glaciers were not static, but could advance and retreat a great distance (de Charpentier, 1841; Haeberli and Zumbühl, 2003).

Hugi's successor Louis Agassiz, a respected natural scientist from Neuchâtel, Switzerland, based on these findings claiming in 1837 that glaciers had once covered most of Eurasia. His theory, today well-known as "ice age theory", caused an uproar in the scientific community. But what else, if not glaciers, Agassiz argued, had left over the giant boulders found in unlikely spots around the continent (Bolles, 1999)?

Agassiz also set off for the Lower Aare Glacier, Switzerland, to prove his theory. In the 1840s he and his interdisciplinary team holed up in a provisional shelter between two boulders dubbed the "Hôtel des Neuchâtelois". There they made the first systematic glacial investigations. Agassiz as the team leader, conducted tests, made observations of glacial movement and composition, and measured ice temperature and atmospheric humidity (Agassiz, 1847).

After these pioneering studies on the Lower Aare Glacier further systematic investigations on glaciers had been made in the second half of the 19th century. As an exemplary joint project between the Swiss Academy of Sciences (SANW) and the Swiss Alpine Club (SAC) the Rhône Glacier, Switzerland,



has been extensively studied. The aim of these thorough investigations was to understand the historical development of the glacier and its flow. Later, measurements have been made of the rate of ablation, precipitation and firnline elevation. Furthermore, data were collected annually on the volume, the area of the glacier and the position of the glacier front during the 1887–1910 period to produce maps on a scale of 1:5000 (Mercanton, 1916; Grove, 2003).

The importance of understanding the relation between climate variations and glacier fluctuations has been recognized before the end of the 19th century:

"Il est un phénomène, dans l'histoire naturelle de nos Alpes, qui est constaté et reconnu depuis bien des siècles, qui a frappé tout le monde, montagnards ignorants et savants physiciens, qui est à peu près décrit dans toutes les théories, mais qui est cependant encore insuffisamment connu, insuffisamment étudié, insuffisamment expliqué. Je veux parler des variations périodiques de grandeur des glaciers. Les montagnards ont de tout temps observé que les glaciers descendent tantôt plus bas, tantôt moins bas dans les vallées, qu'ils subissent des périodes de croissance et de décroissance; les théories ont toutes enregistré ces faits et donné des dates et des chiffres isolés à l'appui de leurs descriptions. Mais nous ne possédons aucun travail d'ensemble qui nous donne les observations, les faits, les lois et la théorie complète du phénomène." (Forel, 1881: 20)

"Les causes des variations en grandeur des glaciers doivent donc être cherchées dans les variations des conditions météorologiques. La grandeur relative des glaciers est un indice de la variation du climat. Nous possédons donc dans le phénomène tangible, tombant directement sous l'observation des variations en grandeur des glaciers, un moyen direct de constater les variations possibles des grands facteurs météorologiques. Cela légitime l'attention du monde savant pour le phénomène que nous étudions." (Forel, 1895: 223)

This led to the founding of the "Commission Internationale des Glaciers" (CIG) in 1894, nowadays known as the International Commission on Snow and Ice (ICSI). The objectives of the CIG were to promote the historical and scientific studies on glaciers throughout the world, to gather and disseminate the data through periodic publication and annual reports. Furthermore, the monitoring strategy should also include indigenous knowledge to be collected by scientists through communication with mountain inhabitants (Forel, 1895). The first phase of international glacier observation around the turn of the century was characterized by the search for regular oscillations in the climate–glacier system as illustrated by the title of the reports ("Les variations périodiques des glaciers").

The first reports contained mainly qualitative observations (advance/retreat) with the exception of the glaciers in the European Alps and Scandinavia, which are quite well documented from the very beginning. A general tendency towards glacier shrinkage was recorded (Haeberli, 1998). Around 1890 and 1920, the majority of glaciers in the European Alps went through a short but marked period of readvance, apart from these periods retreat clearly predominated (Kuhn et al., 1997). This seemed to confirm the impression that climate and glaciers fluctuate in a periodic or at least quasi-periodic way.

After the First World War, the more rarely appearing reports (editor: P.–L. Mercanton) contained numerical data on length changes in European glaciers, as well as references to various national reports. As a consequence of the low scientific interest and the low level of intensity, the strong global warming and glacier shrinkage in the 1930s and 1940s passed rather unnoticed by the scientific literature. Since 1933 the reports were published on behalf of the ICSI, a part of the IAHS, the International Association of Hydrological Sciences (Haeberli and Zumbühl, 2003; Hoelzle et al., 2003).

Thorarinsson (1940) is said to be the first to attempt a global analysis of glaciological information and to extend that information back to the 18th century. His calculation of glacier volume change from

1850 ("Little Ice Age", believed to be the maximum glacier extension since the Ice Age in different areas) and its contribution to sea-level rise is unprecedented. The conclusion at that time, that the present glacier shrinkage is an universal phenomenon and that the global recession of glaciers has taken place in several stages of increasing intensity, interrupted by intervals of stagnation, is still valid (Dyurgerov and Meier, 2000).

Direct measurements of annual glacier mass balance started after 1946 on a regular basis (Houghton et al., 2001; Vincent, 2002). Thereby, the "missing link" between climate fluctuations and glacier length variations has been established (Haeberli and Zumbühl, 2003). In the time before the International Geophysical Year (1957–59), less than 10 glaciers were observed. The number of measured glaciers has grown rapidly since the International Geophysical Year and reached a maximum of 70–90 time series annually in the middle of the 1970s. Mass balances of more than 260 glaciers have been measured at one time or another (Dyurgerov and Meier, 2000).

From 1967 the data of glacier fluctuations were published in five-year intervals first by the PSFG (IAHS(ICS)/UNESCO, 1967; Kasser, 1970), from 1986 by the World Glacier Monitoring Service (WGMS). An extensive overview of the corresponding literature is given in Hoelzle et al. (2003).

## 1.2.2 Glacier variations as climate indicators

As sensitive indicators to climate variability, the data of glacier variations provide us with important and interesting results of history of climate. Changing glaciers therefore, indicate highly visible a changing climate. Primarily two types of data from glaciers contain climatic information: Mass balance observations and data on the geometry of glaciers, notably glacier length (e.g. Houghton et al., 2001).

Glacier mass balance describes the behavior of a glacier or ice sheet. It is the algebraic sum of the accumulation and the ablation within a certain time. The process of gaining ice mass comprises mainly solid precipitation, the process of losing ice mass comprises mainly melting at the surface. Condensation and evaporation are additional processes with minor importance (Paterson, 1994; Dyurgerov, 2002). As a consequence of this, the mass balance can be viewed as the direct and undelayed reaction of a glacier to climate variability and site meteorological conditions, dependent primarily on temperature, solar radiation and precipitation (Reichert et al., 2001). As pointed out before, the available mass balance records are relatively short (usually less than 50 years) when compared with relatively long records of glacier length.

Length variations are the most comprehensive data of glaciers. But in contrast to glacier mass balance, fluctuations in glacier length are the indirect, delayed, filtered and strongly enhanced responses to climate change (Haeberli, 1998). Cumulative glacier mass changes lead to changes in ice thickness and therefore influence the dynamic redistribution of mass by glacier flow and finally glacier length. It represents an intuitively understood and most easily observed phenomenon to illustrate the reality of climate variability (Oerlemans, 2001). Besides the reported measurements of glacier length which extend back into the 19th century, a large amount of length information is available from written documents, sketches, etchings, paintings and old photographs of glaciers, but most of them show the same glaciers (e.g. Holzhauser and Zumbühl, 1996). The number of glaciers where two or more useful pictures from different times in the 18th and 19th century exist is small, maybe fifty (Houghton et al., 2001; Oerlemans, 2001). Nevertheless, due to these proxy data we are given the possibility to reconstruct past glacier variations and to cast further light on regional or world-wide climate change before the instrumental era, eventually in combination with other lines of evidence (e.g. glacier moraine; see Section 1.4.1).

## 1.3 Glacier changes since the 16th century

### 1.3.1 Jostedalsbreen, western south Norway

The reconstruction of Holocene glacier variations in Scandinavia was pioneered by Wibjörn Karlén (see review by Karlén, 1988). In southern Norway, relatively complete records of century- to millennial-scale Holocene glacier variations have been reconstructed from two types of distal sedimentary sequences, downstream of glaciers: firstly, glaciolacustrine sequences (e.g. Nesje et al., 2001; Dahl et al., 2003); secondly, glaciofluvial sediments from stream-bank mires subject to episodic overbank deposition of suspended sediment (e.g. Matthews et al., 2005). These reconstructions complement each other and are more accurate than moraine stratigraphic studies, where large glacier advances were destructive of the evidence of earlier events (Matthews and Briffa, 2005).

During the "Little Ice Age" (LIA; 1300–1900; e.g. Pfister, 1999; Wanner et al., 2000) the glaciers in southern Norway showed their most extensive expansion – apart from early Holocene maxima around 10000 years BP (Nesje and Dahl, 2000; Matthews et al., 2005; Nesje et al., 2005). Please notice that the term "Little Ice Age" still is being discussed controversially. However, it remains useful under restriction being viewed as a modern analogue for earlier similar events (Matthews and Briffa, 2005). As an example, the LIA maxima at the outlets of Jostedalsbreen, a maritime plateau glacier in western south Norway, can be dated to the mid-18th century (Bogen et al., 1989; Chinn et al., 2005). Historic evidence shows that Nigardsbreen, an eastern outlet from Jostedalsbreen, advanced 2800 meters between 1710 and 1735 (see Figure 1.1a), equaling to an average annual advance rate of ~110 meters. Between 1735 and the historically documented LIA maximum in 1748, the glacier advanced 150 meters (Nesje and Dahl, 2003). Local investigations and courts of inquiry produced a wealth of documents showing both the damage caused to farmland/pastures and the suffering of the people who lived near the expanding glacier (Nesje and Dahl, 2000).

The retreat from the LIA maximum positions occurred continuously in southern Norway, but it was slowly and frequently interrupted by short still-stands and some minor readvances. At the outlets of Jostedalsbreen, two readvances during the first decades of the 20th century were studied in detail (Bogen et al., 1989; Winkler, 1996). However, in all glacier regions in Norway, the middle of the 20th century was characterized by considerable and fast glacier retreats. During the 1990s all outlets of Jostedalsbreen were advancing. Currently, Nigardsbreen shows the most positive net balance in Norway (Chinn et al., 2005). Notice that on the one hand the net mass balance on the maritime glaciers in western Norway is best correlated with the winter balance. On the other hand, winter accumulation of these glaciers is closely linked to the NAO index. A positive NAO phase means for example enhanced winter precipitation for maritime glaciers in Scandinavia and reduced winter precipitation for glaciers in the European Alps (Nesje et al., 2005; Nordli et al., 2005).

### 1.3.2 Bernese Alps, Switzerland

The climatic implications of glacier variations have attracted scientific attention from the very beginning of glaciological investigations in the Swiss Alps. Thus, the Swiss were the first to make systematic annual measurements of the changing glacier fronts (see Section 1.2.1; VAW/SANW, 1881–2002). As a result of the scientific activities and the extensive historic sources of glacier variations, the sequence and timing of glacier fluctuations during the LIA have been studied more detailed in the Swiss Alps than elsewhere (Winkler, 2002; Grove, 2003).

Evidence from historical documents (e.g. Zumbühl, 1980) and dendrochronology (e.g. Holzhauser and Zumbühl, 1996) shows that Swiss glaciers advanced in the 1580s, about 1640, 1720, 1740, in

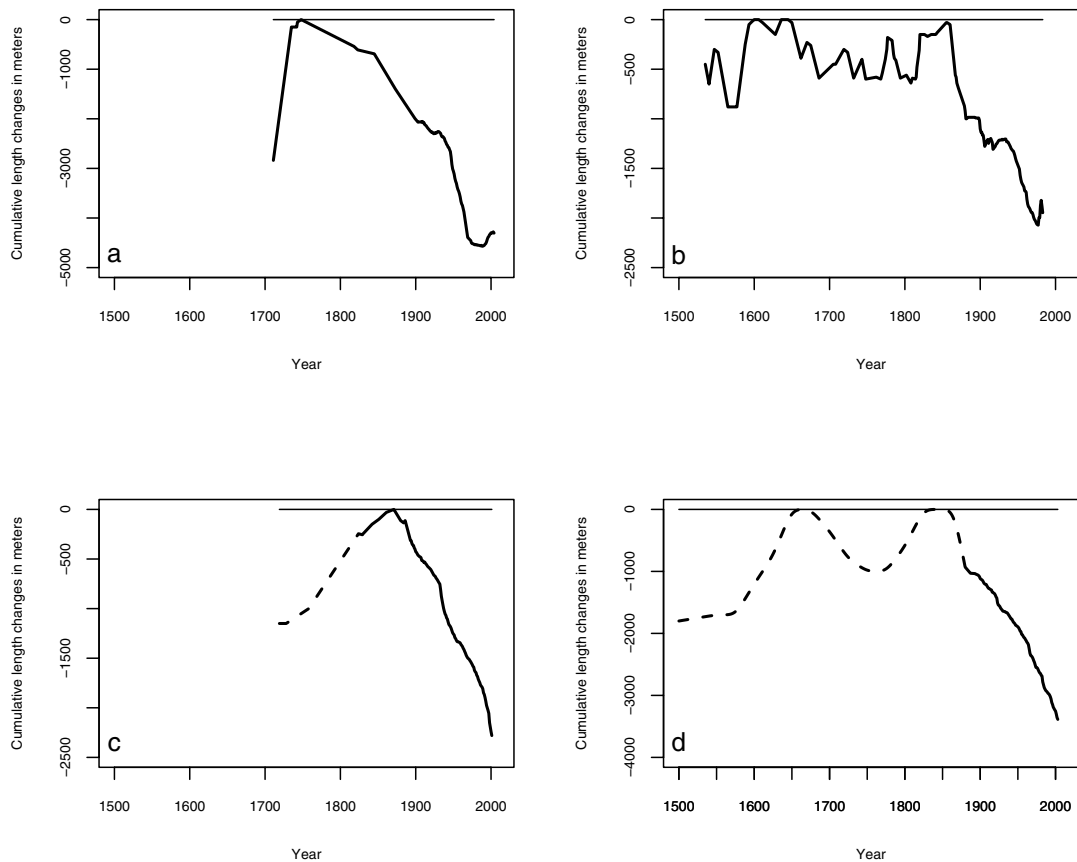


**Figure 1.1:** Cumulative length changes (solid lines) of the four glaciers used in our studies (relative to the particular LIA maxima): (a) Nigardsbreen, Norway (from Østrem et al., 1977; with later updates by the Norwegian Water Resources and Energy Directorate (NVE), Section for Glacier and Snow), (b) Lower Grindelwald Glacier, Switzerland (Zumbühl, 1980; Zumbühl et al., 1983; Holzhauser and Zumbühl, 1999, 2003), (c) Lower Aare Glacier, Switzerland (Zumbühl and Holzhauser, 1988; VAW/SANW, 1881–2002), (d) Great Aletsch Glacier, Switzerland (Zumbühl and Holzhauser, 1988; VAW/SANW, 1881–2002; Haeberli and Holzhauser, 2003). The dashed lines indicate an arguable but likely curve progression (Lower Aare Glacier) or an interpolation (Great Aletsch Glacier), respectively.

the 1770s, about 1818, 1850 and the 1890s. In the 20th century continuous glacier retreat was only interrupted by little readvances around 1920 and in the early 1980s (Grove, 2003). Note that it is very delicate to make general statements about the glacier extension during the LIA. On the one hand, the volume expansion of a particular glacier maximum/minimum can differ significantly from one glacier to another. On the other hand, there are also differences in the number of advances/retreats. Some advances (1600/50s, 1820s, 1850s) are documented for a majority of glaciers. Others are missing or are detected only for a minority of glaciers (Winkler, 2002).

Figures 1.1b–d show the series of cumulative length changes of the Alpine glaciers used in our studies. Obviously, the Lower Grindelwald Glacier (Figure 1.1b) shows the most detailed and best-documented curve of glacier length changes. This is due to the comprehensive studies of Zumbühl

(1980) and Zumbühl et al. (1983) which examined more than 300 historical sources of the Lower Grindelwald Glacier. In contrast to this, the series of Lower Aare (Figure 1.1c) and Great Aletsch Glacier (Figure 1.1d) are less detailed and thus more unconfident. Note that the LIA glacier maximum extent of Lower Aare Glacier is documented in the year 1871, which is two decades later than most of the Alpine glaciers (Zumbühl and Holzhauser, 1988; VAW/SANW, 2002).

## 1.4 Modelling and reconstructing glacier variations

### 1.4.1 Reconstructions



**Figure 1.2:** Samuel Birmann (1793–1847) visited the Lower Grindelwald Glacier, Switzerland, in September 1826 and portrayed in a watercolored pencil drawing the glacier with the clearly recognizable moraine system and the marked fan-shaped tongue ("Schweif") which extended far down into the valley (Zumbühl, 1980). Kupferstichkabinett, Kunstmuseum Basel. Photograph by Heinz J. Zumbühl.

Direct determinations of glacier variations in the (Bernese) Alps were only started with increasing accuracy shortly before the end of the 19th century (see Section 1.2.1). For preceding time periods, we have to analyze the unique natural and documentary archives which are available for some selected glaciers to gain insight into the Holocene glacier history. This can be done by the aid of interdisciplinary approaches which contain both historical and physical methods (e.g. Holzhauser and Zumbühl, 1996). Therefore, the reconstruction of pre-industrial glacier fluctuations in the Swiss Alps reveals the natural range of Holocene climate variability against which the present-day climatic situation can be judged.

Reconstructions of pre-instrumental glacier variations can be based on three methods (Zumbühl and

Holzhauser, 1988; Holzhauser et al., 2005):

- The historical method,
- The glacio–archaeological method,
- The glacio–morphological method.

In case being sufficient in quality and quantity, written documents and pictorial historical records (paintings, sketches, engravings, photographs, chronicles, topographic maps, reliefs) provide quite a detailed picture of glacier fluctuations over the last 450 years. With this method we can achieve a resolution of decades or, in some cases, even single years (Holzhauser et al., 2005). The series of cumulative length changes of the Lower Grindelwald Glacier, Switzerland, is probably the best example of a glacier curve derived from historical sources (see Figure 1.1b). Unfortunately, analyzable material only is available for glaciers that were easily accessible for interested people. In other terms close to human settlement and usually with a spectacular and impressive glacier front. Figure 1.2 shows a high–quality pictorial source of the Lower Grindelwald Glacier, Switzerland, in the year 1826 (Zumbühl, 1980).

The glacio–archaeological method uses anthropogenic traces which are directly related to changes in glacier size/length. Examples are foundations and wooden beams from buildings, old Alpine routes or remains of irrigation channels. Note that such field indices should be proved by written documents or radiocarbon dating (Holzhauser, 1984).

Finally, the glacio–geomorphological method includes the radiocarbon dating of palaeosols and the dating of fossil wood by dendrochronology found within and at the edge of glacier forefields (Hormes et al., 2001). For an exact reconstruction of historic glacier extensions fossil wood has to be found in their original position, i.e. in situ (Zumbühl and Holzhauser, 1988; Holzhauser et al., 2005).

## 1.4.2 Mass balance models

A number of terms are used to describe the different aspects of mass balance on a glacier. The winter balance is the amount of snow accumulated during the winter months. Conversely, the summer balance is a negative quantity, namely the amount of snow and ice lost by melt. The balance over a whole year, which is commonly taken from the end of one melt season to the end of the next, the sum of the winter and summer balances is the net balance. These balances are usually expressed in water equivalents (weq). The specific balance is usually given as

$$b_n = b_m + b_a, \quad (1.1)$$

where  $b_m$  is the specific melt balance, and  $b_a$  is the specific accumulation balance. The sum of both,  $b_n$ , is the specific net balance. The balances are usually measured on stakes placed on the glacier which allow to determine the amount of snow and ice melted after the melting season ( $b_m$ ), and to determine the snow accumulation ( $b_a$ ) during the accumulation season (e.g. Østrem and Bugman, 1991; Dyurgerov, 2002).

As glaciers are sensitive to climate change, therefore the impact of these affects should be assessed on glacier mass balance. Modelling a glacier mass balance consists of two parts, glacier melt and accumulation. In fact, glacier mass balance modelling has received great attention. Even if there is a huge variety of glacier mass balance models with varying sophistication, three basic concepts for glacier mass balance models should be taken into account (Schneeberger, 2003):

- Statistical Models,
- Temperature Index Models,
- Energy Balance Models.

Statistical analysis was introduced by Lliboutry (1974). He examined the statistics of mass balance measurements and developed a linear model to account the independent spatial and temporal variations. This approach is well funded in empirical studies that observe relatively constant spatial differences between stakes but a temporal offset in magnitude of all stakes (Fountain and Vecchia, 1999; Oerlemans, 2001). The nonlinear Neural Network Model (NNM) approaches which were used in our studies are amongst this statistical model concept.

The other two concepts use meteorological measurements to calculate melt and accumulation. The simplest models, temperature index melt models, also known as the degree-day method, are based on an assumed relationship between ablation and air temperature. This relation is usually expressed in the form of positive temperature sums (Braithwaite, 1984; Jóhannesson et al., 1995; Hock, 1998). Many attempts exist to add the physical basis by incorporating more variables, such as radiation components (e.g. Hock, 1999; Hock, 2003).

Energy balance models provide a physically based description of the relevant ablation processes including the assessment of the relevant energy fluxes both to and from the glacier surface. With increasing model complexity the necessary input information increases as well (e.g. Oerlemans, 1992; van de Wal, 1996; Klok and Oerlemans, 2002).

### 1.4.3 Modelling glacier length

Many authors state that in qualitative terms there is a good agreement between proxy climate indicators, instrumental meteorological data and glacier fluctuations (e.g. Oerlemans, 2001; Grove, 2003). However, the explicit simulation and modelling of historical glacier length fluctuations seems to be more complicated. Nevertheless, Greuell (1992) successfully reproduced the retreat of Hintereisferner, Austria, since the mid-19th century. The main problem occurs if the combined advance towards the maximum and the subsequent retreat should be modelled (e.g. Stroeven et al., 1989). Tree rings are often used as climate proxy to force models of glacier length fluctuations because tree ring width and equilibrium line altitude (ELA) are well correlated (Bradley and Jones, 1995). Unfortunately, many attempts to use tree ring width as a glacier mass balance forcing failed (Oerlemans, 2001). The most successful simulation of a long historical glacier record was made by Schmeits and Oerlemans (1997). In his study of the Lower Grindelwald Glacier, Switzerland, he used long records of meteorological stations from sites close to the glacier and extended these backwards in time with climate reconstructions made by Pfister (1999); the latter is based mainly on historical documents.

### 1.4.4 Multiproxy reconstructions of temperature and precipitation

For a relatively short time, new gridded reconstructions of monthly (1659–) and seasonal (1500–1658) temperature (Luterbacher et al., 2004) and seasonal (1500–) precipitation (Pauling et al., 2005) fields for European land areas are available. The temperature reconstruction is based on a comprehensive data set which includes a large number of homogenized and quality-checked instrumental data series. Furthermore, a number of reconstructed sea-ice and temperature indices derived from documentary records for earlier centuries and a few seasonally resolved proxy temperature reconstructions from Greenland ice cores and tree rings from Scandinavia/Siberia are used (Luterbacher

et al., 2004). The precipitation reconstruction includes a combination of instrumental series, documentary indices and natural proxies (tree rings, corals, ice cores; Pauling et al., 2005). As mentioned in Section 1.1, we use these new data sets as forcing variables and selected time series of glacier variations as target function of our NN-based climate–glacier model (see Sections 3 and 4).

## 1.5 Structure of this thesis

Chapter 2 presents a study of glacier perception and fluctuations in the mid–19th century. The first steps of experimental glaciology coincide with a change of glacier representation techniques from paintings and topographic maps to photographs. Simultaneously, it is also the time when a majority of (Alpine) glaciers show their LIA maximum extent. This glacier maximum extent and the subsequent retreat have been extensively studied for two exemplary Swiss Alpine glaciers, the Lower Grindelwald Glacier and the Lower Aare Glacier. The quality of its documentary data allows the development of high-quality digital elevation models (DEMs), probably better than elsewhere in the world. Thus, volume and area changes of these two glaciers since their mid–19th century maximum extent can be determined by DEM comparisons. In addition, these comparisons probably show an unexpected and extraordinary dynamical behavior of the Lower Grindelwald Glacier since the mid–19th century. Additionally to glacier change calculations we are also able to do a unique case study of the evolution of work on two of the best studied glaciers in Europe and to demonstrate its evolution from the very beginnings of glaciology, modern cartography, photography to the exploitation of the latest cartographic techniques.

In Chapter 3 a proxy of annual mass balance changes in the Great Aletsch Glacier, Switzerland, has been reconstructed for the 1500–1999 period. In this study, a nonlinear Backpropagation Neural Network (BPN) has been driven by both monthly resolved instrumental series of local temperature and precipitation (1900–99 period) and multiproxy reconstructions of seasonally resolved temperature and precipitation (1500–1999 period). On the one hand, it can be shown that the BPN approach is a reasonable technique to study the climate–mass balance relation and to reconstruct a proxy of annual mass balance changes. Within this climate–mass balance relation, a significant nonlinear part was discovered. On the other hand, the mass balance changes in the Great Aletsch Glacier are rather driven by summer (JJA) temperature than by winter (DJF) precipitation.

Chapter 4 presents a further development of the BPN technique used in Chapter 3. Instead of using mass balance changes as output data we apply glacier length variations of the Lower Grindelwald Glacier, Switzerland, as training data. The BPN model which also takes into account the varying reaction time of the glacier is then forced with two regional climate scenarios for the 2000–50 period to assess possible future glacier extensions. Furthermore, by processing the used climate parameters with a sensitivity analysis, based on Neural Networks (NNs), we gain insight into the relative importance of different climate configurations of temperature/precipitation that led to advances and retreats of the Lower Grindelwald Glacier in historic times.

Finally, in Chapter 5, the most important results of this dissertation are summarized and overall conclusions are drawn.

## Bibliography

Agassiz, L. (1847). *Système glaciaire ou recherche sur les glaciers, leur mécanisme, leur ancienne extension et le rôle qu'ils ont joué dans l'histoire de la terre. Première partie: Nouvelles études et*



*expériences sur les glaciers actuels: leur structure, leur progression et leur action physique sur le sol.* V. Masson, Paris, L. Voss, Leipzig, 2 Vols.

Bogen, J., B. Wold, and G. Østrem (1989). Historic glacier variations in Scandinavia. In J. Oerlemans (Ed.), *Glacier Fluctuations and Climatic Change. Proceedings of the Symposium on Glacier Fluctuations and Climatic Change*, Amsterdam, The Netherlands, 1–5 June 1987. Kluwer Academic Publishers, Dordrecht, The Netherlands, 109–128.

Bolles, E. B. (1999). *The Ice Finders: How a Poet, a Professor, and a Politician Discovered the Ice Age*. Counterpoint Press, Washington DC, USA.

Bradley, R. S. and P. D. Jones (1995). *Climate Since A.D. 1500*. 2nd edition. Routledge, London and New York.

Braithwaite, R. G. (1984). Calculation of degree-days for glacier-climate research. *Zeitschrift für Gletscherkunde und Glazialgeologie* 20(1–2), 1–8.

Chinn, T., S. Winkler, M. J. Salinger, and N. Haakensen (2005). Recent glacier advances in Norway and New Zealand: a comparison of their glaciological and meteorological causes. *Geografiska Annaler* 87A(1), 141–157, doi:10.1111/j.0435–3676.2005.00249.x.

Dahl, S. O., J. Bakke, Ø. Lie, and A. Nesje (2003). Reconstruction of former glacier equilibrium-line altitudes based on proglacial sites: an evaluation of approaches and selection of sites. *Quaternary Science Reviews* 22(2–4), 275–287, doi:10.1016/S0277–3791(02)00135–X.

de Charpentier, J. (1841). *Essai sur les glaciers et sur le terrain erratique du bassin du Rhône*. M. Ducloux, Lausanne.

Dyrgerov, M. (2002). Glacier Mass Balance and Regime: Data of Measurements and Analysis. In M. Meier and R. Armstrong (Eds.), *INSTAAR Occasional Paper No. 55*, Institute of Arctic and Alpine Research, University of Colorado, Boulder, CO.

Dyrgerov, M. B. and M. F. Meier (2000). Twentieth century glacier change: Evidence from small glaciers. *Proceedings of the National Academy of Sciences* 97(4), 1406–1411.

Forel, F.-A. (1881). Les variations périodiques des glaciers des Alpes. 1er rapport. *Extrait de l'Echo des Alpes* 17, 20–46.

Forel, F.-A. (1895). Les variations périodiques des glaciers. Discours préliminaire. *Extrait des Archives des sciences physiques et naturelles* XXXIV, 209–229.

Fountain, A. G. and A. Vecchia (1999). How many Stakes are Required to Measure the Mass Balance of a Glacier? *Geografiska Annaler* 81A(4), 563–573, doi:10.1111/j.0435–3676.1999.00084.x.

Greuell, J. W. (1992). Hintereisferner, Austria: mass-balance reconstruction and numerical modelling of the historical length variations. *Journal of Glaciology* 38(129), 233–244.

Grove, J. M. (2003). *Little Ice Ages: Ancient and Modern*. 2nd edition. Routledge, London and New York, 2 Vols.

Haeberli, W. (1998). Historical evolution and operational aspects of worldwide glacier monitoring. In W. Haeberli, M. Hoelzle, and S. Suter (Eds.), *Into the second century of worldwide glacier monitoring: prospects and strategies*, UNESCO Studies and Reports in Hydrology, 56, 35–51.

Haeberli, W. and H. Holzhauser (2003). Alpine Glacier Mass Changes During the Past Two Millennia. *PAGES News* 11(1), 13–15.

- Haeberli, W. and H. J. Zumbühl (2003). Schwankungen der Alpengletscher im Wandel von Klima und Perception. In F. Jeanneret, D. Wastl-Walter, and U. Wiesmann (Eds.), *Welt der Alpen – Gebirge der Welt. Ressourcen, Akteure, Perspektiven*, Jahrbuch der Geografischen Gesellschaft Bern, Band 61, 77–92.
- Hock, R. (1998). *Modelling of glacier melt and discharge*. Ph. D. thesis, Swiss Federal Institute of Technology (ETH), Zürich.
- Hock, R. (1999). A distributed temperature–index ice– and snowmelt model including potential direct solar radiation. *Journal of Glaciology* 45(149), 101–111.
- Hock, R. (2003). Temperature index melt modelling in mountain regions. *Journal of Hydrology* 282(1–4), 104–115, doi:10.1016/S0022–1694(03)00257–9.
- Hoelzle, M., W. Haeberli, M. Dischl, and W. Peschke (2003). Secular glacier mass balances derived from cumulative glacier length changes. *Global and Planetary Change* 36(4), 295–306, doi:10.1016/S0921–8181(02)00223–0.
- Holzhauser, H. (1984). *Zur Geschichte der Aletschgletscher und des Fieschergletschers*. Physische Geographie, Vol. 13. Geographisches Institut der Universität Zürich, Zürich.
- Holzhauser, H., M. Magny, and H. J. Zumbühl (2005). Glacier and lake–level variations in west–central Europe over the last 3500 years. *The Holocene* 15(6), 791–803, doi:10.1191/0959683605hl853ra.
- Holzhauser, H. and H. J. Zumbühl (1996). To the history of the Lower Grindelwald Glacier during the last 2800 years – palaeosols, fossil wood and historical pictorial records – new results. *Zeitschrift für Geomorphologie, Neue Folge, Supplementband 104*, 95–127.
- Holzhauser, H. and H. J. Zumbühl (1999). Glacier Fluctuations in the Western Swiss and French Alps in the 16th Century. *Climatic Change* 43(1), 223–237, doi:10.1023/A:1005546300948.
- Holzhauser, H. and H. J. Zumbühl (2003). Nacheiszeitliche Gletscherschwankungen. In R. Weingartner and M. Spreafico (Eds.), *Hydrologischer Atlas der Schweiz*, Bundesamt für Landestopografie, Bern–Wabern, Tafel 3.8.
- Hormes, A., B. U. Müller, and C. Schlüchter (2001). The Alps with little ice: evidence for eight Holocene phases of reduced glacier extent in the Central Swiss Alps. *The Holocene* 11(3), 255–265.
- Houghton, J. T., Y. Ding, D. J. Griggs, M. Noguer, P. J. van der Linden, X. Dai, K. Maskell, and C. A. Johnson (2001). *Climate Change 2001: The Scientific Basis*. Cambridge University Press, Cambridge, UK, and New York, NY, USA.
- Hugi, F. J. (1830). *Naturhistorische Alpenreise*. Amiet-Lutiger, Solothurn.
- IAHS(ICSU)/UNESCO (1967). *Fluctuations of Glaciers 1959–1965*, Volume I (P. Kasser, Ed.). Permanent Service on the Fluctuations of Glaciers (PSFG), Paris.
- Jóhannesson, T., O. Sigurdsson, T. Laumann, and M. Kennett (1995). Degree–day glacier mass–balance modelling with applications to glaciers in Iceland, Norway and Greenland. *Journal of Glaciology* 41(138), 345–358.
- Karlén, W. (1988). Scandinavian glacier and climatic fluctuations during the Holocene. *Quaternary Science Reviews* 7(2), 199–209.

- Kasser, P. (1970). Gründung eines "Permanent Service on the Fluctuations of Glaciers". *Zeitschrift für Gletscherkunde und Glazialgeologie* 6(1–2), 193–200.
- Klok, E. J. and J. Oerlemans (2002). Model study of the spatial distribution of the energy and mass balance of Morteratschgletscher, Switzerland. *Journal of Glaciology* 48(163), 505–518.
- Kuhn, M., E. Schlosser, and N. Span (1997). Eastern Alpine glacier activity and climatic records since 1860. *Annals of Glaciology* 24, 164–168.
- Lliboutry, L. (1974). Multivariate statistical analysis of glacier annual balances. *Journal of Glaciology* 13(69), 371–392.
- Luterbacher, J., D. Dietrich, E. Xoplaki, M. Grosjean, and H. Wanner (2004). European Seasonal and Annual Temperature Variability, Trends, and Extremes Since 1500. *Science* 303(5663), 1499–1503, doi:10.1126/science.1093877.
- Matthews, J. A., M. S. Berrisford, P. Q. Dresser, A. Nesje, S. O. Dahl, A. E. Bjune, J. Bakke, H. J. B. Birks, Ø. Lie, L. Dumayne-Peaty, and C. Barnett (2005). Holocene glacier history of Bjørnbreen and climatic reconstruction in central Jotunheimen, Norway, based on proximal glaciofluvial stream-bank mires. *Quaternary Science Reviews* 24(1–2), 67–90, doi:10.1016/j.quascirev.2004.07.003.
- Matthews, J. A. and K. R. Briffa (2005). The "Little Ice Age": re-evaluation of an evolving concept. *Geografiska Annaler* 87A(1), 17–36, doi:10.1111/j.0435–3676.2005.00242.x.
- Mercanton, P.-L. (1916). *Vermessungen am Rhône-gletscher, 1874–1915*. Neue Denkschriften der Schweizerischen Naturforschenden Gesellschaft (SNG), Kommissions-Verlag von Georg & Co., Basel, No. 52.
- Nesje, A. and S. O. Dahl (2000). *Glaciers and Environmental Change*. Arnold, London, UK.
- Nesje, A. and S. O. Dahl (2003). The 'Little Ice Age' – only temperature? *The Holocene* 13(1), 139–145, doi:10.1191/0959683603hl603fa.
- Nesje, A., E. Jansen, H. J. B. Birks, A. E. Bjune, J. Bakke, C. Andersson, S. O. Dahl, D. K. Kristensen, S.-E. Lauritzen, Ø. Lie, B. Risebrobakken, and J.-I. Svendsen (2005). Holocene Climate Variability in the Northern North Atlantic Region: A Review of Terrestrial and Marine Evidence. In H. Drange, T. Dokken, T. Furevik, R. Gerdes, and W. Berger (Eds.), *The Nordic Seas: An Integrated Perspective*, AGU Monograph 158, American Geophysical Union, Washington DC, 289–322.
- Nesje, A., J. A. Matthews, S. O. Dahl, M. S. Berrisford, and C. Andersson (2001). Holocene glacier fluctuations of Flatebreen and winter-precipitation changes in the Jostedalbreen region, western Norway, based on glaciolacustrine sediment records. *The Holocene* 11(3), 267–280.
- Nordli, Ø., Ø. Lie, A. Nesje, and R. E. Benestad (2005). Glacier Mass Balance in Southern Norway Modelled by Circulation Indices and Spring–Summer Temperatures AD 1781–2000. *Geografiska Annaler* 87A(3), 431–445, doi:10.1111/j.0435–3676.2005.00269.x.
- Oerlemans, J. (1992). Climate sensitivity of glaciers in southern Norway: application of an energy-balance model to Nigardsbreen, Hellstugubreen and Alftobreen. *Journal of Glaciology* 38(129), 223–232.
- Oerlemans, J. (2001). *Glaciers and Climate Change*. A. A. Balkema Publishers, Rotterdam, The Netherlands.

- Østrem, G. and M. Bugman (1991). *Glacier Mass-Balance Measurements: A manual for field and office work*. National Hydrology Research Institute (NHRI), Environment Canada, Saskatoon, Canada, NHRI Science Report No. 4.
- Østrem, G., O. Liestøl, and B. Wold (1977). Glaciological investigations at Nigardsbreen, Norway. *Norsk Geografisk Tidsskrift* 30, 187–209.
- Paterson, W. S. B. (1994). *The physics of glaciers*. 3rd edition. Pergamon, Oxford, UK.
- Pauling, A., J. Luterbacher, C. Casty, and H. Wanner (2005). 500 years of gridded high-resolution precipitation reconstructions over Europe and the connection to large-scale circulation. *Climate Dynamics*, revised.
- Pfister, C. (1999). *Wetternachhersage. 500 Jahre Klimavariationen und Naturkatastrophen 1496–1995*. Paul Haupt Verlag, Bern, Stuttgart, Wien.
- Reichert, B. K., L. Bengtsson, and J. Oerlemans (2001). Midlatitude Forcing Mechanisms for Glacier Mass Balance Investigated Using General Circulation Models. *Journal of Climate* 14(17), 3767–3784, doi:10.1175/1520-0442(2001)014<3767:MFMFGM>2.0.CO;2.
- Schmeits, M. J. and J. Oerlemans (1997). Simulation of the historical variations in length of Unterer Grindelwaldgletscher, Switzerland. *Journal of Glaciology* 43(143), 152–164.
- Schneeberger, C. (2003). *Glaciers And Climate Change: A Numerical Model Study*. Ph. D. thesis, Swiss Federal Institute of Technology (ETH), Zürich.
- Stroeven, A., R. S. W. van de Wal, and J. Oerlemans (1989). Historical fluctuations of the Rhône Glacier: simulation with a numerical model. In J. Oerlemans (Ed.), *Glacier Fluctuations and Climatic Change. Proceedings of the Symposium on Glacier Fluctuations and Climatic Change*, Amsterdam, The Netherlands, 1–5 June 1987. Kluwer Academic Publishers, Dordrecht, The Netherlands, 391–405.
- Thorarinsson, S. (1940). Present Glacier Shrinkage, and Eustatic Changes of Sea-Level. *Geografiska Annaler* 22, 131–159.
- van de Wal, R. S. W. (1996). Mass-balance modelling of the Greenland ice sheet: a comparison of an energy-balance model and a degree-day model. *Annals of Glaciology* 23, 36–45.
- VAW/SANW (1881–2002). *Die Gletscher der Schweizer Alpen. Jahrbücher der Glaziologischen Kommission der Schweizerischen Akademie der Naturwissenschaften (SANW)*. Versuchsanstalt für Wasserbau, Hydrologie und Glaziologie (VAW) der ETH Zürich, Zürich, No. 1–122. (<http://glaciology.ethz.ch/swiss-glaciers/>).
- Vincent, C. (2002). Influence of climate change over the 20th Century on four French glacier mass balances. *Journal of Geophysical Research* 107(D19), 4375, doi:10.1029/2001JD000832.
- Wanner, H., H. Holzhauser, C. Pfister, and H. J. Zumbühl (2000). Interannual to century scale climate variability in the European Alps. *Erdkunde* 54(1), 62–69.
- Winkler, S. (1996). Front variations from outlet glaciers of Jostedalbreen, western Norway, during the 20th century. *Norges Geologiske Undersøkelse Bulletin* 431, 33–47.
- Winkler, S. (2002). *Von der "Kleinen Eiszeit" zum "globalen Gletscherrückzug" – Eignen sich Gletscher als Klimazeugen?* Abhandlungen der Mathematisch-naturwissenschaftlichen Klasse, No. 3. Akademie der Wissenschaften und der Literatur, Mainz.

Zumbühl, H. J. (1980). *Die Schwankungen der Grindelwaldgletscher in den historischen Bild- und Schriftquellen des 12. bis 19. Jahrhunderts. Ein Beitrag zur Gletschergeschichte und Erforschung des Alpenraumes*. Denkschriften der Schweizerischen Naturforschenden Gesellschaft (SNG), Birkhäuser, Basel/Boston/Stuttgart, Band 92.

Zumbühl, H. J. and H. Holzhauser (1988). Alpengletscher in der Kleinen Eiszeit. Sonderheft zum 125jährigen Jubiläum des SAC. *Die Alpen* 64(3), 129–322.

Zumbühl, H. J., B. Messerli, and C. Pfister (1983). *Die kleine Eiszeit: Gletschergeschichte im Spiegel der Kunst. Katalog zur Sonderausstellung des Schweizerischen Alpen Museums Bern und des Gletschergarten-Museums Luzern vom 09.06.–14.08.1983 (Luzern), 24.08.–16.10.1983 (Bern)*.



## Chapter 2

# Two Alpine glaciers over the last two centuries: a scientific view based on pictorial sources

Daniel **Steiner**<sup>1,2</sup>, Heinz Jürg **Zumbühl**<sup>1</sup>, Andreas **Bauder**<sup>3</sup>

<sup>1</sup> Meteorology and Climatology, Institute of Geography, University of Bern, Switzerland

<sup>2</sup> NCCR Climate, University of Bern, Switzerland

<sup>3</sup> Laboratory of Hydraulics, Hydrology and Glaciology (VAW), ETH Zürich, Switzerland

Revised for publication in: B. Orlove, E. Wiegandt and B. Luckman (Eds.), *The Darkening Peaks: Glacial Retreat in Scientific and Social Context*, University of California Press, Berkeley, CA

### Abstract

*Starting with the idea of an ice age hypothesis, Louis Agassiz initiated a research program on the Lower Aare Glacier, Switzerland, which marked the beginning of modern experimental glacier research. The results of this new scientific view were published in 1847, and included the first scientific maps of a glacier on a large scale. The original drawing of the panorama by Jacques Bourkhardt, which was missing for a long time and has recently been rediscovered, shows the extension of the Lower Aare Glacier in the 1840s and the extreme conditions under which the scientists and artists had been living and working. Since 1849, the material of the Lower Aare Glacier was updated with the first photographs of Swiss Alpine glaciers. Therefore, this period of the beginning of experimental glaciology on the one hand coincides with a change of glacier representation techniques from drawings/paintings and maps to photographs within 15 years. On the other hand, it is also the time when a majority of (Alpine) glaciers show their last maximum extent.*

*The Lower Grindelwald Glacier, Switzerland, plays a similar important role to the Lower Aare Glacier for scientific glacier research. Its well-documented record of length variations back to 1535 illustrates*

*the Little Ice Age climate changes. Newly discovered (stereo) photographs and old topographic maps of the Lower Grindelwald Glacier also show the impressive dimension of the 1855/56 maximum extent and the rapid glacier retreat since then.*

*In general, this glacier maximum extent in the mid-19th century and the subsequent retreat have been extensively studied for both, the Lower Grindelwald and the Lower Aare Glacier. The quality of its documentary data allows, probably better than elsewhere in the world, the development of accurate digital elevation models (DEMs). Thus, volume and area changes of these two glaciers since their mid-19th century maximum extent were determined by DEM comparisons.*

*It can be shown that the Lower Grindelwald Glacier has lost 5.5 km<sup>2</sup> of area and 1.56 km<sup>3</sup> of ice and the Lower Aare Glacier 4.3 km<sup>2</sup> of area and 1.59 km<sup>3</sup> of ice since their last maximum extent. However, for the Lower Grindelwald Glacier the spatial distribution of thickness changes could possibly signify extraordinary dynamical behavior since the mid-19th century.*

**Keywords:** Bernese Alps, glacier perception, glacier variations, glacier history, pictorial sources, digital elevation model, photogrammetry, historical cartography

## 2.1 Introduction

For centuries the high mountains and the glaciers have been a source of both paralysing fear and strange fascination. At the beginning of the 18th century the interest in Alpine glaciers first increased when natural scientists focussed their attention on them. Although first simple observations of glacier movements and moraines were made, no systematic scientific investigations on glaciers had been done (Zumbühl, 1980).

Thus, the 19th century stands not only for the break-through of the "ice age hypothesis", but also for the beginning of modern experimental glaciology. Initial detailed studies of glacier-related phenomena were undertaken on the Lower Aare Glacier, Switzerland, in the 1840s by the zoologist and geologist Louis Agassiz (1807–1873). His contributions to the newly established scientific field made him known as the "Father of Glaciology" (Lurie, 1960).

At about the same time impressive glacier advances which affected the majority of Alpine glaciers can be deduced from natural archives and documentary evidence (Maisch et al., 1999; Nicolussi and Patzelt, 2000). Furthermore, new kinds of documentary data which can be used to analyze glacier fluctuations appear in the mid-19th century. The technical progress of photography made it on the one hand possible to record a glacier position without any artistic distortion (Gernsheim, 1983). On the other hand, the first geometrically exact topographic maps of Switzerland, the so-called "Dufour map", were published between 1844 and 1864 (Wolf, 1879; Graf, 1896; Locher, 1954).

In general, all these historical records can give a very detailed picture of glacial fluctuations in the Swiss Alps during the late Holocene. They allow the study of glacier history to extend further into the past than would be possible from the use of direct measurements alone (e.g. Holzhauser et al., 2005). Empirical qualitative and/or quantitative data, mainly on the length, but also on the area and volume of glaciers, can be derived. Unfortunately, the potential for using documentary data outside the area of glaciology is still underestimated.

With methods based on historical records a temporal resolution of decades or, in some cases, even single years, is achieved in the reconstruction of glacier time series. Probably the best example in this context is the Lower Grindelwald Glacier, Switzerland. Fluctuations in its length have been reconstructed with the aid of numerous texts and pictorial representations back to 1535 (Zumbühl, 1980; Holzhauser and Zumbühl, 1996, 2003). It must also be noted that for many other glaciers



in the European Alps the historical material appears exceptionally rich (e.g. Mont Blanc region). However, there might well be untapped documentation for further research in many other areas of the world.

The objective of this paper is to bring together the different documentary data to quantify the fluctuations of the Lower Aare Glacier and the Lower Grindelwald Glacier, Switzerland, since their mid-19th century glacier maximum extent. Whereas many other studies of glacier change focus on a regional or even global scale, we are studying two exemplary glaciers in a relatively small area within the Swiss Alpine region. Besides the comparable climatic conditions and similar glacier characteristics (e.g. area) both glaciers show a particularly rich sample of documentary data. However, for reliable results a great labour-intensive effort is needed to calibrate this local documentation.

Finally, we also analyze the remarkable development of the representation techniques from drawings/paintings and topographic surveys to first scientific photographs within few centuries as a background to the beginning of modern glaciology.

## 2.2 The area investigated

Our study is focussed on the Lower Aare Glacier and the Lower Grindelwald Glacier, both located in the Bernese Alps, Switzerland, in close vicinity (Figures 2.1, 2.11).

The Lower Aare Glacier (46° 35' N, 8° 15' E) is a valley glacier, 13.5 km long and covering a surface of 24.1 km<sup>2</sup>. A prominent feature is the large ice-cored medial moraine and the extensive debris cover of typically 5–15 cm thickness (Table 2.3b; Bauder, 2001; Schuler et al., 2004).

The tongue of the Lower Aare Glacier is formed by the two main tributaries Lauteraar Glacier and Finsteraar Glacier. Mass balance measurements, conducted between 1996 and 1999, indicate that the present equilibrium line altitude (ELA) of Lower Aare Glacier is at 2850 meters asl. (Bauder 2001). The present glacier terminus, 1.5 kilometers from Lake Grimsel, is at an elevation of 1950 meters asl. The cumulative length fluctuations of the Lower Aare Glacier (Figure 2.2b) show a continuous retreat of the glacier since the first observations in the 1880s (VAW/SANW, 2002).

The Lower Grindelwald Glacier (46° 35' N, 8° 5' E) is also a valley glacier, 8.85 km long and covering a surface of 20.6 km<sup>2</sup> (Table 2.3a, Figure 4.11). Ischmeer in the east and the Bernese Fiescher Glacier in the west join to form the tongue of the Lower Grindelwald Glacier (Figure 2.1). The main contribution of ice nowadays originates from the Bernese Fiescher Glacier (Holzhauser and Zumbühl, 1996; Holzhauser and Zumbühl, 1999; Schmeits and Oerlemans, 1997).

The approximated ELA (AAR=0.67; Table 2.1), derived from digital elevation models (DEMs) and confirmed by the maximum elevation of lateral moraines (Gross et al., 1976; Maisch et al., 1999), is situated at 2640 meters asl. in relatively flat areas. As a consequence of this specific hypsography, the relatively little rise of the ELA of about +40 meters in the last 140 years affected a big increase of the ablation area and thus a large glacier retreat since the mid-19th century (Nesje and Dahl, 2000). Today, the Lower Grindelwald Glacier terminates at about 1297 meters asl. in a narrow gorge and reliable observations are difficult to obtain. The last-published quantitative observation was made in 1983 (VAW/SANW, 2002). Due to the extraordinary low position of the terminus and its easy accessibility the Lower Grindelwald Glacier is one of the best-documented glaciers in the Swiss Alps. Figure 2.2a shows the cumulative length fluctuations of the Lower Grindelwald Glacier, derived from documentary evidence, for the period 1535–1983 including the two well-known glacier maxima around 1600 and 1855/56 (Zumbühl, 1980; Holzhauser and Zumbühl, 1996; Holzhauser and Zumbühl, 2003).

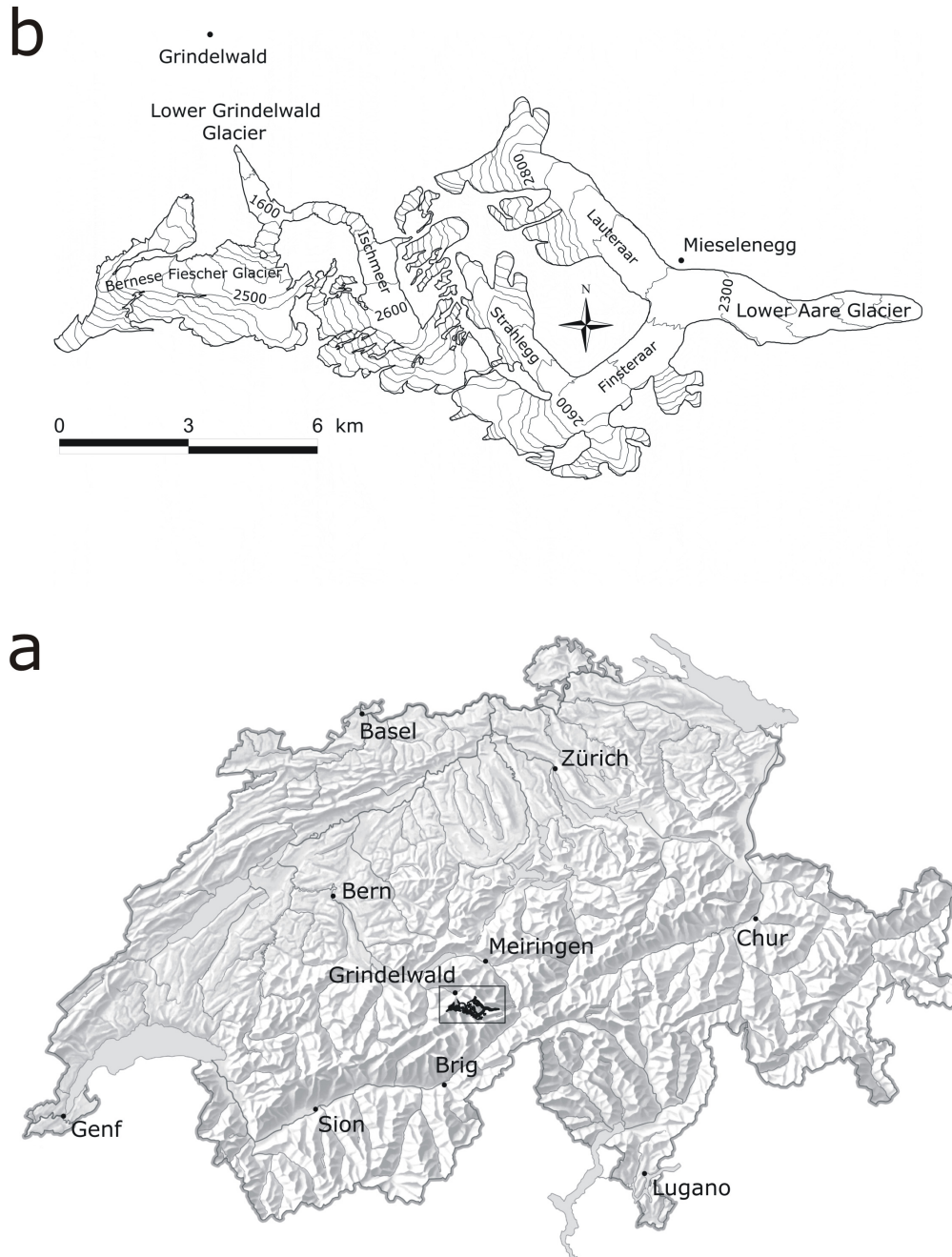


**Figure 2.1:** Maps showing (a) the Lower Aare and the Grindelwald region (area with solid outline) within Switzerland, (b) the outlines of the Lower Grindelwald and the Lower Aare Glacier with their main branches and tributaries.



**Figure 2.2:** Cumulative length variations of (a) the Lower Grindelwald Glacier from 1535 to 1983, relative to the 1600s maximum extent ( $=0$ ), and (b) the Lower Aare Glacier from 1719 to 2001, relative to 1871 ( $=0$ ). Maximal extensions of the Lower Grindelwald Glacier are represented by a thick line, minimal extensions by a dashed line. The Lower Aare Glacier is represented by a solid line (1830–2001 period), resp. a dashed line (1719–1829 period) which indicates an arguable, but likely curve progression.

Note that the geometry of both the Lower Aare Glacier and the Lower Grindelwald Glacier does not resemble that of ideal "model glaciers": They show a large variety of surface slopes and/or many basins that deliver ice to the main streams.

### 2.2.1 From first observations to detailed studies

The beginning of systematic observations on the Lower Aare Glacier is marked by the naturalist Franz Josef Hugi (1796–1855) who visited the Lower Aare Glacier from 1827 to 1831. He was the first to make observations on the surface-velocity of the glacier (Hugi, 1830). When his successor Louis Agassiz (1807–1873) visited the Lower Aare Glacier in 1839, he realized to his big surprise that the hut of Hugi on the medial moraine had moved away since 1827. This was the most important indication for Agassiz in confirming glacier movement (Agassiz, 1885; Portmann, 1975)

Agassiz also set off for the Lower Aare Glacier to prove his theory of ice ages. The idea that glaciers have been transporting erratic material was not new and was probably started by the mountain farmer Jean-Pierre Perraudin (1767–1858) who explained the hypothesis in 1815 to the geologist Jean de Charpentier (1786–1855) (Haeberli and Zumbühl, 2003). Charpentier argued that the Swiss glaciers of today had once been much more extensive. His ideas were taken up from Agassiz who went further and postulated the hypothesis, that the whole Northern Hemisphere from the North Pole to the Mediterranean Sea was once covered with a gigantic glacier. This "ice age hypothesis" was denied by quite a lot of people because this idea questioned the Bible-based Christian world

	<b>1860/61/72</b>	<b>2004</b>
Length (measured along the longest flowline 1; see Figure 2.10)	10.8 km	8.85 km
Elevation of head (Mönch)	4107 m asl.	4107 m asl.
Elevation of terminus	972 m asl.	1297 m asl.
Surface area (incl. all subglaciers which have been connected with the main streams in 1860/61/72)	26.1 km <sup>2</sup>	20.6 km <sup>2</sup>
Estimation of glacier-snowline ELA (Accumulation Area Ratio AAR=0.67)	2600 m asl.	2640 m asl.
Average slope in %	29.0 %	31.8 %
Average slope in degrees	16.2°	17.6°
Exposure	N-NW	N-NW
Absolute ice volume change 1860/61/72–2004	–1.56 km <sup>3</sup>	
Average thickness change 1860/61/72–2004 in meters per year	–0.42 m	

**Table 2.1:** *Topographical characteristics of the Lower Grindelwald Glacier in 1860/61/72 and 2004. The calculations are based on the DEMs 1861 and 2004 (Table 2.2a). For the techniques used see section 2.2.4.*

view of that time where no huge glaciers are mentioned. In addition to this, comparable glaciers or ice sheets had not yet been discovered (Bolles, 1999).

However, from 1840 to 1845, Agassiz conducted a research program on the Lower Aare Glacier, Switzerland, which proved to be the beginning of modern experimental glaciology. In his interdisciplinary team Agassiz initially acted as the leader and program manager who was also responsible for climatic data. His secretary and personal friend at that time, the naturalist Jean Édouard Desor (1811–1882), did glaciological and geomorphological investigations. The results of the numerous observations were summarized in Agassiz (1847) in comprehensive documentation. Notice that Desor later broke with Agassiz. The clash between Desor and Agassiz has actually been triggered by personal motives, based on their long and intense friendship, as well as by scientific, religious and political reasons (Kaeser, 2004).

Besides these extensive glaciological studies, the accompanying artists and engineers produced the first outstanding representations of the Lower Aare Glacier, such as the panorama of Jacques Bourkhardt (1811–1867) and the glacier maps of Johannes Wild (1814–1894) and Johann Rudolf Stengel (1824–1857) (see Sections 2.2.2 and 2.2.4; Zumbühl and Holzhauser, 1988).

## 2.2.2 Panorama of Jacques Bourkhardt (1842)

We recently discovered the original drawing of Jacques Bourkhardt's (1811–1867) large size lithography "Panorama de la mer de glace du Lauteraar et du Finsteraar – Hôtel des Neuchâtelois", which had been missing for a long time (Figure 2.3a). This drawing is probably the most beautiful and in topographical terms the richest panorama ever done of the Lower Aare Glacier. Different mountain

peaks were named for the first time. Bourkhardt chose the Mieselenegg (see Figure 2.1b for the location) as the position from which to draw.

The partial panorama includes the main mountain peaks in the background, the confluence area of the Finsteraar and the Lauteraar, and the artist is sitting drawing on the right hand side under an umbrella. Desor (1847) praised the panorama of Bourkhardt, but he also mentioned the time-consuming drawing process. The importance of the panorama of Bourkhardt may also be confirmed by the double portrayal (Figure 2.4) of the two friends Agassiz and Desor by Fritz Berthoud (1812–1890). The panorama was of course used as the dominant background, as a reminder of the great scientific work done by the two naturalists.

On the medial moraine, below the confluence area, Bourkhardt shows the "Hôtel des Neuchâtelois", a huge metamorphic boulder, which served Agassiz and his team as accommodation and especially as a shelter during the summer campaigns (Figure 2.14; Zumbühl and Holzhauser, 1988). We also see on the panorama, for the first time ever, a newly built tent, 20 meters long and 5 meters high. The wooden frame with a wooden floor was constructed by the guides and used as sleeping-, drawing- and study room and even had a little bookshelf.

### 2.2.3 First photographs of glaciers

Besides portraiture, early photographers also paid special attention to architecture, travel views and landscapes. One possible reason, besides publicity, why the scientific and public interest focussed specifically on glacier photographs lies probably in the dramatic Greenland expedition of the arctic explorer Elisha Kent Kane (1820–1857) from 1853 to 1855. During the voyage to search for survivors of an other expedition, Kane's ship became icebound, so instead his objective changed to one of survival. After two years of hardship and a difficult journey over ice and open water to Greenland, they were finally rescued (Kane, 1856). Kane's widespread reports about an "ice-ocean of boundless dimensions" or "Land-ice" confirmed the existence of huge ice masses and brought the final breakthrough of the ice age theory after 40 years of discussions and opposition. This prompted the curiosity and attracted more and more tourists to visit locations where they could admire even "little" glaciers, such in the Swiss Alps.

Probably the oldest photos of Swiss glaciers were made in summer 1849 and 1850 by Jean-Gustave Dardel (1824–1899) and Camille Bernabé (1808–?) (Morand and Kempf, 1989; Lagoltièrre, 1989). In September 1855, Auguste-Rosalie Bisson, took a panoramatic photo of the Lower Aare Glacier (Figure 2.15a) with the remarkable size of 1.85 meters which was praised as "a gigantic ensemble with a wonderful effect" (Chlumsky et al., 1999). The Bisson Brothers, Auguste-Rosalie (1826–1900) and Louis-Auguste (1814–1876), were among the best-known European photographers of the 1850s and 1860s. Their most famous body of work is comprised of the high-altitude photographs they made in the Alps, such as the first photographs of the peak of Mont Blanc. Thus, photography opened up new regions which were not usually possible with previous representation techniques (Guichon, 1984). It is probable that the photo of Lower Aare Glacier was also shown at the "Exposition Universelle" 1855 in Paris. Because the mega size photos of the Bisson Brothers were among the attractions, the Lower Aare Glacier could have become also a "megastar" of the "Exposition Universelle". However, the work of the Bisson Brothers was praised and awarded the "Médaille de 1re classe" (Bonaparte, 1856; Chlumsky et al., 1999).

Figure 2.5 shows the Bisson photo "Glacier inférieur du Grindelwald (Oberland bernois)" which is most probably the first photograph of the Lower Grindelwald Glacier. The black ink stamp "Bisson frères" at the edge of the photo, the snow-free glacier front and an advertisement of the Bisson Brothers in the journal "L'Artiste" (14 December 1856) show that the photo was taken in



**Figure 2.3:** (a) Original drawing (24.4 × 126 cm; pencil, pen, ink, watercolor, gouache) for the lithography "Panorama de la mer de glace du Lauteraar et du Finsteraar – Hôtel des Neuchâtelois" of Jacques Bourkhardt (1811–1867) from the Mieselenegg (Figure 2.1b; Swiss national coordinates: approx. 657'500/158'700; altitude: approx. 2620 m asl.) of the year 1842 (cut-out). Private collection. Photograph by Heinz J. Zumbühl.  
 (b) Recent panorama of the Lower Aare Glacier, taken east from Mieselenegg (Swiss national coordinates: approx. 657'600/158'600; altitude: approx. 2520 m asl.). Photograph by Daniel Steiner, Heinz J. Zumbühl, 22.8.2004.



**Figure 2.4:** Double portrayal (Oil painting) of the two friends Louis Agassiz (sitting) and Jean Édouard Desor (standing) by Fritz Berthoud (1812–1890) with Jacques Bourkhardt's panorama in the background. Musée d'art et d'histoire Neuchâtel (Inv.-Nr. 762). Photograph by Heinz J. Zumbühl.

summer/autumn 1855/56. It shows the Lower Grindelwald Glacier exactly at its mid-19th century maximum extent.

After Queen Victoria took a fancy to the stereoscope at the Crystal Palace Exhibition in 1851, stereo viewing, a special application of photography, became all the rage (Gernsheim, 1983). The stereoscope slides that were produced allowed people to sit in their own home and tour the world in an easy, but spectacular way. Furthermore, because of the small size they were not too expensive. The most popular slides were travelogue type slides that showed the world from the countrysides of Europe to the pyramids and tombs of ancient Egypt (Schönfeld, 2001). However, both travelogue slides and books (cf. Kane's expedition reports to Greenland) have produced an increasing interest in natural phenomena that had so far been unreachable. Thus, historical sources of glaciers also provide cultural information on the interest and the social attitude to glaciers and about how glaciers have been perceived over time. The perception of glaciers therefore ranges from paralysing fear and romantic transfiguration (until the 18th century, but also up to the present day) to a broad scientific interest and non-scientific curiosity at a safe distance (from the 19th century). In a similar way, representations of glacier retreat today could be interpreted as a social danger signal in a changing climate.

The earliest stereo views from the Lower Grindelwald Glacier were taken by Adolphe Braun (1812–1877) in summer/autumn 1858 (Figure 2.6a). A list of Swiss stereo views by Braun, published in the journal "La Lumière" (21 May 1859), and including Figure 2.6a, shows that Braun began to



**Figure 2.5:** *The Lower Grindelwald Glacier in summer or autumn 1855/56 in the valley floor, exactly at its mid-19th century maximum extent. Photograph "Glacier inférieur du Grindelwald (Oberland bernois)" by the Bisson Brothers. Alpine Club Library, London. Photograph by Heinz J. Zumbühl.*

commercialize his series of Swiss views, depicting the most chic tourist destinations in Switzerland, a year earlier than had been assumed until now (Kempf, 1994; personal communication with Christian Kempf, 19.12.2003). Figure 2.6 is a wonderful example of the impressive changes which can be observed in the forefield of the Lower Grindelwald Glacier since the mid-19th century.

Braun's stereo views were taken two years after the mid-19th century maximum extent of the Lower Grindelwald Glacier in 1855/56. Due to incomplete stereographic effects in the background of the photographs, the stereo views could not unfortunately be interpreted by modern digital photogrammetric methods. Nevertheless, a qualitative comparison of the stereo views with the Bisson photo of 1855/56 shows no significant differences in the extension of the Lower Grindelwald Glacier. In fact, Zumbühl (1980) compute a change in length of less than -10 meters for the period 1855/56-1858.

In contrast to this, the following 2-3 years brought a slightly accelerated tendency to retreat. This can be seen in a projection of the 1855/56 moraine ridges, extracted from an ortho photo map (scale: 1:2000) of the year 1974 (Zumbühl, 1980), onto the original plane-table sheet "Grindelwald 1860/61" (Figure 2.7). According to this, the glacier had withdrawn 30-60 meters from the outer 1855/56 moraines. Furthermore, the arrangement of the moraine ridges and the glacier extent of 1870, extracted from the Siegfried map of the year 1870 ("Grindelwald 1870"), suggest that the glacier had been retreating in a rapid and asymmetric pattern since 1860/61.



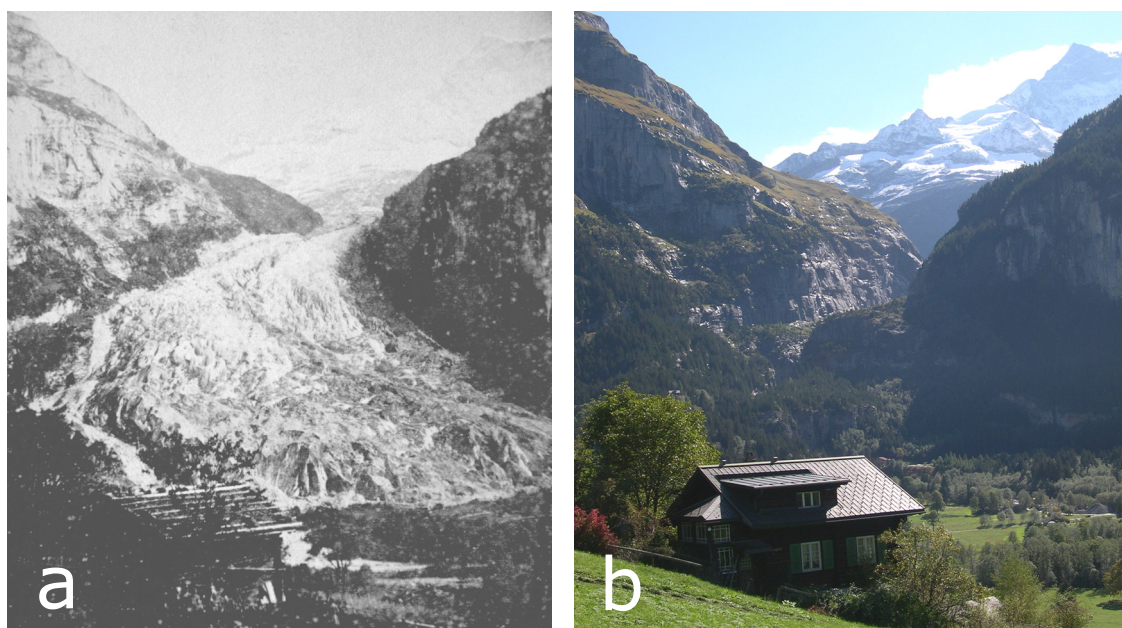


**Figure 2.6:** (a) *The Lower Grindelwald Glacier 1858 in the valley floor, 2–3 years after the maximum extent in 1855/56. Stereograph (left) by Adolphe Braun (1812–1877) at Dornach ("Suisse/No. 511"). Private Collection of Jaroslav F. Jebavy, Geneva. Photograph by Heinz J. Zumbühl.*

(b) *Recent view to the glacier gorge and the Fiescherhorn/Pfaffestecki from upper Stotzhallen (Swiss national coordinates: approx. 645'900/163'700; altitude: approx. 1030 m asl.). Photograph by Daniel Steiner, 25.9.2003.*

## 2.2.4 (First) topographic maps and digital elevation models (DEMs)

The Lower Aare Glacier was the subject of the first topographic map of a glacier with scientific value, generated by Wild in 1842. The lithography (scale: 1:10000), published by Agassiz (1847), shows the tongue of the Lower Aare Glacier which was more than eight kilometers long, east of the confluence area, and designed by a system of hachures (Figure 2.12). On the map, the Lower Aare Glacier ended in a steep, impressive, partially ice covered ice front, approx. 2.1 km in front of the present glacier terminus (Zumbühl and Holzhauser, 1988; VAW/SANW, 2002; Haeberli and Zumbühl, 2003). Due to the missing contour lines, no reliable interpretation in terms of glacier volume changes can be deduced.

The glacier map "Carte Orographique du Glacier de l'Aar Montrant les détails de la Stratification et l'origine des glaciers de second ordre", surveyed by Stengel in 1846 and also published by Agassiz (1847), shows the same glacier extent as on the Wild map, but for the first time we find contour lines of the glacier surface (Figure 2.13).

The leading role of Swiss cartography is mainly based on the first modern official map series of Switzerland carried out between 1832 and 1864 under the supervision of General Guillaume–Henri Dufour (1787–1875). The map in 25 sheets (scale: 1:100000) was published between 1842 and 1865, and is an admirable specimen of cartography. After the "Dufour map" had been published, the desire for a map in 1:25000 or 1:50000 scale became known. Some areas surveyed by regional topographic surveys were no longer satisfactory and had to be completely resurveyed. In contrast, most surveys carried out by the Federal topographic survey met the requirements after a few minor revisions. These efforts resulted in the first official map series of a high resolution and continuous

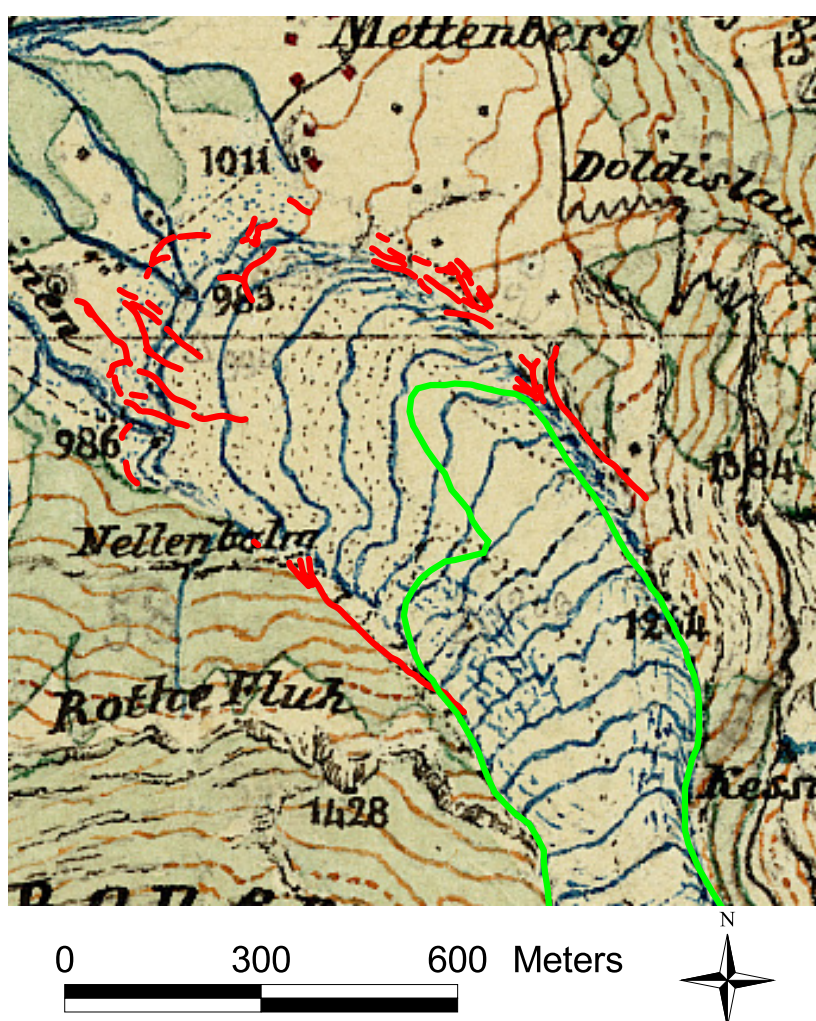


**Figure 2.7:** Forefield of the Lower Grindelwald Glacier, extracted from the original plane-table sheet "Grindelwald 1860/61" with a projection of the 1855/56 moraine ridges (Zumbühl, 1980). Given are also the glacier extent in 1860/61 from "Grindelwald 1860/61" (blue contour lines) and 1870 from "Grindelwald 1870" (green outline).

scale, known as the "Siegfried map" and published from 1870 onwards (Oberli, 1968).

The entire glaciated area of the Lower Aare Glacier spreads over four, and the glaciated area of the Lower Grindelwald Glacier spreads over two individual map sheets.

Two plane-table sheets of the Dufour map and two first editions of the Siegfried map, covering the Lower Grindelwald Glacier, were available in the mid-19th century. The date of survey or revision of the maps was partly determined by intensive archive studies. As mentioned before, the Siegfried maps were often based on a revision of the Dufour surveys (Zölly, 1944). This is also valid for the Siegfried edition "Jungfrau 1872" (Table 2.2a; BAR E 27 20040) which was used for the accumulation area of the glacier instead of Stengel's original plane-table sheet from 1851 due to its inaccurate glacier texture.

Both the original plane-table sheet "Grindelwald 1860/61" of Wilhelm August Gottlieb Jacky (1833–1915) and the Siegfried map "Jungfrau 1872" have been geo-referenced based on the recent Swiss

a					
<b>DEM name</b>	DEM1861	DEM1926	DEM1993	DEM2000	DEM2004
<b>Data basis</b>	Plane-table sheet, topographic map	Topographic maps	Digital photogrammetrical analysis	Digital photogrammetrical analysis	Digital photogrammetrical analysis
<b>Name</b>	Grindelwald, Jungfrau	Interlaken, Jungfrau	DHM25 (Level2)		
<b>Survey/revision</b>	Terrestrial survey	Terrestrial photographs	Aerial photographs	Aerial photographs	Aerial photographs
<b>Date</b>	1860/61, 1872	1926/1934	1993	1999/2000	2004
<b>Scale</b>	1:50000	1:50000			
<b>Equidistance</b>	30 meters	20 meters			
b					
<b>DEM name</b>	DEM1880	DEM1927	DEM1947	DEM1961	DEM1997
<b>Data basis</b>	Plane-table sheet	Photogrammetrical contour analysis	Photogrammetrical contour analysis	Cadastral map	Digital photogrammetrical analysis
<b>Survey/revision</b>	Terrestrial survey	Terrestrial photographs	Aerial photographs	Aerial photographs	Aerial photographs
<b>Date</b>	1879/80, 1872	1927	1947	1961	1997
<b>Scale</b>	1:50000	1:25000	1:25000	1:10000	
<b>Equidistance</b>	30 meters	20 meters	20 meters	10 meters	

**Table 2.2:** The DEMs used and their sources: (a) Lower Grindelwald Glacier, (b) Lower Aare Glacier

geodetic datum "CH1903". Figure 2.8 shows the composition of the two topographic maps used. The precise transitions between the two maps are remarkable. Even though the old topographic maps are originally based on an older geodetic reference system (ellipsoid of Schmidt 1828, equivalent conical projection), they have not been transformed to the present reference system. The shifts in  $xy$ -direction between the two different reference systems amounts to  $<0.5$  meters and are therefore negligible for our studies (Bolliger, 1967; personal communication with Urs Marti, swisstopo, 5.6.2002). Because the origin of elevation measurements has changed from 376.2 m asl. (Dufour map), 376.86 m asl. (Siegfried map) to 373.6 m asl. (Swiss geodetic datum "CH1903") the  $z$ -coordinates of historical data have been corrected by  $-3$  meters to obtain a comparable data basis.

A comparison of a recent pixel map (PK50@swisstopo) and the geo-referenced maps shows an accuracy which lies within the expected range (15 meters in  $xy$ -direction, 1 meter in  $z$ -direction; personal communication with Urs Marti, swisstopo, 25.11.2002, 16.8.2004). This result may be explained by the extraordinary work of many topographers at this time. The sheet of Jacky, as an

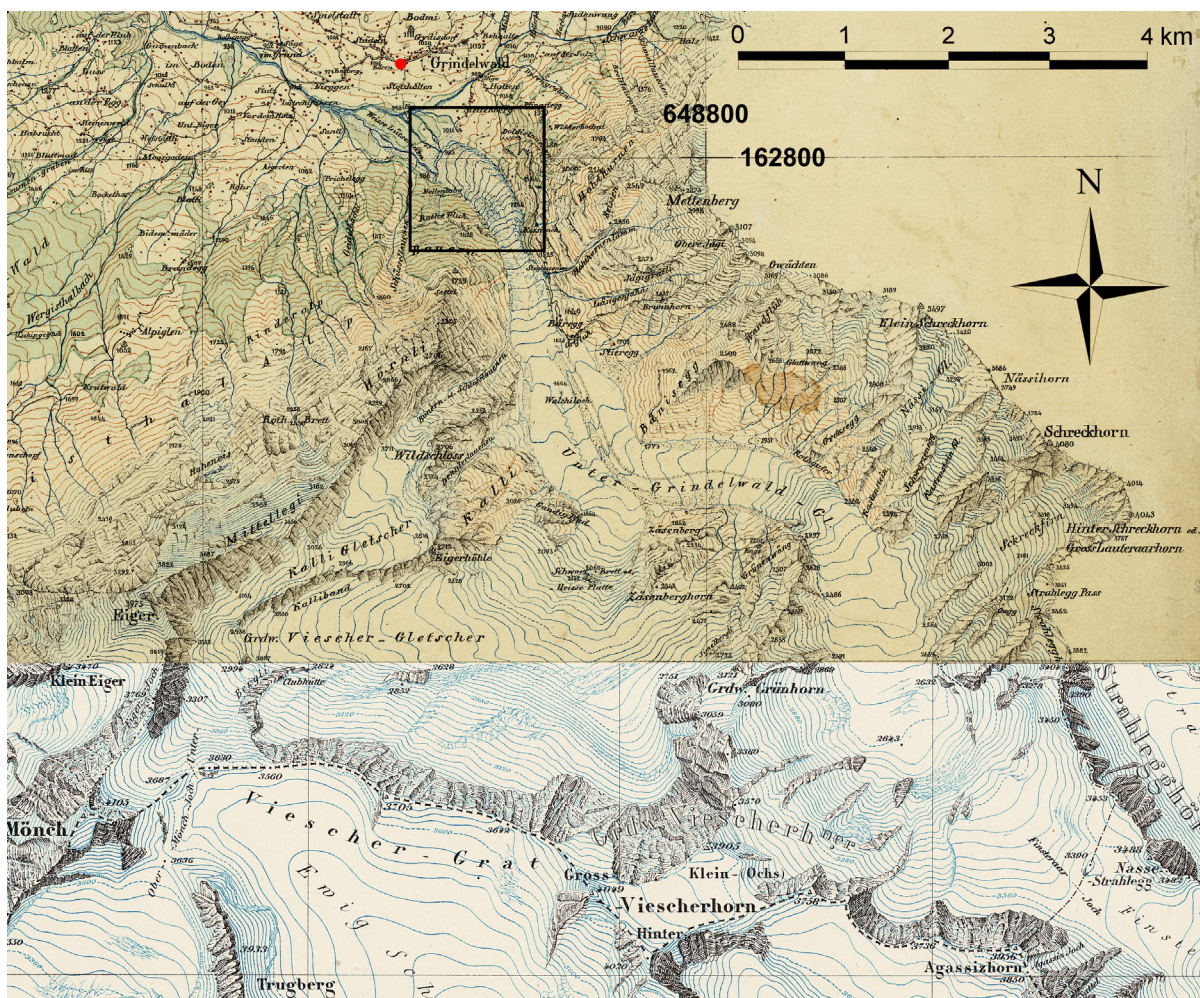


**Figure 2.8:** Map composition of the Lower Grindelwald Glacier. Upper part: "Grindelwald 1860/61". Lower part: "Jungfrau 1872" (see Table 2.2a for details). The area with a solid outline represents the forefield region shown in Figure 2.7. Given are also the approximate photographer's locations of Figures 2.6 (red point).

example, has been judged as blameless and exemplary by the responsible cartographic commission in 1862 (Locher, 1954).

The DEM1861 (Table 2.2a) has been generated by digitalizing contour lines and reference points from the map composition, given in Figure 2.8 (Hoinkes, 1970; Funk et al., 1997; Wipf, 1999; Bauder, 2001). Note that the quality of these early maps makes the development of modern DEMs from these data possible, probably better than elsewhere in the world. These in turn probably allow the most precise calculations possible of surface and volumetric glacier loss in the Alps.

Using the first and completely revised edition of the official Swiss maps (scale: 1:50000), based on terrestrial stereo-photogrammetry in 1926 and additional field surveys in 1934, a DEM1926 of the Lower Grindelwald Glacier was determined (BAR E 27 20042).

Additional DEMs of the current state of the glaciers have been extracted from a recent set of aerial photographs, applying digital stereo-photogrammetry (Kääb and Funk, 1999; Kääb, 2001). Digital color aerial photos of the Lower Grindelwald Glacier were produced in the years 1999 (accumulation area), 2000 (ablation area) and 2004 (©swisstopo). The photogrammetric interpretation and

automatic generation of the DEM was performed by standard photogrammetric software. In order to refine the modelled deglaciated glacier forefield, the contour lines of the ortho photo map of the year 1974 mentioned before, have also been digitalized and merged to the DEMs 2000 and 2004. The automatic procedures for DEM generation is limited in areas with low texture, such as flat snowfields. In a time-consuming procedure points were checked manually and deleted or corrected. The resulting high-resolution DEMs 2000 and 2004 show an average grid width of ~10 meters. Finally, the DHM25 (Level 2) of the Federal Office of Topography (DHM25@swisstopo) has been interpreted as the status of the Lower Grindelwald Glacier in 1993 (Swisstopo, 2004).

For the Lower Aare Glacier five plane-table sheets of the Dufour map and four first editions of the Siegfried map do exist. The quality of the maps covering the firn areas turned out to be insufficient. Therefore, we restrict our study on the ablation area below the confluence of Lauteraar and Finsteraar where the major changes are expected (Table 2.2b). Four additional DEMs exist for the Lower Aare Glacier, dating from 1927, 1947, 1961 and 1997, respectively (Bauder, 2001). They are based on digitalized contours of two original, analytical photogrammetrical analysis, a map of a regional cadastral survey and a recent digital photogrammetrical analysis as presented before (Table 2.2b). All data set have been interpolated on a equally spaced grid of typical 25 m grid spacing (Bauder, 2001).

## 2.2.5 Results

Based on these DEMs, calculation of glacier volume, area and length and their changes are possible (Wipf, 1999; Maisch et al., 1999). The spatial distribution of volume and thickness changes have been calculated for both the Lower Grindelwald Glacier and the Lower Aare Glacier. They are based on the area of larger extension, which includes areas of complete retreat and new advance.

The results are summarized in Table 2.3. After the well-documented maximum extents of the Lower Grindelwald Glacier in 1855/56 and the Lower Aare Glacier in 1871 (Zumbühl and Holzhauser, 1988), we find a relatively high rate of thickness change of  $-0.55$  meters per year for the Lower Grindelwald Glacier and a lower rate of  $-0.24$  meters per year for the Lower Aare Glacier until the late 1920s. From then a lower rate of thickness change is evaluated for the Lower Grindelwald Glacier while the mass loss of the Lower Aare Glacier is increasing.

A rapid volume loss of  $-0.90$  meters per year in the 1990s can be calculated for the Lower Grindelwald Glacier. It is striking that this mass loss occurred almost without any substantial change in glacier length (Table 2.3a). This is probably due to the fact that the glacier terminus is recently in a narrow gorge. This down-wasting of the glacier surface in the front basin of the glacier (Figures 2.9, 2.17) that is also known from other glaciers (Paul et al., 2004) primarily effected a decrease of glacier width/area and not of length. The cumulative mass balance of three Swiss Alpine glaciers (Gries, Basòdino, Silvretta) observed, amounts to approx.  $-2$  meters for the period 1993–2000 and  $-2.6$  meters for the period 2001–04 which includes the European heatwave of 2003 (VAW/SANW, 2002, unpublished data from Andreas Bauder, VAW). Therefore, the decrease of the Lower Grindelwald Glacier of  $-6.3$  meters for the period 1993–2000 was above average, the thickness change of  $-2.8$  meters for the period 2001–04 was comparable to the mass balance of other Alpine glaciers.

The overall mass loss of  $-1.56$  km<sup>3</sup> ice ( $-1.4$  km<sup>3</sup> water; assumed ice density:  $0.9$  kg·m<sup>-3</sup>) for the Lower Grindelwald Glacier, resp.  $-1.59$  km<sup>3</sup> ice ( $-1.43$  km<sup>3</sup> water) for the Lower Aare Glacier since their last maximum extents is comparable to one and a half times of the annual water consumption ( $1.06$  km<sup>3</sup>) of Switzerland in 2000 (SVGW, 2002).

Finally, the developing of average thickness changes is similar to other investigations on Alpine

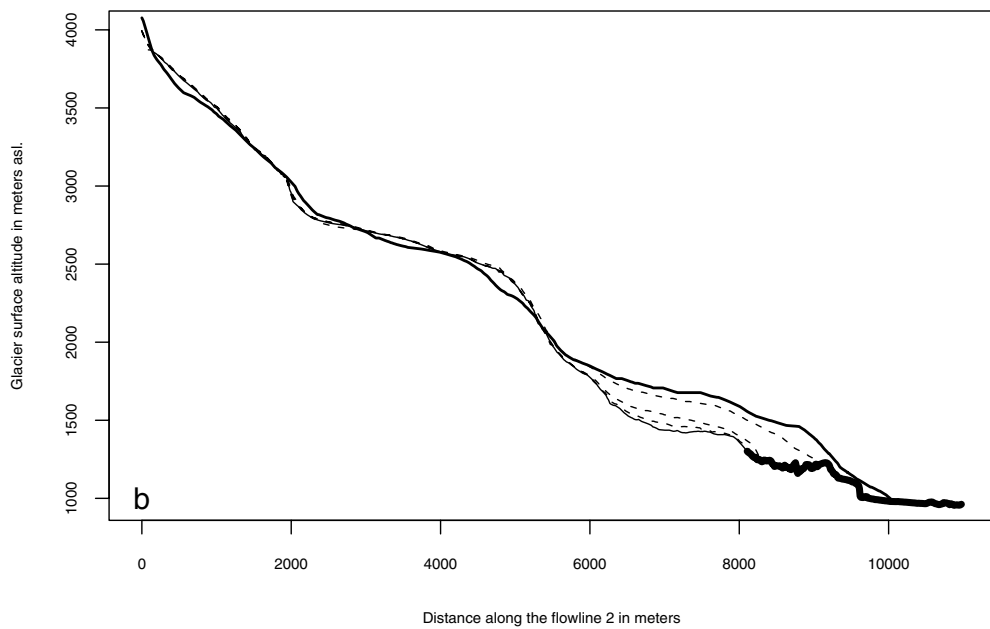
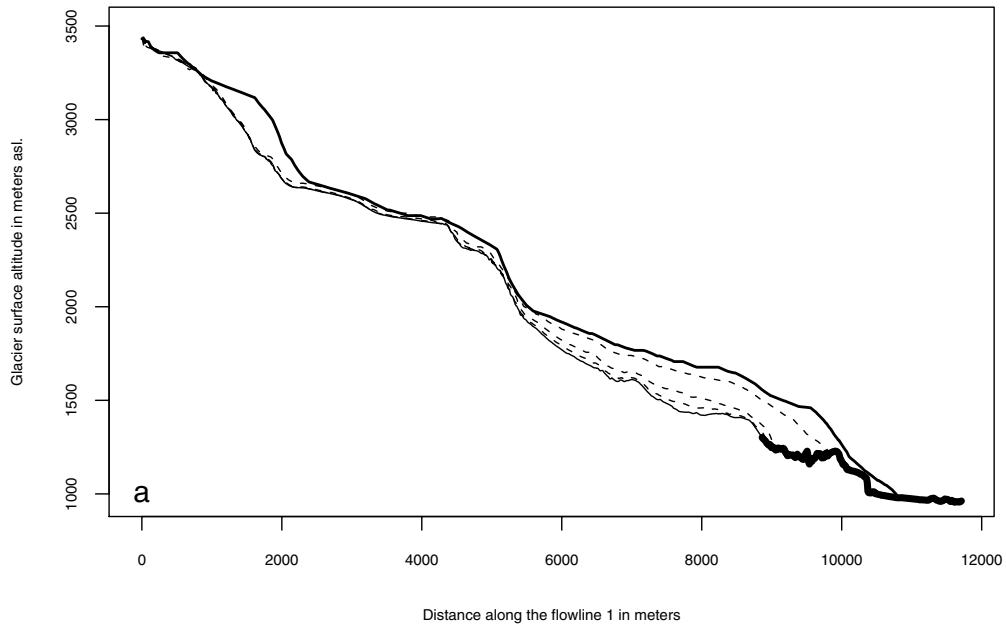


**Figure 2.9:** Surface profiles along (a) flowline 1 and (b) flowline 2 (see Figure 2.10) of the Lower Grindelwald Glacier for 1860/61 (thick line), 1926 (dashed line), 1993 (dashed line), 1999/2000 (dashed line) and 2004 (solid line), derived from DEMs. The thick line at down-glacier distances indicates the recent visible glacier forefield with the two pronounced and well-known "Schopffelsen".

a					
Year	1860/61/72	1926	1993	2000	2004
Area in km <sup>2</sup>	26.1	24.3	22.3	21.4	20.6
Length in km	10.8	9.8	9.0	8.9	8.85
Period	1860/61/72–2004	1860/61/72–1926	1926–1993	1993–1999/2000	1999/2000–2004
Absolute volume change in km <sup>3</sup>	–1.56	–0.94	–0.42	–0.14	–0.06
Absolute thickness change in meters	–59.8	–36.0	–17.3	–6.3	–2.8
Average thickness change in meters per year	–0.42	–0.55	–0.26	–0.90	–0.70
b					
Year	1880	1927	1947	1961	1997
Area in km <sup>2</sup>	28.4	27.5	27.4	25.5	24.1
Period	1880–1997	1880–1927	1927–1947	1947–1961	1961–1997
Absolute volume change in km <sup>3</sup>	–1.59	–0.32	–0.42	–0.34	–0.51
Absolute thickness change in meters	–56.0	–11.3	–15.3	–12.4	–20.0
Average thickness change in meters per year	–0.48	–0.24	–0.76	–0.89	–0.56

**Table 2.3:** Changes in glacier parameters of (a) the Lower Grindelwald Glacier and (b) the Lower Aare Glacier, based on DEMs at different time.

glaciers, such as Aletsch, Rhône and Trift. Generally, an increased mass loss since the 1980s has been observed. Rates and timing depend on available DEMs.

Figure 2.10 shows the spatial distribution of the thickness change for Lower Grindelwald Glacier between DEM1861 and DEM2004. The average overall thickness change for this period amounts to –0.42 meters per year. The average standard error of the thickness changes for the same period is 0.51 meters per year. In general, the widespread decrease (blue areas) of glacier thickness expected since 1860 can be determined from Figure 2.10. Absolute negative thickness changes up to –330 meters can be seen in the ablation area, the upper Ischmeer part and in the south of the Bernese Fiescher Glacier. These big differences in areas of accumulation do not correspond to the

typical thickness change distribution patterns in which we would expect smaller changes in the accumulation zone (Figure 2.16; Bauder, 2001).

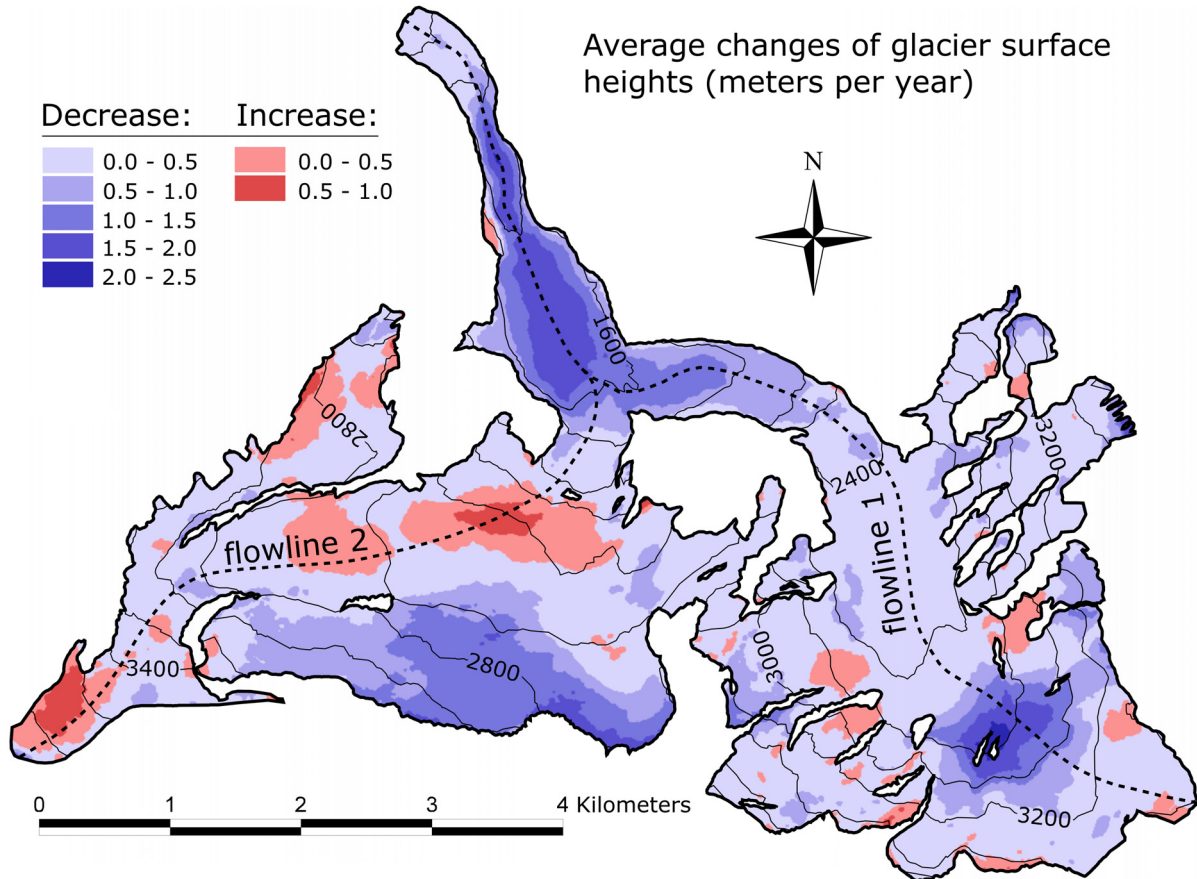


**Figure 2.10:** Average changes of surface heights (meters per year) between 1860/61/72 and 2004 (difference model DEM1861–DEM2004). The glacier outlines of 1860/61/72 and the contour lines of 2004 are also given.

Nevertheless, there are some regions where a totally unexpected increase (red areas) of glacier surface height is stated. In some cases, such as the upper part of the Bernese Fiescher Glacier or different small areas of increase, we can assume a lower quality of both the DEM1861 and the DEM2004 due to low snow/ice surface contrasts and/or complex terrain. This can also be seen in a sparse point density of DEM1861 and DEM2004 in such areas.

This argument does not apply to the lower part of the Bernese Fiescher Glacier which has shown a big area of surface height increase of up to +100 meters since the mid-19th century maximum extent (see also Figure 2.9b for the surface profile along the flowline 2). What is the reason behind this area of increase? Is it a mistake? According to the newly discovered field book, the topographer of the plane table sheet, Jacky, one of the best topographer of that time, surveyed the Grindelwald region in July 1861. For this purpose, he worked very close to the area of increase which also represents a relatively flat region easy to survey. Jacky has measured a large number of trigonometric points with full spatial information on the Lower Grindelwald Glacier or close by, including a profile crossing exactly the assumed area of increase (Jacky, 1861). So, Jacky has measured these points in situ to use them for drawing the contour lines (personal communication with Martin Gurtner, swisstopo,



28.8.2003). Big systematic mistakes in Jacky's survey are therefore very doubtful.

However, it is also possible that the area of increase could be dynamically linked with the decrease of surface heights in the south part of the Bernese Fiescher Glacier. Because we have no intensive dynamical investigations for the Lower Grindelwald Glacier, this statement cannot be followed up.

## 2.3 Summary and conclusions

First systematic investigations on the Lower Aare Glacier are in place for modern glacier research to make a start and represent an important proof of the ice age theory. Louis Agassiz acted as a moving power behind both the first systematic and scientific glaciological studies and exceptional glacier representations in the form of drawings and topographic maps.

A few years later, first (glacier) photographs were showing a new possibility of making a glacier photograph in a relatively easy way. Thus, the photographic technique marks a new era of scientific representations (of glaciers) because even inaccessible areas could now be recorded quickly and easily. This change of scientific representation techniques from drawings/paintings and maps to photographs only within 15 years can be studied against the background of beginning modern glaciology.

During the same period an increased glaciation in widely spread regions all over the world can be detected. This last glacier maximum extent is well-documented for few glaciers, e.g. for the Lower Grindelwald and the Lower Aare Glacier, Switzerland. Thus, we are able to do a unique case study of the evolution of work on two of the best studied glaciers in Europe and to demonstrate its evolution from the very beginnings of glaciology, modern cartography and photography to the exploitation of the latest cartographic techniques. We also noted that the quality of documentary evidence from these two glaciers is a benchmark against which other glaciers and studies should be measured.

The maximum extents of the Lower Grindelwald and the Lower Aare Glacier around the mid-19th century and their subsequent retreat were also studied by an approach including a critical discussion of documentary data combined with the application of recent technical possibilities in photogrammetry. New photographic material and the evaluation of old topographic maps confirm that the retreat of Lower Grindelwald Glacier was relatively slow in a first period after the mid-19th century maximum extent and then accelerated dramatically in the following period 1861–1870. The results of DEM comparisons show reliable rates of thickness changes of  $-0.42$  meters per year for the Lower Grindelwald Glacier and  $-0.48$  meters per year for the Lower Aare Glacier since their mid-19th century maximum extent.

Finally, the Lower Grindelwald Glacier's spatial distribution of thickness changes shows some surprising patterns. Either, the basic data material is much more inaccurate than assumed so far or the Lower Grindelwald Glacier demonstrates an interesting dynamical behavior that affected only parts of the area. Because a mass shift could have taken place within less than a decade additional information between the two DEMs 1860 and 1926 is needed in order to investigate this question further.

## Acknowledgements

This work has been supported by the Swiss National Science Foundation (SNSF) through its National Center of Competence in Research on Climate (NCCR Climate), project PALVAREX.

We are grateful to Hermann Bösch (VAW, ETH Zürich) for his never-ending help in photogrammetric problems, Pierre Gerber, Urs Marti, Martin Gurtner and Martin Rickenbacher (swisstopo) for their competent help concerning problems in historical cartography.

Thanks also to the Federal Office of Topography (swisstopo) for providing their topographical material, to Heinz Wanner and the Scientific Editors, Ben Orlove, Ellen Wiegandt and Brian Luckman, for their fruitful suggestions on various aspects of this paper.

## Bibliography

- BAR (Bundesarchiv) E 27 20040. Geschäftsberichte des Eidgenössischen Stabsbureaus, 1872.
- BAR (Bundesarchiv) E 27 20042. Geschäftsberichte der Eidgenössischen Landestopographie, 1926 (Band 2); 1934 (Band 3).
- Agassiz, E. C. (1885). *Louis Agassiz. His Life and Correspondence*. Houghton, Mifflin and Co., Boston, 2 Vols.
- Agassiz, L. (1847). *Système glaciaire ou recherche sur les glaciers, leur mécanisme, leur ancienne extension et le rôle qu'ils ont joué dans l'histoire de la terre. Première partie: Nouvelles études et expériences sur les glaciers actuels: leur structure, leur progression et leur action physique sur le sol*. V. Masson, Paris, L. Voss, Leipzig, 2 Vols.
- Bauder, A. (2001). *Bestimmung der Massenbilanz von Gletschern mit Fernerkundungsmethoden und Fließmodellierungen. Eine Sensitivitätsstudie auf dem Unteraargletscher*. Versuchsanstalt für Wasserbau, Hydrologie und Glaziologie (VAW) der Eidgenössischen Technischen Hochschule Zürich (ETHZ), Mitteilungen No. 169.
- Bolles, E. B. (1999). *The Ice Finders: How a Poet, a Professor, and a Politician Discovered the Ice Age*. Counterpoint Press, Washington DC, USA.
- Bolliger, J. (1967). *Die Projektionen der Schweizer Plan- und Kartenwerke*. Druckerei Winterthur, Winterthur.
- Bonaparte, Napoléon-Joseph-Charles-Paul, P. (1856). *Exposition Universelle de 1855. Rapports du jury mixte international*. Imprimerie impériale, Paris.
- Chlumsky, M., U. Eskildsen, and B. Marbot (1999). *Die Brüder Bisson. Aufstieg und Fall eines Fotografenunternehmens im 19. Jahrhundert. Katalog zur gleichnamigen Ausstellung: Museum Folkwang, Essen, 07.02.–28.03.1999; Fotomuseum im Münchner Stadtmuseum, 11.04.–30.05.1999; Bibliothèque nationale de France, Paris, 15.06.–15.08.1999*. Verlag der Kunst, Amsterdam, The Netherlands.
- Desor, J. E. (1847). *Agassiz' und seiner Freunde geologische Alpenreisen in der Schweiz, Savoyen und Piemont. Unter Agassiz', Studer's und Carl Vogt's Mitwirkung verfasst von J. E. Desor. Herausgegeben von Dr. Carl Vogt*. Zweite, stark vermehrte Auflage. Literarische Anstalt, Frankfurt am Main.
- Funk, M., R. Morelli, and W. Stahel (1997). Mass balance of Griesgletscher 1961–1994: Different methods of determination. *Zeitschrift für Gletscherkunde und Glazialgeologie* 33(1), 41–56.
- Gernsheim, H. (1983). *Geschichte der Photographie. Die ersten 100 Jahre*. Propyläen Verlag, Frankfurt am Main.

- Graf, J. H. (1896). *Die Schweizerische Landesvermessung 1832–1864. Geschichte der Dufourkarte*. Buchdruckerei Stämpfli & Cie., Bern.
- Gross, G., H. Kerschner, and G. Patzelt (1976). Methodische Untersuchungen über die Schneegrenze in alpinen Gletschergebieten. *Zeitschrift für Gletscherkunde und Glazialgeologie* 12(2), 223–251.
- Guichon, F. (1984). *Montagne. Photographies de 1845 à 1914*. Denoël, Paris.
- Haeberli, W. and H. J. Zumbühl (2003). Schwankungen der Alpengletscher im Wandel von Klima und Perzeption. In F. Jeanneret, D. Wastl-Walter, and U. Wiesmann (Eds.), *Welt der Alpen – Gebirge der Welt. Ressourcen, Akteure, Perspektiven*, Jahrbuch der Geografischen Gesellschaft Bern, Band 61, 77–92.
- Hoinkes, H. (1970). Methoden und Möglichkeiten von Massenhaushaltsstudien auf Gletschern. Ergebnisse der Messreihe Hintereiserner (Öztaler Alpen) 1953–1968. *Zeitschrift für Gletscherkunde und Glazialgeologie* 6(1–2), 37–90.
- Holzhauser, H., M. Magny, and H. J. Zumbühl (2005). Glacier and lake-level variations in west-central Europe over the last 3500 years. *The Holocene* 15(6), 791–803, doi:10.1191/0959683605hl853ra.
- Holzhauser, H. and H. J. Zumbühl (1996). To the history of the Lower Grindelwald Glacier during the last 2800 years – palaeosols, fossil wood and historical pictorial records – new results. *Zeitschrift für Geomorphologie, Neue Folge, Supplementband 104*, 95–127.
- Holzhauser, H. and H. J. Zumbühl (1999). Glacier Fluctuations in the Western Swiss and French Alps in the 16th Century. *Climatic Change* 43(1), 223–237, doi:10.1023/A:1005546300948.
- Holzhauser, H. and H. J. Zumbühl (2003). Nacheiszeitliche Gletscherschwankungen. In R. Weingartner and M. Spreafico (Eds.), *Hydrologischer Atlas der Schweiz*, Bundesamt für Landestopografie, Bern–Wabern, Tafel 3.8.
- Hugi, F. J. (1830). *Naturhistorische Alpenreise*. Amiet-Lutiger, Solothurn.
- Jacky, W. A. G. (1861). *Feldbuch. Blatt Grindelwald. Topographische Aufnahme 1:50000, 1860/61*. Bundesamt für Landestopografie, Bern–Wabern.
- Kääb, A. (2001). Photogrammetric reconstruction of glacier mass balance using a kinematic ice-flow model: a 20 year time series on Grubengletscher, Swiss Alps. *Annals of Glaciology* 31, 45–52.
- Kääb, A. and M. Funk (1999). Modelling mass balance using photogrammetric and geophysical data: a pilot study at Griesgletscher, Swiss Alps. *Journal of Glaciology* 45(151), 575–583.
- Kaerer, M.-A. (2004). *L'Univers du Préhistorien. Science, foi et politique dans l'oeuvre et la vie d'Édouard Desor (1811–1882)*. L'Harmattan, Paris.
- Kane, E. K. (1856). *Arctic Explorations. The Second Grinnell Expedition in Search of Sir John Franklin: 1853, '54, '55*. Childs and Peterson, Philadelphia, 2 Vols.
- Kempf, C. (1994). *Adolphe Braun et la photographie, 1812–1877*. Editions Lucigraphie/Valblor, Illkirch, France.
- Lagolthière, R. M. (1989). Mulhouse et la conquête photographique des Alpes et du Mont-Blanc. *Annuaire historique de la ville de Mulhouse* 2, 39–63.
- Locher, T. (1954). *Bernische Kartierung zur Zeit der Dufourkarte und Vorarbeiten zum bernischen Kataster*. Ph. D. thesis, Philosophisch-naturwissenschaftliche Fakultät der Universität Bern, Bern.

- Lurie, E. (1960). *Louis Agassiz: A Life in Science*. University of Chicago Press, Chicago, USA.
- Maisch, M., A. Wipf, B. Denneler, J. Battaglia, and C. Benz (1999). *Die Gletscher der Schweizer Alpen. Gletscherhochstand 1850, Aktuelle Vergletscherung, Gletscherschwund-Szenarien*. vdf Hochschulverlag, ETH Zürich.
- Morand, S. and C. Kempf (1989). *Le Temps suspendu: Le daguerréotype en Alsace au XIXe siècle*. Editions Oberlin, Strasbourg.
- Nesje, A. and S. O. Dahl (2000). *Glaciers and Environmental Change*. Arnold, London, UK.
- Nicolussi, K. and G. Patzelt (2000). Untersuchungen zur holozänen Gletscherentwicklung von Pasterze und Gepatschferner (Ostalpen). *Zeitschrift für Gletscherkunde und Glazialgeologie* 36(1–2), 1–87.
- Oberli, A. (1968). Vor 100 Jahren: Wie es zur Herausgabe der Siegfriedkarte kam. *Hauszeitung der Eidgenössischen Landestopographie (Wabern)* 23, 7–22.
- Paul, F., A. Käab, M. Maisch, T. Kellenberger, and W. Haeberli (2004). Rapid disintegration of Alpine glaciers observed with satellite data. *Geophysical Research Letters* 31(21), L21402, doi:10.1029/2004GL020816.
- Portmann, J. P. (1975). Louis Agassiz (1807–1873) et l'étude des glaciers. In *Denkschriften der Schweizerischen Naturforschenden Gesellschaft (SNG)*, Zürich, Band 89, 113–164.
- Schmeits, M. J. and J. Oerlemans (1997). Simulation of the historical variations in length of Unterer Grindelwaldgletscher, Switzerland. *Journal of Glaciology* 43(143), 152–164.
- Schönfeld, J. (2001). Die Stereoskopie. Zu ihrer Geschichte und ihrem medialen Kontext. Master's thesis, Fakultät für Kulturwissenschaften der Universität Tübingen.
- Schuler, T., U. H. Fischer, and G. H. Gudmundsson (2004). Diurnal variability of subglacial drainage conditions as revealed by tracer experiments. *Journal of Geophysical Research* 109(F2), F02008, doi:10.1029/2003JF000082.
- SVGW. Schweizerischer Verein des Gas- und Wasserfaches (2002). Der Trinkwasserkonsum in der Schweiz sinkt weiter. *TWI* 9, 1–2.
- Swisstopo (2004). *DHM25 – The digital height model of Switzerland. Product Information*. Bundesamt für Landestopografie (swisstopo), Bern–Wabern.
- VAW/SANW (1881–2002). *Die Gletscher der Schweizer Alpen. Jahrbücher der Glaziologischen Kommission der Schweizerischen Akademie der Naturwissenschaften (SANW)*. Versuchsanstalt für Wasserbau, Hydrologie und Glaziologie (VAW) der ETH Zürich, Zürich, No. 1–122. (<http://glaciology.ethz.ch/swiss-glaciers/>).
- von Klebelsberg, R. (1948). *Handbuch der Gletscherkunde und Glazialgeologie. Band 1: Allgemeiner Teil*. Springer, Wien.
- Wipf, A. (1999). *Die Gletscher der Berner, Waadtländer und nördlichen Walliser Alpen. Eine regionale Studie über die Vergletscherung im Zeitraum "Vergangenheit" (Hochstand 1850), "Gegenwart" (Ausdehnung 1973) und "Zukunft" (Gletscherschwundsszenarien, 21. Jhdt.)*. Physische Geographie, Vol. 40. Geographisches Institut der Universität Zürich, Zürich.
- Wolf, J. R. (1879). *Geschichte der Vermessungen in der Schweiz*. Commission von S. Höhr, Zürich.

Zölly, H. (1944). Geodätische Grundlagen der Vermessungen im Kanton Bern. Geschichtlicher Überblick. *Sonderdruck aus: Schweizerische Zeitschrift für Vermessungswesen und Kulturtechnik*, Winterthur.

Zumbühl, H. J. (1980). *Die Schwankungen der Grindelwaldgletscher in den historischen Bild- und Schriftquellen des 12. bis 19. Jahrhunderts. Ein Beitrag zur Gletschergeschichte und Erforschung des Alpenraumes*. Denkschriften der Schweizerischen Naturforschenden Gesellschaft (SNG), Birkhäuser, Basel/Boston/Stuttgart, Band 92.

Zumbühl, H. J. and H. Holzhauser (1988). Alpengletscher in der Kleinen Eiszeit. Sonderheft zum 125jährigen Jubiläum des SAC. *Die Alpen* 64(3), 129–322.

## 2.4 Appendix 1



**Figure 2.11:** (a) *The Lower Aare Glacier, Switzerland. Photograph by Martin Funk, 9.8.2005.*  
(b) *The snout of the Lower Aare Glacier. Photograph by Daniel Steiner, 22.8.2004.*

## 2.5 Appendix 2

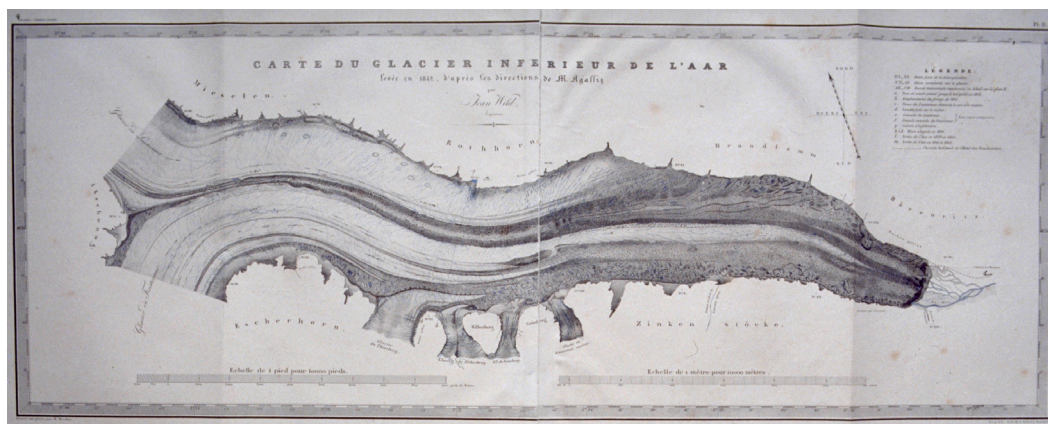


**Figure 2.12:** During the most important and longest field campaign on the Lower Aare Glacier (4 July–5 September 1842) the engineer and late professor Johannes Wild (1814–1894) surveyed the "Carte du glacier inférieur de l'Aar" in the scale of 1:10'000 (no contour lines). This even today admirable unique time document in a great scale (von Klebelsberg, 1948) was published five years later in Agassiz (1847). On this lithography in black and blue colors, also aesthetically a masterpiece, we see the more than 8 kilometers long tongue of the Lower Aare Glacier east of the Abschwung, designed by a system of hachures. Wild surveyed in black also plenty of ice surface-related phenomena like moraines, with dark gravel covered ice pyramids, craters, huge boulders of rock, but also the rock and tent of the "Hôtel des Neuchâtelois". Systems of crevasses, ice surface rivers, intraglacial waterfalls and ice lakes were marked in blue color. In 1842, the Lower Aare Glacier was ending in a steep, impressive, partially ice covered ice front, approx. 2.1 km in front of the present glacier terminus (Zumbühl and Holzhauser, 1988; VAWISANW, 2002; Haerberli and Zumbühl, 2003). It must be noted that this lithography can be viewed as the first map of a glacier with scientific value. Photograph by Heinz J. Zumbühl.

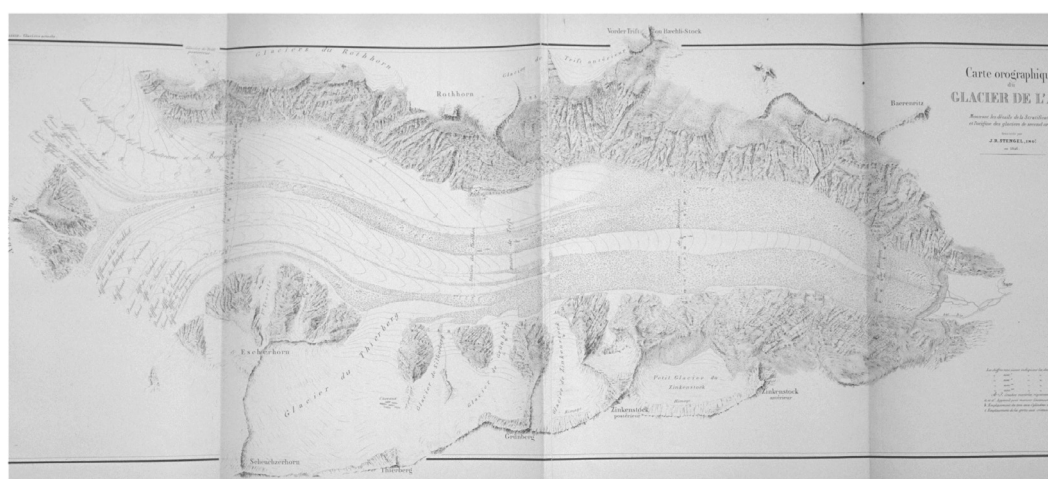


**Figure 2.13:** Lithography "Carte Orographique du Glacier de l'Aar Montrant les détails de la Stratification et l'origine des glaciers de second ordre" in the scale of 1:10'000 (with contour lines), surveyed by Johann Rudolf Stengel (1824–1857) in (until?) 1846 (Agassiz, 1847). Photograph by Heinz J. Zumbühl.

## 2.6 Appendix 3



**Figure 2.14:** Oil painting "Hôtel des Neuchâtelois Glacier de l'Aar" (with added Finsteraarhorn as background) of Jacques Bourkhardt (1811–1867). Archives de l'Etat Château Neuchâtel, Agassiz-Archiv. Photograph by Heinz J. Zumbühl.



## 2.7 Appendix 4

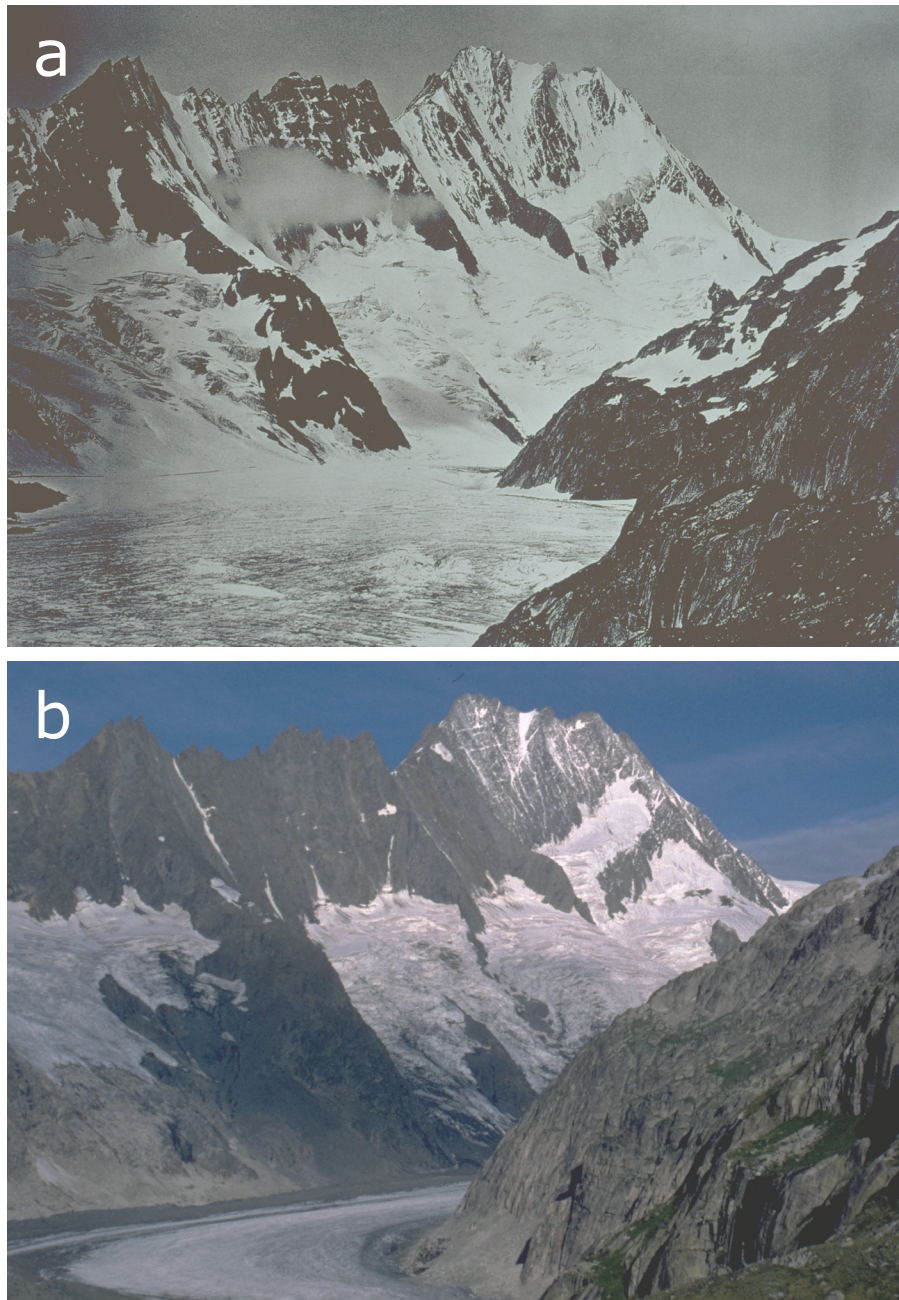


**Figure 2.15:** (a) The Lower Aare Glacier 1855 from the Pavillon Dollfus. Photograph by the Bisson Brothers ("Suisse", No. 24). Alpine Club Library, London. Photograph by Heinz J. Zumbühl.  
(b) Recent panorama from the Lauteraarhütte. Photograph by Heinz J. Zumbühl, 23.8.2004.

## 2.8 Appendix 5

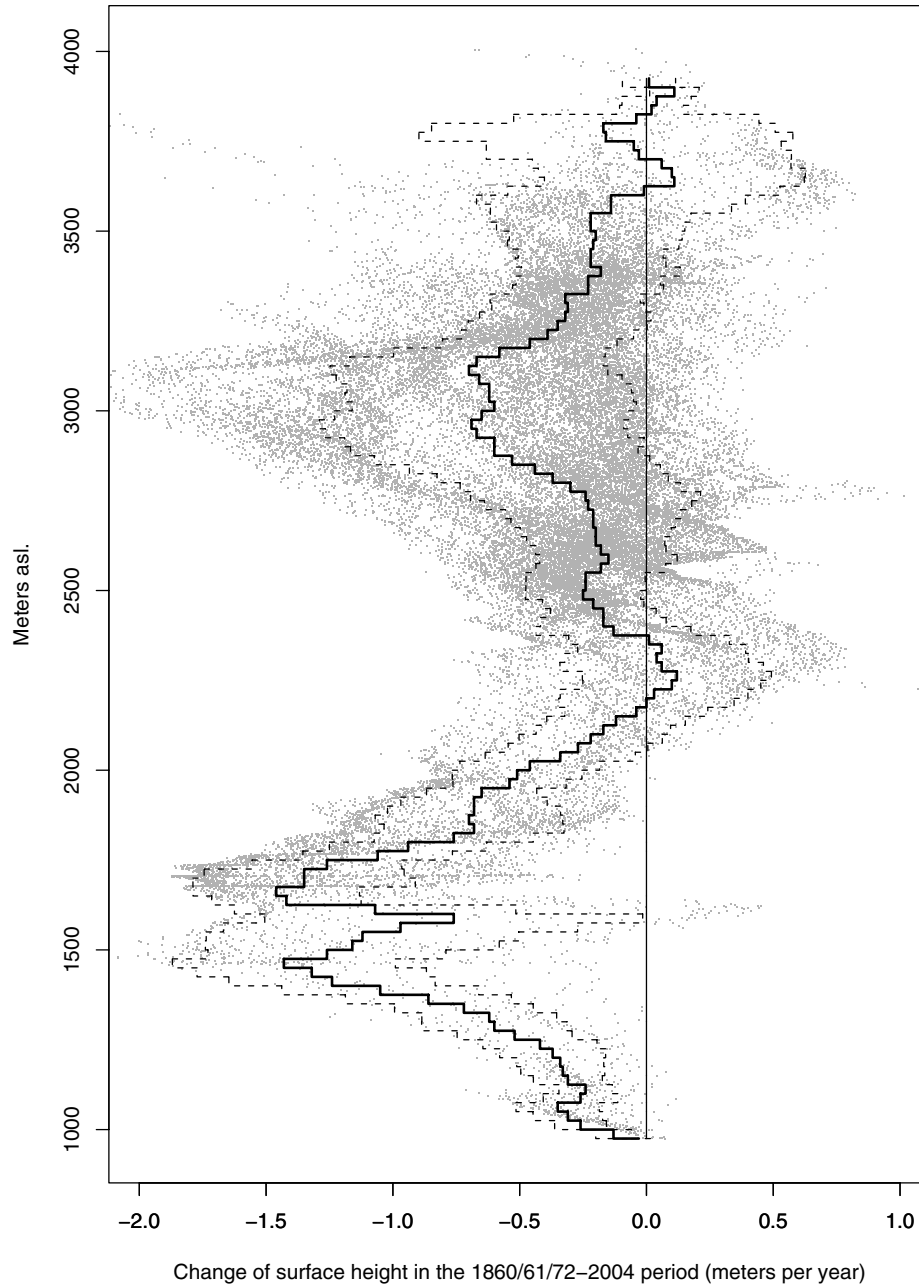


**Figure 2.16:** Distribution of the glacier surface thickness changes (41689 points) for the difference model DEM1861-DEM2004 (gray points). Given are also the average surface thickness changes (solid line) and the  $\pm 1$  standard errors (dashed lines) depending on the elevation range. The overall average thickness change for the 1860/61/72-2004 period is  $-0.416$  meters with a standard error of  $0.514$  meters.

## 2.9 Appendix 6

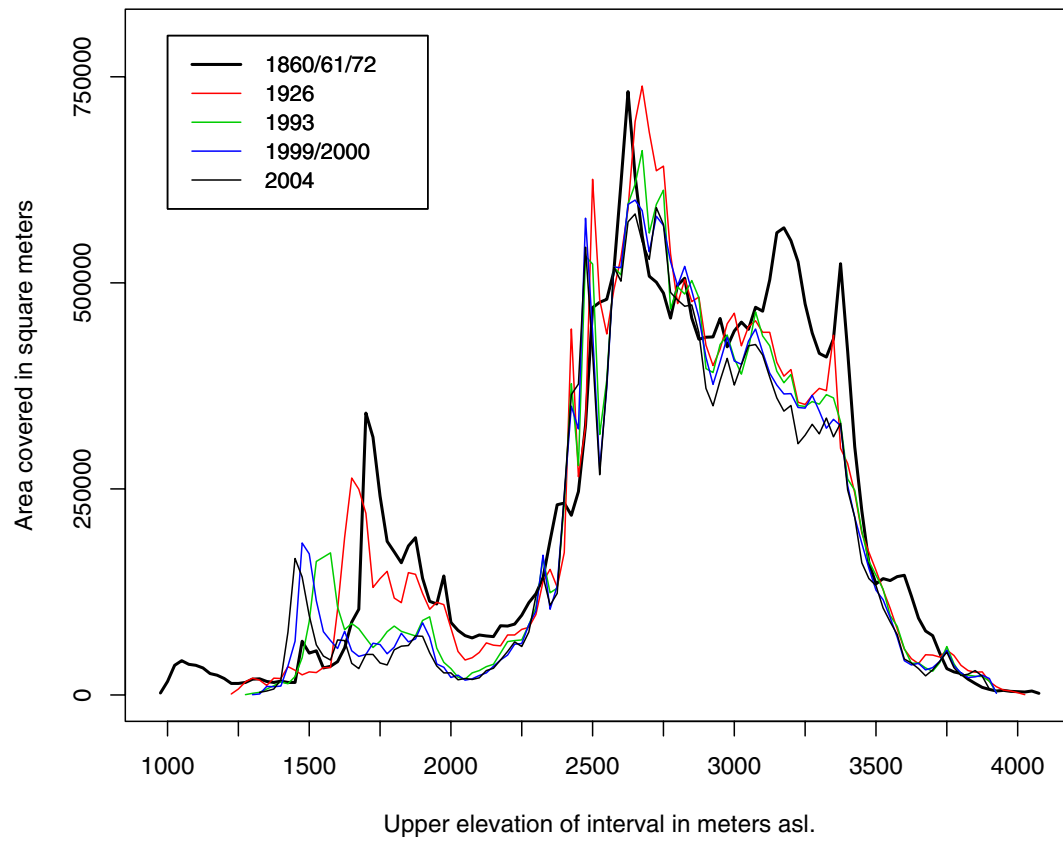


**Figure 2.17:** Glacier hypsography with 25 meter equidistance for the years 1860/61/72 (black thick line), 1926 (red line), 1993 (green line), 1999/2000 (blue line) and 2004 (black solid line), derived from DEMs.



## Chapter 3

# The application of a nonlinear Backpropagation Neural Network to study the mass balance of Great Aletsch Glacier, Switzerland

Daniel **Steiner**<sup>1,2</sup>, Andreas **Walter**<sup>3</sup>, Heinz Jürg **Zumbühl**<sup>1</sup>

<sup>1</sup> Meteorology and Climatology, Institute of Geography, University of Bern, Switzerland

<sup>2</sup> NCCR Climate, University of Bern, Switzerland

<sup>3</sup> Deutscher Wetterdienst (DWD), Offenbach a.M., Germany

*Journal of Glaciology* 51 (173); in press

### Abstract

*Glacier mass changes are considered to represent key variables related to climate variability. We have reconstructed a proxy for annual mass balance changes in the Great Aletsch Glacier, Swiss Alps, back to AD 1500 using a nonlinear Backpropagation Neural Network (BPN). The model skill of the BPN performs better than reconstructions using conventional stepwise multiple linear regression.*

*The BPN, driven by monthly instrumental series of local temperature and precipitation, provides a proxy for 20th-century mass balance. The long-term mass balance reconstruction back to AD 1500 is based on a multiproxy approach of seasonally resolved temperature and precipitation reconstructions (mean over a specific area) as input variables. The relation between the driving factors (temperature, precipitation) used and the reconstructed mass balance series is discussed. Mass changes in the Great Aletsch Glacier are shown to be mainly influenced by summer (June–August) temperatures, but winter (December–February) precipitation also seems to contribute.*

*Furthermore, we found a significant nonlinear part within the climate–mass balance relation of Great*

**Keywords:** European Alps, climate variability, glacier variations, temperature, precipitation, mass balance reconstruction, Backpropagation Neural Network

### 3.1 Introduction

Modern climatology faces the question of whether anthropogenically induced climate change is already observable in climatic variables. Because the climate system can be regarded as nonlinear (Houghton et al., 2001), traditional linear statistical models can not describe the full complexity of its behavior, and thus fail to answer this question. Nonlinear Neural Network Models (NNMs) provide a statistical solution to this problem.

NNMs originated in the study of the cognitive abilities of biological brain functions, i.e. how the brain processes information and how it learns (Adrian, 1926; Rosenblatt, 1958; Grossberg, 1982). A comprehensive overview of the wide range of applications of NNMs to time series analysis is summarized in Anderson and Rosenfeld (1986) and Rumelhart and McClelland (1986).

As an analogue to biological brains, a typical NNM consists of a yet to be defined number of simple processing units. The task of a (supervised learning) NNM is to 'learn' certain features of the data, which consist of input variables and desired output responses, using a training subset. After the training process these features are interpolated on an unknown validation subset, on which the performance of the NNM can be determined. Internal parameters of the network architecture are adjusted according to a specific learning rule so that the network ideally captures all intrinsic data features.

What distinguishes NNMs from traditional statistical methods is its nonlinear character, due to a nonlinear mapping function. This mapping function is commonly chosen out of the class of sigmoid functions, because it has been shown experimentally by Adrian (1926) that biological neurons respond to a stimulus in a sigmoidal fashion, i.e. no output until a certain threshold is exceeded, followed by a nearly linear input–output relation and saturation from a certain input level onward.

Conventional studies of climate change are based either on physical climate models, e.g. General Circulation Models (GCMs) with a high computing and CPU time demand, or on statistical models such as Multiple Linear Regression (MLR) models, which allow only a limited exploration of the state of the climate system. There is a wide variety of models for studying the behavior of the climate system that can be ordered by increasing complexity (e.g. Radiative Convective Models, Energy Balance Models). The MLR and GCM approaches represent the extremes of this model hierarchy. Nevertheless, NNM represents a quite simple nonlinear method for gaining insight into the behavior of the climate system.

The nonlinear NNM combines the advantages of physically motivated (possibly nonlinear) climate models, with high complexity, and linear statistical models, with a low CPU time demand. Two recent climatological applications of NNMs have been the detection and attribution of anthropogenic climate change (Walter and Schönwiese, 2002; Walter and Schönwiese, 2003) and forecasting tropical Pacific sea surface temperatures in the El Niño region (Wu and Hsieh, 2003). For a general overview of climatological applications of neural networks, see Hsieh and Tang (1998) or Walter (2001).

In this paper we simulate and reconstruct a proxy for annual mass balance of the Great Aletsch Glacier, Switzerland, using a Backpropagation Network (Rumelhart et al., 1986). This is the first

time that a Neural Network approach has been used in this glaciological context to simulate and reconstruct glacier mass balance.

The mass balance of glaciers varies with changing climate, many studies and measurements have been carried out to investigate this connection (e.g. Oerlemans and Reichert, 2000, and references therein). To relate annual glacier mass balance to meteorological data, a suitable combination of climate data is required. In many studies (summer) temperature and (winter) precipitation are assumed to be the best predictors for this objective (Oerlemans and Reichert, 2000). Because mass balance is a complex function dependent on climate, time and other factors, it may be well-suited to nonlinear approaches. In fact, nonlinear functions in the glacier–climate system have been found in several recent studies (e.g. Braithwaite and Raper, 2002; Lie et al., 2003). The aim of this study is to use an easy nonlinear model, driven only by a combination of temperature and precipitation data.

In Section 3.2 we provide an overview of the data used in this study and the concept behind a BPN. In Section 3.3 we discuss how the BPN can be used to simulate a proxy for annual glacier mass balance by a suitable selection of monthly instrumental data (temperature, precipitation) for the 20th century. As well as simulating glacier mass balance, this work aims to reconstruct a longer term mass balance series. Applying the BPN technique, we propose to use multiproxy seasonal reconstructions of temperature (Luterbacher et al., 2004) and precipitation (Pauling et al., 2005) to calculate a new annual mass balance series back to 1500. In Section 3.4 the performance of the BPN is discussed, questions are presented, and further investigations are proposed.

## 3.2 Data and methods

### 3.2.1 Instrumental data of the 20th century

Figure 3.1 shows the topography and the locations of the meteorological stations within the greater region of Aletsch Glacier, the largest stream of ice in the Alps, lying in the Bernese Alps of south–central Switzerland. Aletsch Glacier (Figure 3.8) is divided into main (Great Aletsch), middle and upper parts. The main glacier ( $46^{\circ} 30' \text{ N}$ ,  $8^{\circ} 2' \text{ E}$ ) is 24.7 km long and covers an area of 86.76 square km. Its head is at 4160 meters asl., the glacier terminates at 1556 meters asl. and its average height is about 3140 meters asl. (IAHS(ICSU)/UNEP/UNESCO, 1998). The exposure of Great Aletsch Glacier is to the south–east (accumulation area) and to the south (ablation area). As shown in Figure 3.1a, the ice stream consists of three large firn fields: the Aletschfirn, the Jungfraufirn, and the Ewigschneefeldfirn. In 1994, depth soundings made by means of radio echolot (radar) located the glacier bed at depths of 600–700 meters in the Konkordia region (VAW/SANW, 1881–2002; No. 115/116).

The study site which borders on the Upper Valais (Rhône Valley) is characterized by a generally temperate humid climate. It is more subcontinental than that of the northern–Alpine region, which is more suboceanic (van der Knaap and van Leeuwen, 2003). Frei and Schär (1998) point out that the dry inner–Alpine conditions of the Valais contrast with the wet anomalies along the Alpine rims, especially in the north of the Aletsch region. Because the Valais has a complex topography, like the whole Alpine region, marked vertical temperature gradients are found over short distances. Furthermore, the major west–east orientation of the Valais, occasionally across the main airflow direction, can cause mesoscale meteorological phenomena like the foehn (Schüepf et al., 1978).

The fluctuations in length of Great Aletsch Glacier have been carefully reconstructed on the basis of documents, archaeological field studies, and precise dendrochronological dating. In the last 500 years, a very small advance around 1500 is dated by both, dendrochronology and archaeology.

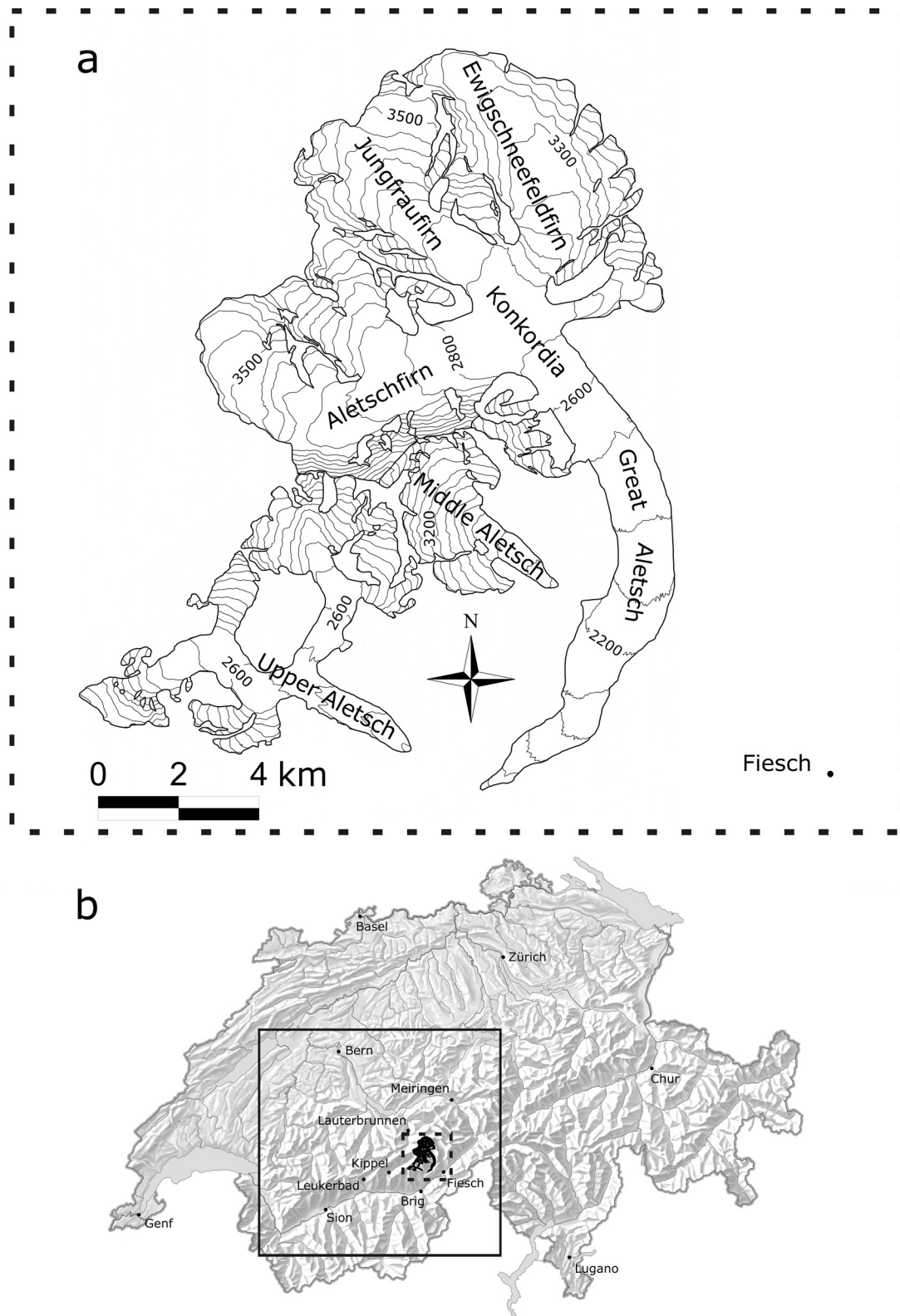


**Figure 3.1:** (a) Map showing the Aletsch Glacier with its main branches and tributaries. (b) The Aletsch region (area with dashed outline) and the meteorological stations used as forcing or reference data in this study. Also shown is the grid range (area with solid outline) over which seasonal averages have been calculated.



Dendrochronological analysis allows an exact reconstruction of the marked advance, leading to a maximum glacier extent from 1670 to 1680. Pictures and texts document fluctuations during the 18th and 19th centuries, especially the final advance to the last Little Ice Age maximum extent around 1856. From 1892 to the present, the continuously decreasing tongue has been precisely measured every year (Holzhauser and Zumbühl, 1999; Haeberli and Holzhauser, 2003; VAW/SANW, 1881–2002).

As a continuation of the mass balance studies of the 1950s (Kasser, 1954; IAHS(ICSU)/UNESCO, 1967), Aellen and Funk (1990) estimated an average yearly net balance for the period 1931–87 from a simple hydrological model, calculating daily to annual water storage variations in the basin of the Massa river. Based on water flux measurements of the Massa river, a tributary of the Rhone river which issues from Great Aletsch Glacier, and precipitation data from the surrounding area, a proxy for annual mass balances can be calculated (Paterson, 1994). Later, in order to correct systematic errors in these calculations (under- or overestimations of areal precipitation), the data were revised by a linear regression approach. Besides the uncorrected data series from Aellen and Funk (1990), information from direct glaciological mass balance measurements on Great Aletsch Glacier and a reference mass balance series (average of Great Aletsch (uncorrected), Limmeren and Plattalva glacier) were incorporated into the linear model to determine a corrected proxy for annual mass balances (Müller-Lemans et al., 1994).

As a control of the Aletsch data, variations of total volume, surface area and mean thickness were determined for the years 1926/27, 1957, 1980 and 1999, using geodetic methods (terrestrial or aerial surveys). There is clear agreement between the Aletsch cumulative mass balance and these geodetic measurements (Vincent et al., 2004). An annual check is also provided by the average net balances computed from a stake network observed on Great Aletsch Glacier from 1950–86 (Aellen, 1995). Finally, new data made it possible to expand the mass balance data to the 1919–99 period with the model approach presented here.

It should be noted that this proxy for annual balances of Great Aletsch Glacier comes from a hydrological model and not directly from field measurements. So the resulting series is probably not as reliable as direct measurements, even though the data have been checked against independent geodetic measurements (Vincent et al., 2004). Nevertheless, this proxy will serve as target function in our neural network modelling approach.

The forcing data, monthly temperature and precipitation series from the surroundings of Great Aletsch Glacier, were provided by MeteoSwiss (online database of MeteoSwiss). The data are homogenized, i.e. they are adjusted for non-climatic factors like changes in station location or changes in observation practices (Begert et al., 2003). Table 3.1 represents all climate series used in this study. In agreement with Schüepp et al. (1978), we found a lack of long climatic time series in this region of the Swiss Alps.

As the Alpine precipitation field shows large spatiotemporal variability, there is a strong need for long-term precipitation data close to a glacier in order to relate climatic conditions to glacier activities. The precipitation series (Fiesch, Kippel) were selected according to the study by Aellen and Funk (1990). But instead of the precipitation series for Grindelwald applied there, which is missing values for the period 1903–10, we chose the highly-correlated ( $r=0.92$ ) nearby precipitation series for Lauterbrunnen. Furthermore, the Sion and Meiringen data were used as temperature data sets. With this data selection, we climatically represent both the inner-Alpine dry valley of the Upper Valais and the wetter northern part of the Bernese Alps. However, these data series serve as potential model inputs for the BPN.

To complete the precipitation series of Fiesch and Kippel for the missing periods 1992–2003 and 1974–2003, a method derived from the homogenization process at MeteoSwiss was used (Begert

climate parameter	usage in study	station name	altitude in m asl.	time period	geographic coordinates
temperature	forcing	Sion	483	1864–2003	46° 13' N, 7° 20' E
temperature	forcing	Meiringen	595	1890–2003	46° 44' N, 8° 11' E
precipitation	forcing	Fiesch	1060	1899–1991	46° 24' N, 8° 08' E
precipitation	reduction	Ernen	1000	1967–1999	46° 24' N, 8° 08' E
precipitation	reduction	Fieschertal	1095	1999–2003	46° 25' N, 8° 09' E
precipitation	reference	Brig	666	1899–1906 1959–2003	46° 19' N, 7° 58' E
precipitation	forcing	Kippel	1376	1899–1974	46° 24' N, 7° 46' E
precipitation	reduction	Ried	1500	1974–2003	46° 25' N, 7° 48' E
precipitation	reference	Leukerbad	1285	1898–2003	46° 23' N, 7° 37' E
precipitation	forcing	Lauterbrunnen	818	1899–2003	46° 36' N, 7° 54' E

**Table 3.1:** Principal meteorological stations used in this study (data from the online database of MeteoSwiss).

et al., 2003). Based on a highly-correlated reference series, nearby precipitation series were reduced to the level of the series with missing values. For this, average ratios between all precipitation series and the reference series were calculated for the overlapping periods. Based on the proportion of these average ratios, it is possible to determine reduction factors for the nearby precipitation stations (personal communication from Thomas Schlegel, MeteoSwiss, 26.2.2004).

The Fiesch precipitation data series ( $P_{\text{Fiesch}}$ ) was completed as follows:

- (i) The highly-correlated ( $r=0.92$ ) precipitation series from Brig was used as reference series.
- (ii) The two nearby precipitation stations, Ernen ( $P_{\text{Ernen}}$ ; 1.3 km from Fiesch) and Fieschertal ( $P_{\text{Fieschertal}}$ ; 2.2 km from Fiesch), were then reduced to the level of Fiesch.
- (iii) For the missing time period 1992–98,

$$(P_{\text{Fiesch}}) = q_{\text{Fiesch}} \cdot \frac{(P_{\text{Ernen}})}{q_{\text{Ernen}}} = 1.043 \cdot (P_{\text{Ernen}}). \quad (3.1)$$

- (iv) For the missing time period 1999–2003,

$$(P_{\text{Fiesch}}) = q_{\text{Fiesch}} \cdot \frac{(P_{\text{Fieschertal}})}{q_{\text{Fieschertal}}} = 0.764 \cdot (P_{\text{Fieschertal}}), \quad (3.2)$$

where  $q_{\text{Fiesch}}$ ,  $q_{\text{Ernen}}$  and  $q_{\text{Fieschertal}}$  are the average ratios between the Fiesch, Ernen and Fieschertal precipitation series and the Brig reference series for the overlapping measured period.

In an analogous procedure, the Kippel data series ( $P_{\text{Kippel}}$ ) was completed using the Leukerbad reference series ( $r=0.90$ ) and the nearby Ried precipitation series ( $P_{\text{Ried}}$ ; 3.1 km from Kippel) as a reduction series.

For the missing time period 1974–2003,

$$(P_{\text{Kippel}}) = q_{\text{Kippel}} \cdot \frac{(P_{\text{Ried}})}{q_{\text{Ried}}} = 1.044 \cdot (P_{\text{Ried}}), \quad (3.3)$$

where  $q_{\text{Kippel}}$  and  $q_{\text{Ried}}$  are the average ratios between the Kippel and Ried precipitation series and the Leukerbad reference series for the overlapping measured period.

### 3.2.2 Multiproxy reconstructions of temperature and precipitation back to 1500

In the absence of widespread instrumental data, we must rely upon indirect lines of evidence to provide information about climate variability over the past several centuries. To determine annual or higher-resolution climate variations, however, high-resolution "proxy" climate indicators such as ice cores and tree ring measurements, combined with the scant available documentary or instrumental evidence available in prior centuries, are required (e.g. Mann, 2002; Jones and Mann, 2004; Luterbacher et al., 2004).

In this study two new gridded ( $0.5^\circ \times 0.5^\circ$  resolution) multiproxy reconstructions of seasonal temperature (Luterbacher et al., 2004) and precipitation fields (Pauling et al., 2005) from 1500–2000 for European land areas were used. The temperature reconstruction is based on a data set that includes instrumental data series, reconstructed sea-ice and temperature indices, and proxy temperature reconstructions from ice cores and tree rings (see Luterbacher et al., 2004, for a detailed description of the method and the data used). Like the temperature reconstructions, the precipitation estimates were based on a combination of instrumental series, documentary indices (precipitation) and natural proxies (tree rings, corals, ice cores). As these reconstructions share no common predictors, they can be compared in terms of climate dynamics or temporal stability of the precipitation–temperature relationship. The temperature reconstructions end in 2004; the precipitation reconstructions in 2000. As a consequence we studied the period mentioned above (1500–2000).

As input data for the model, a seasonal average of both temperature and precipitation sums was calculated over an area of  $7^\circ \text{ E}$  to  $8.5^\circ \text{ E}$  and  $46^\circ \text{ N}$  to  $47^\circ \text{ N}$ , comprising  $xy$  gridpoints (see Figure 3.1b for the grid range). This grid extent covers the entire Aletsch region and clearly reflects its climatic conditions, presented in Section 3.2.1. The seasonal averages generally show higher correlations with the observed precipitation (Fiesch, Kippel, Lauterbrunnen) and temperature measurements (Sion, Meiringen) for the overlapping 1900–2000 period than nearby single grid points. The correlation coefficients range from 0.87 (JJA period; Meiringen) to 0.95 (MAM period; Sion) for temperature and from 0.61 (JJA period; Fiesch) to 0.77 (DJF period; Kippel) for precipitation. The generally lower correlation coefficients for precipitation probably reflect the greater difficulty in reconstructing and/or representing precipitation fields in mountainous regions due to their large spatiotemporal variability. As with all models, the output of a BPN depends on the quality of the input data, and possible uncertainties in the precipitation data will significantly reduce the accuracy of the trained neural networks. Related to this issue, Klein and Rossin (1999) found that errors in training data affect neural network models more severely than linear regression models.

### 3.2.3 Backpropagation Neural networks as modelling tools

Neural networks use nonlinear functions and a large number of processing units to reduce the risk of model mismatch errors. Instead of matching the architecture of the model to a problem, a model

is used that can describe almost anything, and careful training of the model is used to constrain it to describe the data.

In this study the standard NNM, the Backpropagation Network (BPN), was applied (Rumelhart et al., 1986). This network architecture is based on a supervised learning algorithm to find the minimum of a cost function. Unlike a simulated annealing schedule (Metropolis et al., 1953), the BPN does not guarantee that the global minimum of this cost function will be reached, though it is very likely that a minimum good enough to reproduce responses in the data can be found. This approach also bears a certain risk of overfitting, so the data have to be separated into a training and a validation subset (calibration/verification in reconstruction exercises). The 'learning' process of the network is performed on the training subset only, whereas the validation subset serves as an independent reference for the simulation quality. This technique is called Cross-Validation (Stone, 1974; Michaelson, 1987). When applying NNM to a nonstationary time series, as in this approach, the choice of the training subset must ensure that the entire amplitude range of all forcing mechanisms considered is covered. Otherwise the algorithm will fail if confronted with an extreme value during the validation process, and such an extreme value never occurred in the learning period. The training must be carried out using a representative data subset. Therefore the training data cannot be chosen continuously out of all data available but must be chosen so that all the amplitudes are covered. We used 75% of all data for training and the remaining 25% for validation (Walter and Schönwiese, 2003).

A typical NNM consists of three layers: input, processing and output layers. Figure 3.2 shows a simplified neural network. Although the units of the processing layer are sometimes called 'hidden units', their weights, activation and all other internal parameters are easily accessible from the outside.

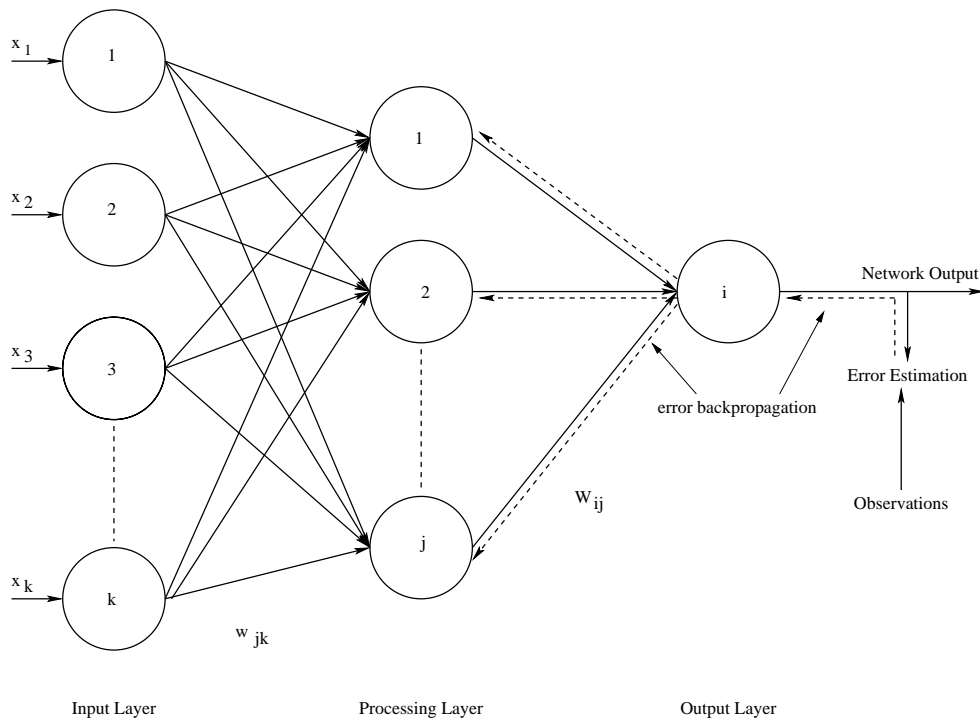


**Figure 3.2:** An example of a simplified three-layer  $k$ - $j$ -1 BPN architecture. Also shown is by arrows the concept behind the Backpropagation training algorithm.

The input to an NNM is a vector of elements  $(x_k)$ , where the index  $k$  stands for the number of input

units in the network. In our study,  $k=12$  indicates the major short-term climatic influences on the mass balance of Great Aletsch Glacier in the 20th century. For the long-term reconstructions of annual glacier mass balance since 1500, we chose  $k=2$  (see Section 3.3 for the selection of the input variables). These inputs are weighted with weights  $w_{jk}$ , where  $j$  represents the number of processing units, to give the inputs to the processing units

$$h_j = \sum_k w_{jk} x_k. \quad (3.4)$$

Using too few/many processing units can lead to underfitting/overfitting problems. That is, the simulation results are highly sensitive to the number of processing units and learning parameters chosen. The best number of processing units can be determined by repeated simulations with increasing numbers of processing units, i.e.  $j = 1, 2, \dots, n$  and by observing the performance of these different network architectures on the validation sample. Multiple versions of the BPN must be tried to obtain robust results. Typically, the validation error decreases with increasing numbers of processing units until the network has too many degrees of freedom, i.e. too many processing units. After that, the validation error increases and the model with the optimal number of processing units, i.e. the model configuration with the lowest validation error, must be chosen for the final simulations.

For the 20th century we used 12 input units as forcings. In addition, there are 6 processing units in 1 processing layer and 1 output unit as a target function. This neural network architecture is abbreviated as 12–6–1. For long-term simulations back to 1500, a 2–2–1 architecture was applied.

After weighting and summation of the inputs, the nonlinear aspects of the BPN were encountered first as the results were passed to nonlinear activation functions in each processing unit. These functions produced the output of the processing layer

$$X_j = g(h_j) = g\left(\sum_k w_{jk} x_k\right). \quad (3.5)$$

To retain the original analogy between NNM and learning mechanisms in the brain (Adrian, 1926; Amit, 1989), the activation functions are commonly chosen from the class of sigmoid functions, which also will keep the model response bounded. We have chosen

$$g(h) = \tanh(h) = \frac{e^h - e^{-h}}{e^h + e^{-h}}. \quad (3.6)$$

The outputs of the processing units are fed to the output layer where they are again weighted

$$H_i = \sum_j W_{ij} X_j = \sum_j W_{ij} g\left(\sum_k w_{jk} x_k\right). \quad (3.7)$$

The use of a second activation function will finally produce the output of the network

$$Y = f(H_i) = f\left[\sum_j W_{ij} g\left(\sum_k w_{jk} x_k\right)\right], \quad (3.8)$$

where  $f$  is the output activation function,  $x_k$  are the chosen input variables,  $w_{jk}$  are the weights from the  $k$  input units to the  $j$  processing units, and  $W_{ij}$  are the weights from the processing units to the output unit. As an output activation function we apply the identity function  $f(x) = x$ , so that Equation (3.7) is the complete BPN function.

This model is very general. However, it has been shown that 'with one layer and an arbitrary continuous sigmoidal function, this model can approximate any continuous function, provided that no constraints are placed on the number of units or the size of the weights' (Cybenko, 1989).

### 3.2.4 The Backpropagation Architecture

The purpose of training an NNM is to find a set of coefficients that reduces the error between the model outputs and the given test data  $y(x_k)$ . This is usually done by adjusting the weights  $W_{ij}$  and  $w_{jk}$  to minimize the least square error

$$\begin{aligned}\chi^2 &= \frac{1}{2} \sum_n \sum_i [y(x_k) - Y(x_k)]^2 \\ &= \frac{1}{2} \sum_n \sum_i \left[ y(x_k) - g \left( \sum_j W_{ij} g \left( \sum_k w_{jk} x_k \right) \right) \right]^2,\end{aligned}\quad (3.9)$$

where  $n$  is the length of the time series. One way to adjust these weights, and thus to reduce  $\chi^2$ , is gradient descent. The update step in the output weights can be found by differentiating

$$\begin{aligned}\Delta W_{ij} &= -\gamma \frac{\partial \chi^2}{\partial W_{ij}} \\ &= \gamma \sum_n [y(x_k) - Y(x_k)] g'(H_i) X_j \\ &= \gamma \sum_n \Delta_i X_j,\end{aligned}\quad (3.10)$$

defining

$$\Delta_i = [y(x_k) - Y(x_k)] g'(H_i).\quad (3.11)$$

The so-called learning constant  $\gamma$ , given in Equation (3.10), is a scale factor which controls how big the update step is, and  $g'$  is the derivation of the sigmoidal activation function used, here  $\tanh(x)$ . The choice of  $\gamma$  is crucial because  $\gamma$  determines the step width of the gradient descent algorithm. If  $\gamma$  is too small, the algorithm might get stuck in steep canyons of the  $\chi^2$  hypersurface. If it is too large, the algorithm might just jump over minima.

The update in the input weights can be found using the chain rule:

$$\begin{aligned}\Delta w_{jk} &= -\gamma \frac{\partial \chi^2}{\partial w_{jk}} \\ &= \gamma \sum_n \sum_i [y(x_k) - Y(x_k)] g'(H_i) W_{ij} g'(h_j) x_k \\ &= \gamma \sum_n \sum_i \Delta_i W_{ij} g'(h_j) x_k \\ &\equiv \gamma \sum_n \delta_j x_k,\end{aligned}\quad (3.12)$$

defining

$$\delta_j = g'(h_j) \sum_i W_{ij} \Delta_i. \quad (3.13)$$

The deltas for the input layer are found in terms of the deltas for the output layer by running them backwards through the networks  $W_{ij}$ 's. Thus, the errors between model output and observations are propagated backwards through the weights of the output and the processing layer, and these errors are used to adjust the weights throughout the network. Training a network by gradient descent and feeding the errors backwards through the network is called *error back propagation*.

As mentioned above, this network architecture risks being stuck in local minima on the  $\chi^2$  hypersurface. To reduce this risk, an enhanced version of standard backpropagation with a momentum term  $\alpha$  was used. The momentum term introduces the old weight change as a parameter for computing the new weight change. This avoids the oscillation problems common with the standard backpropagation algorithm when the error hypersurface has a very narrow minimum area. The new weight change is computed by

$$\Delta w(t) = -\gamma \frac{\partial \chi^2}{\partial w} + \alpha \Delta w(t-1). \quad (3.14)$$

The term  $\alpha$ , a number between 0 and 1, is the so-called momentum parameter and  $\Delta w(t-1)$  the weight change in the time step  $t-1$ . The effect of these enhancements is that flat spots of the error hypersurface are traversed relatively rapidly with a few large steps, while the step size is decreased as the hypersurface gets rougher. This adaption of the step size increases learning speed significantly.

One obvious problem concerning BPN is that Equation (3.14) contains two parameters,  $\gamma$  and  $\alpha$ , whose optimum values will typically vary from one iteration to the next. We might therefore seek some procedure for setting these automatically as part of the training algorithm. One approach for doing this is the Polak–Ribière variant of the conjugate gradient descent. Conjugate gradient is a method of accelerating gradient descent in which the learning rate  $\gamma$  and the momentum parameter  $\alpha$  are determined in each iteration. In ordinary gradient descent, one uses the gradient to find the steepest downhill direction, then moves along that line to the minimum in that direction. With conjugate gradient, a search is made along the conjugate gradient direction to determine the step size, which minimizes the error function along that line. The momentum term  $\alpha$  is calculated by the Polak–Ribière formula, since this controls the search direction while the learning rate  $\gamma$  is determined by the golden section method for line minimization (Press et al., 1992; Bishop, 1995). For an excellent overview of the conjugate gradient descent method, see the unpublished draft by J.R. Shewchuk (<http://www.cs.cmu.edu/~quake-papers/painless-conjugate-gradient.ps>). It should be noted that for many applications the Polak–Ribière method gives slightly better results than other conjugate gradient methods or even the conventional gradient descent approach (Press et al., 1992; Bishop, 1995; Dao and Vemuri, 2002).

A second uncertainty in the BPN simulation is related to the fact that the minimum, found from the algorithm, is dependant on the initial starting point on the  $\chi^2$  hypersurface. Since the BPN represents a nonlinear mapping function slightly different initial conditions can lead to large differences in the simulation results. To eliminate this kind of uncertainty, the BPN was driven 30 times, each time only varying the initial starting point for the conjugate gradient algorithm on the  $\chi^2$  hypersurface.

## 3.3 Results

### 3.3.1 Mass Balance in the 20th century

One of the most important factors in determining the success of a practical application of neural networks is the form of pre-processing applied to the data. In the simplest case, pre-processing may take the form of a linear transformation of the input and output data (see the z-transformation below). More complex pre-processing may also involve reduction of the dimensionality of the input data. The fact that such dimensionality reduction can improve performance may at first appear somewhat paradoxical, since it will decrease the information content of the input data in most cases (Bishop, 1995). Some of these techniques, such as genetic algorithms, are highly heuristic, while other methods such as principal components analysis make assumptions as to the linearity of relationships between the input data items. Finally, an exhaustive search of optimal input configurations is highly effective but computationally intensive. With the 60 input variables used in this study (5 data sets with monthly resolution, each) there are  $2^{60} \approx 10^{18}$  possible subsets to consider.

In the present study we therefore used the stepwise multiple linear regression approach to extract the potential influences on the mass balance of Great Aletsch Glacier. Although there is an assumption of linearity behind this method, Addison et al. (2004) show that the use of stepwise multiple linear regression could perform comparably to, if not better than, most other reduction methods. Stepwise multiple linear regression examines variables incorporated in the model at every stage of the regression. A variable that may have been the best choice to enter the model at an early stage may later be nonsignificant because of the relationships between it and other variables now in the regression. Once a variable is proven to be nonsignificant, it is removed from the model. This process continues until no more variables can be accepted and no more can be rejected (von Storch and Zwiers, 1999).

We performed a stepwise multiple linear regression with the monthly averages of temperature and precipitation as independent variables and the proxy of annual mass balance of Great Aletsch Glacier as an output data set (dependent). As model inputs for the BPN, we found the following subset of 12 independent variables (>99% confidence level): Meiringen (Aug, Sep), Sion (Jun, Jul), Fiesch (Jan, May, Jul, Nov) and Kippel (Feb, Jul, Oct, Dec).

Changes in glacier mass balance can be viewed as a direct, undelayed reaction of a glacier to climatic variations (Reichert et al., 2001; Nesje and Dahl, 2003). Furthermore, glacier mass is determined by taking into account the accumulation of snow, mostly in winter, and warm season ablation, and thus shows an immediate response to climate variability and site meteorological conditions. Therefore, it is not surprising that 'summer' (JJAS) temperature and 'winter' (ONDJF) precipitation turn out to be highly-correlated with the annual glacier mass balance. The high correlations of May and July precipitation could indicate that the mass balance also responds to effects of spring and summer precipitation. Furthermore, it seems that there is no (linear) relationship between the mass balance series of Great Aletsch Glacier and the Lauterbrunnen precipitation series.

In contrast to the proxy-based reconstruction back to 1500 (see next Section 3.3.2), we use monthly data for a reconstruction of the 20th-century mass balance. In this way a choice of potential climatic driving factors is more differentiated and probably leads to better model performance.

Before feeding the BPN, the data are standardized to 1919–99 mean and standard deviation (z-transformation) so that temperature and precipitation are in comparable units (for robust NN performance). After fitting the BPN with the conjugate gradient descent method, the full model was used to reconstruct a proxy of annual mass balance from the forcing data when no output data were available. In a final step, the data were rescaled by the inverse z-transformation.



Figure 3.3 is the composite made up of the annual glacier mass balance for the 1919–99 training/validation period, presented in Section 3.2.1, and BPN predictions for those years when estimations are missing (1900–18, 2000–03). An error envelope (95% confidence interval) based on the RMS errors in predictions appears around each section of BPN prediction (Mann and Jones, 2003; Reusch and Alley, 2004). The simulation and the reconstruction are the average outputs of 30 model runs to reduce the effect of falling into local minima (see Section 3.2.4).

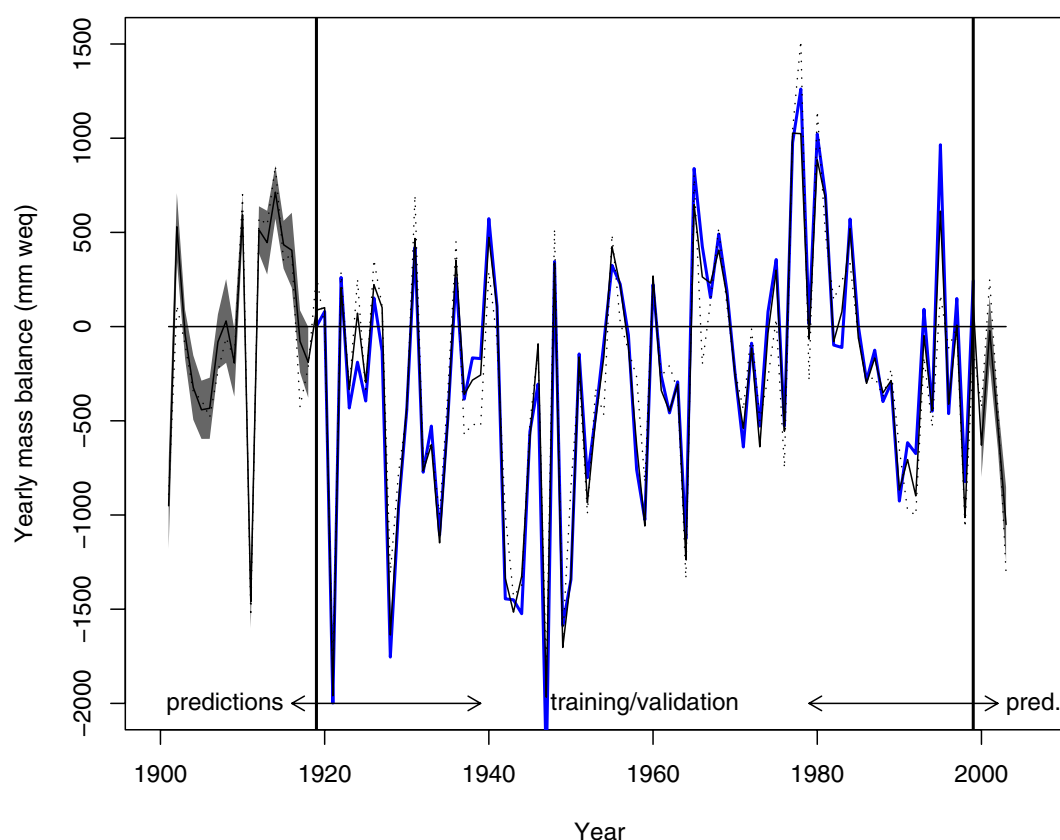


**Figure 3.3:** Results of the Backpropagation Network (BPN) simulation and reconstruction (solid black line). Also shown is the proxy of annual glacier mass balance (thick blue line) for the 1919–99 period and the output of the stepwise multiple linear regression (dotted black line). Confidence intervals derived from RMS errors appear as gray envelopes around predictions.

The simulation quality over the 1919–99 training/validation period amounts to 97.3% of explained variance, while the stepwise multiple linear regression model driven by the same input data ends with an explained variance of 86.3%. Chen and Funk (1990) applied a similar multiple linear regression approach to reconstruct the mass balance of Rhone Glacier. They used mean annual precipitation and mean summer temperature of nearby stations as model inputs. So our stepwise multiple linear regression model represents a refinement of their approach with higher resolution data.

To ensure that the neural network has captured most relevant mechanisms, the residuals of the simulations must be tested. This is usually done by testing for Gaussian distribution of the residuals.

In the case of a nonlinear neural network, the residuals undergo nonlinear transformations during the training of the network. Therefore, the residuals do not have to be Gaussian distributed even if the model captured all relevant mechanisms and the residuals are in fact (white) noise. An alternative statistical method for testing residuals of this kind is the autocorrelation function. If the residuals are indeed white noise, i.e. uncorrelated at all lags, the autocorrelation function should have no structure (von Storch and Zwiers, 1999; Walter and Schönwiese, 2002).

The autocorrelation coefficient of our simulations shows no significant deflection from zero (95% confidence level). Therefore the BPN captured all relevant mechanisms and the remaining residuals can be treated as white noise.

The BPN used here can simulate a proxy of annual glacier mass balance for the 20th century. While the stepwise multiple linear regression approach often under- or overestimates the extremes of the mass balance function, the trained BPN is better able to learn the intrinsic data features. A small number of NN misfits were found. Furthermore, it is possible to reconstruct missing mass balance data. For the 2000–03 period we estimated a cumulative mass balance of about –2.2 meters (Figure 3.3). This is consistent with several studies and measurements that show persistent melting of Alpine glaciers during the last two decades (Vincent et al., 2004; BUWAL et al., 2004). The beginning of the 20th century is characterized by a short period of negative mass balances (minimum around 1905) followed by a relative maximum in 1910. In 1911, a strongly negative mass balance was found, after which a period with mainly positive mass balances can be detected (maximum around 1914). Again, this is in good agreement with other mass balance reconstructions of Alpine glaciers, such as Hintereisferner, Austria (Nicolussi, 1994; Kuhn et al., 1997).

### 3.3.2 Proxy-based reconstructions of mass balance back to 1500

To reconstruct annual glacier mass balance back to 1500, we used the same method described in Section 3.3.1 but with different inputs. We focussed attention on a longer term reconstruction of mass balance. Because our data were not available in monthly resolution back to 1500, we used seasonal averages. After a stepwise multiple linear regression with the seasonal averages, calculated from gridded data sets, as independent variables and with annual glacier mass balance as output data set (dependent), the potential climate influences were chosen. Significant data sets (>99% confidence level) were winter (DJF) precipitation and summer (JJA) temperature. As presented in Section 3.3.1, the input data were standardized before training.

Figure 3.4 shows the simulation (1919–99) and the reconstruction (1500–1918) of the annual glacier mass balance, with an error envelope (grey shaded) around each section of BPN predictions based on its RMS errors (95% confidence interval). Also given are a 20-year low-pass filtered time series for the BPN simulation and reconstruction of yearly mass balance (thick blue line), and the output of the stepwise multiple linear regression (solid red line).

Figure 3.5 represents the cumulative glacier mass balance changes back to 1500, also with an error envelope (95% confidence interval). A positive slope in Figure 3.5 is the result of years with positive mass balance, indicating a mass gain and the opposite for the negative slope.

Again, the BPN was trained by the conjugate gradient descent method to simulate the mass balance over the 1919–99 training/validation period. The model was then used to reconstruct annual mass changes since 1500 by averaging 30 different BPN runs that started from different points in the space of possible weights. In this case the simulation skill amounts to 60.8% of explained variance, while the stepwise multiple linear regression approach driven by the same input data accounts for 54.8% of explained variance. Again, the autocorrelation coefficient function indicates no significant

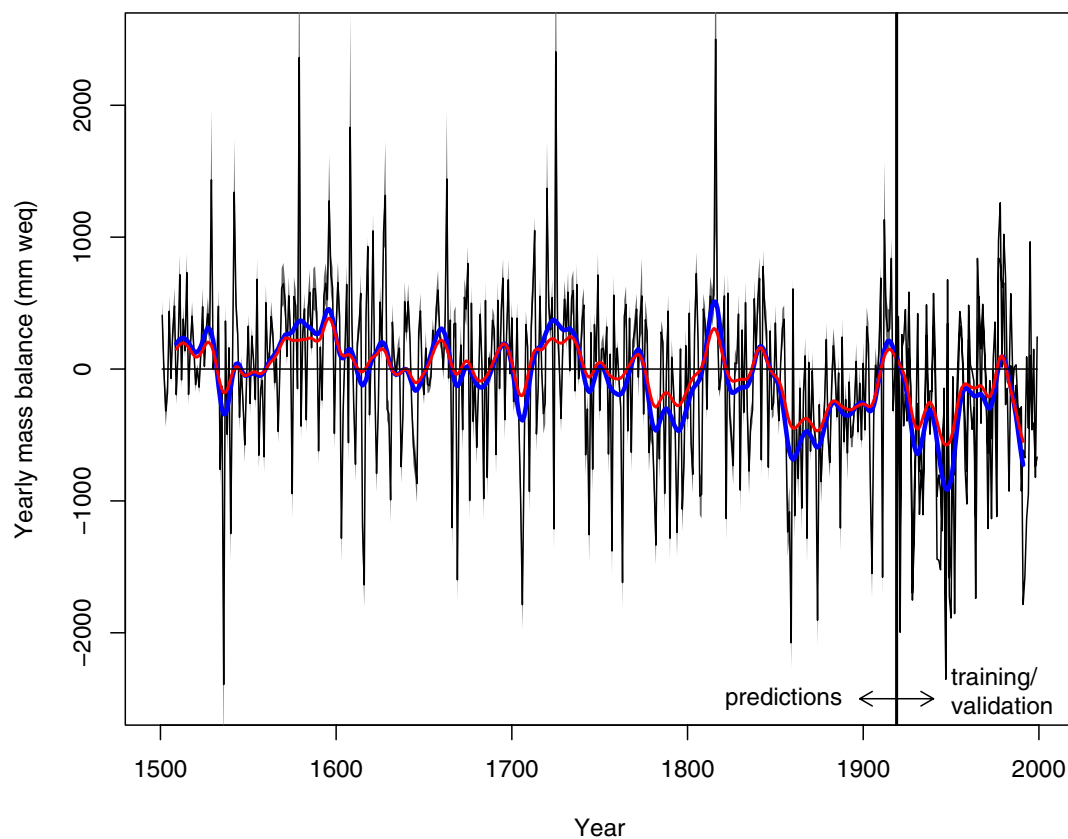


**Figure 3.4:** Results of the Backpropagation Network (BPN) simulation and reconstruction (solid black line) of yearly mass balance. Confidence intervals derived from RMS errors appear as gray envelopes around predictions. Also shown is the proxy of annual glacier mass balance for the 1919–99 period. The smoothed thick blue line represents the 20-year low-pass filtered time series of the results of the BPN simulation and reconstruction. The smoothed solid red line is the 20-year low-pass filtered output of the stepwise multiple linear regression model.

deflection from zero (95% confidence level).

A comparison of the reconstructed cumulative mass balance of Great Aletsch Glacier and the statistics of front positions of nearby Lower Grindelwald Glacier (e.g. Zumbühl et al., 1983; Holzhauser and Zumbühl, 2003), provided in Figure 3.5, shows correlation coefficients of  $r=0.89$  for the overlapping 1535–1983 period and  $r=0.69$  for the 1535–1918 reconstruction period.

Figures 3.4 and 3.5 show significant trends in glacier mass balance fluctuations over the past five centuries.

Around the mid-16th century, Great Aletsch Glacier showed generally negative mass balances, with a consequent minimum in cumulative mass balance at this time. As shown in Figures 3.6 and 3.7 (Luterbacher et al., 2004; Pauling et al., 2005), this coincides with an extended period of higher summer temperatures. This period ends when winter precipitation increases.

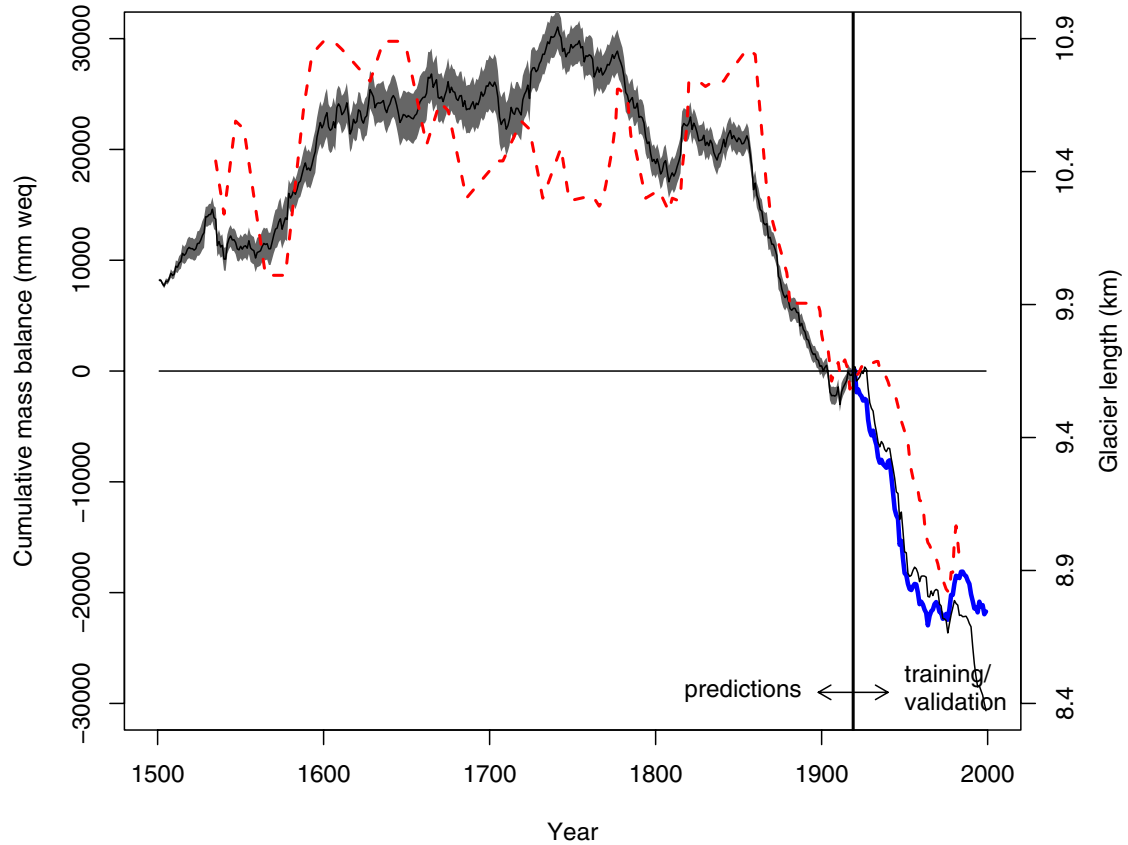


**Figure 3.5:** Cumulative glacier mass balance changes in Great Aletsch Glacier for the 1500–1999 period (1919=0). The thick blue line represents the mass changes observed (1919–99); the solid black line is the result of the BPN simulation and reconstruction. Also shown is an error envelope (gray shading) around the predictions of cumulative mass balance. The dashed red line shows the length fluctuations of nearby Lower Grindelwald Glacier, 1535–1983.

The maximum mass balances around 1600 are connected with low summer temperatures and average winter precipitation. These conditions led to low ablation rates and an extended period of increasing mass balance.

During the next century (~1610–1710) mass balance remained static and showed a slight negative trend. Summer temperature and winter precipitation are also found to stagnate. Cumulative mass balance shows a broad plateau in the 17th century, with two relative minima in the mid-17th century and at the beginning of the 18th century.

From around 1710, decreasing summer temperatures and very high winter precipitation caused a phase of uniform positive mass balance with a mass gain. The later stagnancy of glacier mass balance is represented by a nearly constant cumulative mass balance. This period of maximal cumulative mass balance coincides with a minimum in glacier length (Haeberli and Holzhauser, 2003).

From 1770 to 1810, low winter accumulation potential and high summer ablation potential overlap,

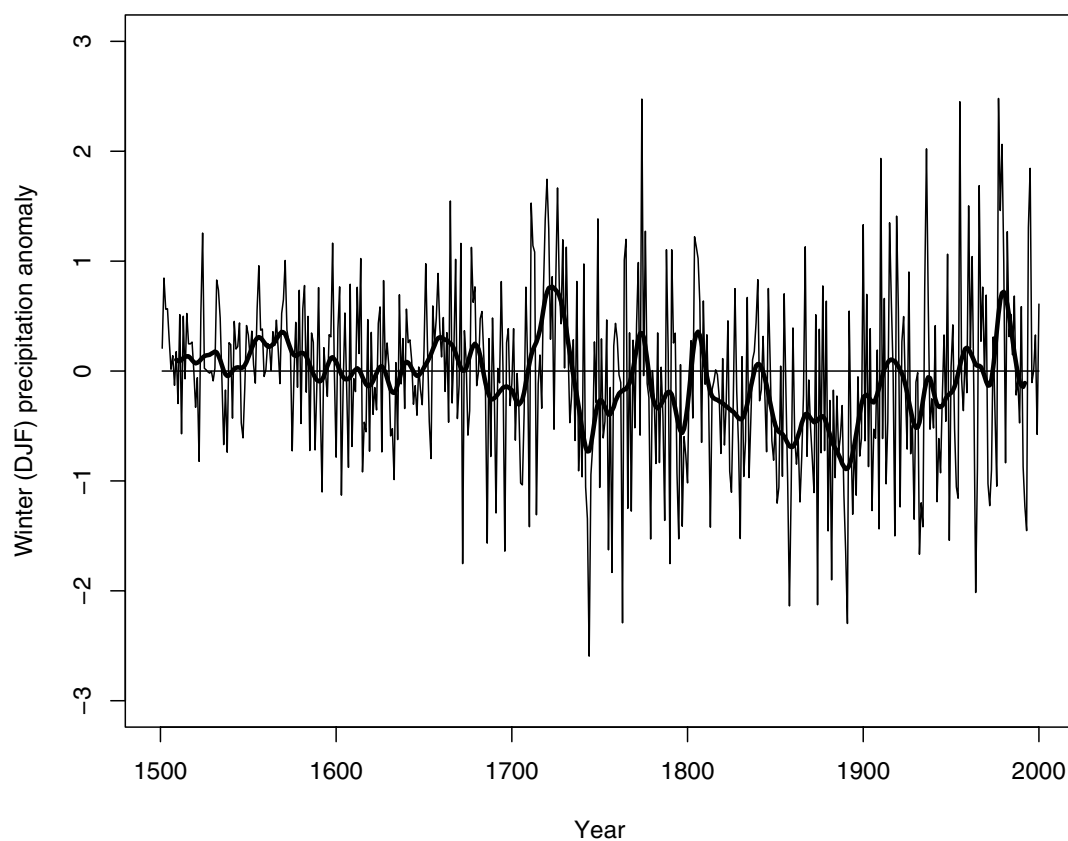


**Figure 3.6:** Winter (DJF) precipitation anomalies for the 1500–1999 period (solid line) over the grid range used in this study (after Pauling et al., 2005). Also shown is the 20-year low-pass filtered time series of the winter precipitation model input (thick line). The time series is z-standardized relative to the 1919–99 calibration average.

producing conditions favorable for negative mass balances and a resulting continuous mass loss, with a minimum of cumulative mass balance around 1810.

The 1856 glacial maximum was likely produced by 40–50 years of cool summers without anomalous positive winter precipitation, identifiable as two short periods of positive mass balance.

After 1856, higher summer temperatures and low winter precipitation caused an extended ablation-dominated mode with an enormous mass loss until the beginning of the 20th century.

From then up until the 1920s, retreat rates slowed substantially, and a small mass gain was determined. Low summer temperatures coupled with increasing winter precipitation coincided with an increasing (positive) mass balance. Note that for this time a little stagnancy in length was documented for Great Aletsch Glacier (VAW/SANW, 1881–2002; Zumbühl and Holzhauser, 1988).

The mid 1950s mass loss was characterized by high summer temperatures, while the subsequent positive mass balances in the 1980s can be explained by lower summer temperatures and high winter precipitation.

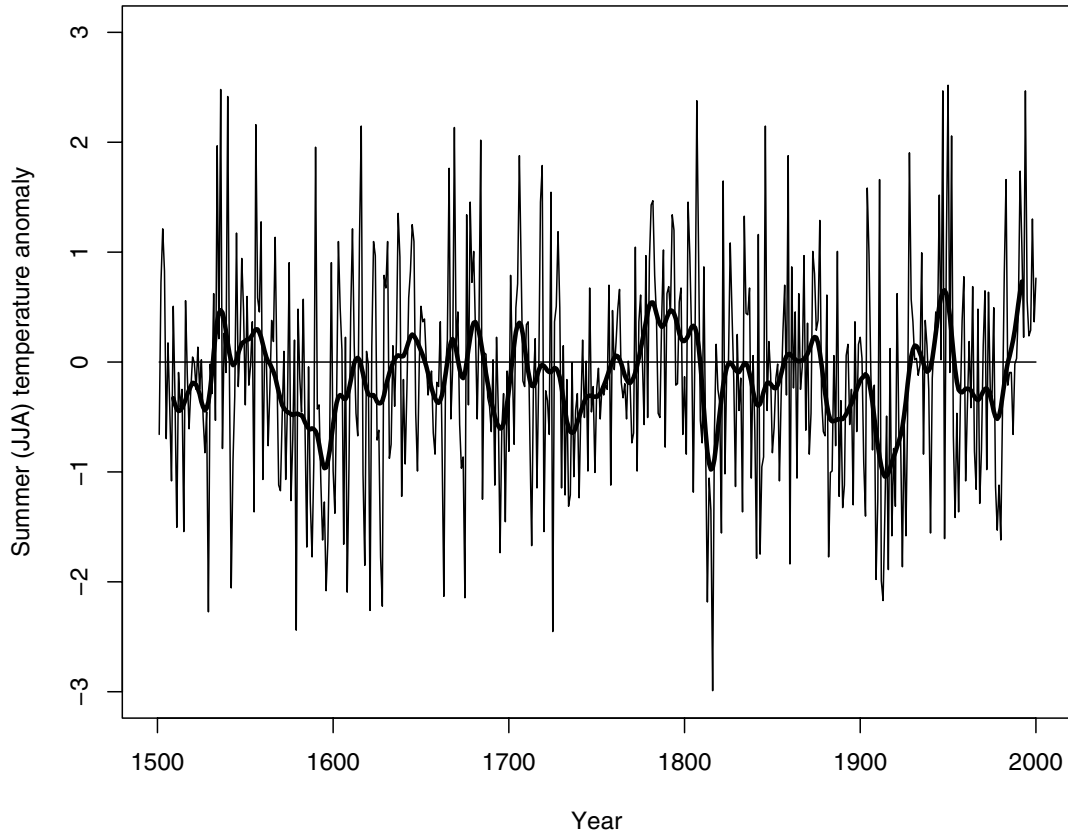


**Figure 3.7:** Summer (JJA) temperature anomalies for the 1500–1999 period (solid line) over the grid range used in this study (after Luterbacher et al., 2004). Also shown is the 20-year low-pass filtered time series of the summer temperature model input (thick line). The time series is z-standardized relative to the 1919–99 calibration average.

The evidence presented here suggests that maxima in the mass balance of Great Aletsch Glacier are predominantly caused by cold summers, often coupled with high winter precipitation. This is in good agreement with Oerlemans and Reichert (2000), who show that summer temperature is the important factor in drier (inner-Alpine) climates. Negative mass balance is mainly driven by high summer temperature. There is probably a weaker dependence on low winter precipitation, which can be influential under strong enough forcing. This longer-term model was driven by a very small number of forcing factors. So spring and fall conditions, and the effects of summer precipitation, are not taken into account.

### 3.4 Conclusions and Outlook

For the first time a NNM has been used to reconstruct the mass balance of Great Aletsch Glacier. Two new gridded data sets of temperature and precipitation were applied to the NNM as potential

driving factors of the glacier system. This was a unique opportunity to bring these two aspects, a new method and two new data sets, together.

The results of this study show that the NNM approach is a useful tool for quantifying Great Aletsch Glacier's mass balance changes in a nonlinear way. In fact, the reconstructed mass balance is the result of a combination of several climatic input variables (precipitation and temperature) that vary in their composition and input importance. It can be shown how the mass balance reacts to changes in local to regional temperature and precipitation. We observed maximum mass balances for Great Aletsch Glacier around 1600, 1730, 1815/45 and 1920. Minima in glacier mass balance were found in the 1540s, 1790s, 1870s and 1950s.

Furthermore, we confirm that summer temperature is an important driving factor for variations in mass balance. Thus the results presented here suggest that NNMs capture the appropriate dependence on the relevant inputs that likely affect a glacier system. We also conclude that the climate–mass balance relation of Great Aletsch Glacier consists of a significant nonlinear part.

In our approach we used only temperature and precipitation data as inputs for the BPN. It would be interesting to see whether other data, e.g. North Atlantic Oscillation (NAO), solar irradiance or tree rings, could improve the quality of the model. In the absence of widespread mass balance data that can be used as training sets, the possibility of using the present approach to model glacier length variations should be further investigated.

## Acknowledgments

This study was supported by the following institutions: Stiftung Marchese Francesco Medici del Vascello, and the Swiss National Science Foundation (SNSF), through its National Center of Competence in Research on Climate (NCCR Climate), project PALVAREX. The authors are grateful to MeteoSwiss, Jürg Luterbacher and Andreas Pauling for providing instrumental and multiproxy reconstructions of temperature and precipitation. Thanks also go to Andreas Bauder for providing data from Great Aletsch Glacier and for his helpful advice. The detailed comments and fruitful suggestions of Heinz Wanner, David B. Reusch, an anonymous reviewer and the Scientific Editor, Robert A. Bindenschadler, helped to improve this paper.

## Bibliography

- Addison, J. F. D., K. J. McGarry, S. Wermter, and J. MacIntyre (2004). Stepwise Linear Regression for Dimensionality Reduction in Neural Network Modelling. In M. Hamza (Ed.), *Artificial Intelligence and Applications. Proceedings of the IASTED International Conference on Artificial Intelligence and Applications*, Innsbruck, Austria, 16-18 February 2004. ACTA Press Inc., Calgary, 2 Vols., 363–368.
- Adrian, E. (1926). The impulses produced by sensory nerve endings. Part I. *Journal of Physiology (London)* 61, 49–72.
- Aellen, M. (1995). Glacier mass balance studies in the Swiss Alps. *Zeitschrift für Gletscherkunde und Glazialgeologie* 31(1–2), 159–168.
- Aellen, M. and M. Funk (1990). Bilan hydrologique du bassin versant de la Massa et bilan de masse des glaciers d'Aletsch (Alpes bernoises, Suisse). In H. Lang and A. Musy (Eds.), *Hydrology in Mountainous Regions. I – Hydrological Measurements; the Water Cycle, International Association of Hydrological Sciences (IAHS) Publ. 193*, 89–98.

- Amit, D. J. (1989). *Modeling brain function: The world of attractor neural networks*. Cambridge University Press, Cambridge.
- Anderson, J. A. and E. Rosenfeld (1986). *Neurocomputing: Foundations of Research*. MIT Press, Cambridge, MA.
- Begert, M., G. Seiz, T. Schlegel, M. Musa, G. Baudraz, and M. Moesch (2003). *Homogenisierung von Klimamessreihen der Schweiz und Bestimmung der Normwerte 1961–1990*. MeteoSchweiz, Zürich, No. 67.
- Bishop, C. M. (1995). *Neural Networks of Pattern Recognition*. Oxford University Press, Oxford, UK.
- Braithwaite, R. J. and S. C. B. Raper (2002). Glaciers and their contribution to sea level change. *Physics and Chemistry of the Earth* 27(32–34), 1445–1454, doi:10.1016/S1474–7065(02)00089–X.
- BUWAL, BWG, and MeteoSchweiz (2004). *Auswirkungen des Hitzesommers 2003 auf die Gewässer*. Bundesamt für Umwelt, Wald und Landschaft (BUWAL), Bern, No. 369.
- Chen, J. and M. Funk (1990). Mass balance of Rhône-gletscher during 1882/83–1986/87. *Journal of Glaciology* 36(123), 199–209.
- Cybenko, G. (1989). Approximation by superpositions of a sigmoidal function. *Mathematics of Control, Signal and Systems* 2(4), 303–314.
- Dao, V. N. P. and V. R. Vemuri (2002). A Performance Comparison of Different Back Propagation Neural Networks Methods in Computer Network Intrusion Detection. *Differential Equations and Dynamical Systems* 10(1/2), 201–214.
- Frei, C. and C. Schär (1998). A precipitation climatology of the Alps from high-resolution rain-gauge observations. *International Journal of Climatology* 18(8), 873–900, doi:10.1002/(SICI)1097–0088(19980630)18:8<873::AID-JOC255>3.0.CO;2–9.
- Grossberg, S. (1982). How does a brain build a cognitive code? In S. Grossberg (Ed.), *Studies of Mind and Brain: Neural principles of learning, perception, development, cognition and motor control*, Reidel Publishing, Boston, 1–52.
- Haeberli, W. and H. Holzhauser (2003). Alpine Glacier Mass Changes During the Past Two Millennia. *PAGES News* 11(1), 13–15.
- Holzhauser, H. and H. J. Zumbühl (1999). Glacier Fluctuations in the Western Swiss and French Alps in the 16th Century. *Climatic Change* 43(1), 223–237, doi:10.1023/A:1005546300948.
- Holzhauser, H. and H. J. Zumbühl (2003). Nacheiszeitliche Gletscherschwankungen. In R. Weingartner and M. Spreafico (Eds.), *Hydrologischer Atlas der Schweiz*, Bundesamt für Landestopografie, Bern–Wabern, Tafel 3.8.
- Houghton, J. T., Y. Ding, D. J. Griggs, M. Noguer, P. J. van der Linden, X. Dai, K. Maskell, and C. A. Johnson (2001). *Climate Change 2001: The Scientific Basis*. Cambridge University Press, Cambridge, UK, and New York, NY, USA.
- Hsieh, W. W. and B. Tang (1998). Applying Neural Network Models to Prediction and Data Analysis in Meteorology and Oceanography. *Bulletin of the American Meteorological Society* 79(9), 1855–1870, doi:10.1175/1520–0477(1998)079<1855:ANNMTP>2.0.CO;2.



- IAHS(ICSU)/UNEP/UNESCO (1998). *Fluctuations of Glaciers 1990–1995*, Volume VII (W. Haeberli, M. Hoelzle, S. Suter, R. Frauenfelder, Eds.). World Glacier Monitoring Service (WGMS), Paris.
- IAHS(ICSU)/UNESCO (1967). *Fluctuations of Glaciers 1959–1965*, Volume I (P. Kasser, Ed.). Permanent Service on the Fluctuations of Glaciers (PSFG), Paris.
- Jones, P. D. and M. E. Mann (2004). Climate over past millennia. *Reviews of Geophysics* 42(2), RG2002, doi:10.1029/2003RG000143.
- Kasser, P. (1954). Sur le bilan hydrologique des bassins glaciaires avec application au Grand Glacier d'Aletsch. *International Association of Hydrological Sciences (IAHS) Publ.* 39, 331–350.
- Klein, B. D. and D. F. Rossin (1999). Data Errors in Neural Network and Linear Regression Models: An Experimental Comparison. *Data Quality Journal* 5(1), 1–25.
- Kuhn, M., E. Schlosser, and N. Span (1997). Eastern Alpine glacier activity and climatic records since 1860. *Annals of Glaciology* 24, 164–168.
- Lie, Ø., S. O. Dahl, and A. Nesje (2003). Theoretical equilibrium–line altitudes and glacier buildup sensitivity in southern Norway based on meteorological data in a geographical information system. *The Holocene* 13(3), 373–380, doi:10.1191/0959683603hl630rp.
- Luterbacher, J., D. Dietrich, E. Xoplaki, M. Grosjean, and H. Wanner (2004). European Seasonal and Annual Temperature Variability, Trends, and Extremes Since 1500. *Science* 303(5663), 1499–1503, doi:10.1126/science.1093877.
- Mann, M. E. (2002). The Value of Multiple Proxies. *Science* 297(5586), 1481–1482, doi:10.1126/science.1074318.
- Mann, M. E. and P. D. Jones (2003). Global surface temperatures over the past two millennia. *Geophysical Research Letters* 30(15), 1820, doi:10.1029/2003GL017814.
- Metropolis, N., A. W. Rosenbluth, M. N. Rosenbluth, A. H. Teller, and E. Teller (1953). Equations of State Calculations by Fast Computing Machines. *Journal of Chemical Physics* 21(6), 1087–1092.
- Michaelson, J. (1987). Cross-Validation in Statistical Climate Forecast Models. *Journal of Applied Meteorology* 26(11), 1589–1600, doi:10.1175/1520-0450(1987)026<1589:CVISCF>2.0.CO;2.
- Müller-Lemans, H., M. Funk, M. Aellen, and G. Kappenberger (1994). Langjährige Massenbilanzreihen von Gletschern in der Schweiz. *Zeitschrift für Gletscherkunde und Glazialgeologie* 30(1–2), 141–160.
- Nesje, A. and S. O. Dahl (2003). The 'Little Ice Age' – only temperature? *The Holocene* 13(1), 139–145, doi:10.1191/0959683603hl603fa.
- Nicolussi, K. (1994). Jahrringe und Massenbilanz. Dendroklimatische Rekonstruktion der Massenbilanzreihe des Hintereisferners bis zum Jahr 1400 mittels *Pinus cembra*-Reihen aus den Ötztaler Alpen, Tirol. *Zeitschrift für Gletscherkunde und Glazialgeologie* 30(1–2), 11–52.
- Oerlemans, J. and B. K. Reichert (2000). Relating glacier mass balance to meteorological data by using a seasonal sensitivity characteristic. *Journal of Glaciology* 46(152), 1–6.
- Paterson, W. S. B. (1994). *The physics of glaciers*. 3rd edition. Pergamon, Oxford, UK.
- Pauling, A., J. Luterbacher, C. Casty, and H. Wanner (2005). 500 years of gridded high-resolution precipitation reconstructions over Europe and the connection to large-scale circulation. *Climate Dynamics*, revised.

- Press, W. H., S. A. Teukolsky, W. T. Vetterling, and B. P. Flannery (1992). *Numerical recipes in C: The art of scientific computing*. Cambridge University Press, Cambridge.
- Reichert, B. K., L. Bengtsson, and J. Oerlemans (2001). Midlatitude Forcing Mechanisms for Glacier Mass Balance Investigated Using General Circulation Models. *Journal of Climate* 14(17), 3767–3784, doi:10.1175/1520-0442(2001)014<3767:MFMFGM>2.0.CO;2.
- Reusch, D. B. and R. B. Alley (2004). A 15-year West Antarctic climatology from six automatic weather station temperature and pressure records. *Journal of Geophysical Research* 109(D4), D04103, doi:10.1029/2003JD004178.
- Rosenblatt, F. (1958). The Perceptron: A probabilistic model for information storage and organization in the brain. *Psychological Review* 65, 386–408.
- Rumelhart, D. E., G. E. Hinton, and R. J. Williams (1986). Learning Internal Representations by Error Propagation. In D. E. Rumelhart and J. L. McClelland (Eds.), *Parallel Distributed Processing: Explorations in the Microstructure of Cognition*, MIT Press, Cambridge, MA, 318–362.
- Rumelhart, D. E. and J. L. McClelland (1986). *Parallel Distributed Processing: Explorations in the Microstructure of Cognition*. MIT Press, Cambridge, MA, 2 Vols.
- Schüepp, M., M. Bouët, M. Bider, and C. Urfer (1978). *Regionale Klimabeschreibungen. Teil 1*. Schweizerische Meteorologische Zentralanstalt, Zürich.
- Stone, M. (1974). Cross-validation choice and the assessment of statistical predictions. *Journal of the Royal Statistical Society* B36(1), 111–147.
- van der Knaap, W. O. and J. F. N. van Leeuwen (2003). Climate–pollen relationships AD 1901–1996 in two small mires near the forest limit in the northern and central Swiss Alps. *The Holocene* 13(6), 809–828, doi:10.1191/0959683603hl657rp.
- VAW/SANW (1881–2002). *Die Gletscher der Schweizer Alpen. Jahrbücher der Glaziologischen Kommission der Schweizerischen Akademie der Naturwissenschaften (SANW)*. Versuchsanstalt für Wasserbau, Hydrologie und Glaziologie (VAW) der ETH Zürich, Zürich, No. 1–122. (<http://glaciology.ethz.ch/swiss-glaciers/>).
- Vincent, C., G. Kappenberger, F. Valla, A. Bauder, M. Funk, and E. Le Meur (2004). Ice ablation as evidence of climate change in the Alps over the 20th century. *Journal of Geophysical Research* 109(D10), D10104, doi:10.1029/2003JD003857.
- von Storch, H. and F. W. Zwiers (1999). *Statistical Analysis in Climate Research*. Cambridge University Press, Cambridge.
- Walter, A. (2001). *Zur Anwendung neuronaler Netze in der Klimatologie*. Deutscher Wetterdienst (DWD), Offenbach a.M., Deutschland, No. 218.
- Walter, A. and C.-D. Schönwiese (2002). Attribution and detection of anthropogenic climate change using a backpropagation neural network. *Meteorologische Zeitschrift* 11(5), 335–343, doi:10.1127/0941-2948/2002/0011-0335.
- Walter, A. and C.-D. Schönwiese (2003). Nonlinear statistical attribution and detection of anthropogenic climate change using simulated annealing algorithm. *Theoretical and Applied Climatology* 76(1–2), 1–12, doi:10.1007/s00704-003-0008-5.
- Wu, A. and W. W. Hsieh (2003). Nonlinear interdecadal changes of the El Niño–Southern Oscillation. *Climate Dynamics* 21(7–8), 719–730, doi:10.1007/s00382-003-0361-1.

Zumbühl, H. J. and H. Holzhauser (1988). Alpengletscher in der Kleinen Eiszeit. Sonderheft zum 125jährigen Jubiläum des SAC. *Die Alpen* 64(3), 129–322.

Zumbühl, H. J., B. Messerli, and C. Pfister (1983). *Die kleine Eiszeit: Gletschergeschichte im Spiegel der Kunst. Katalog zur Sonderausstellung des Schweizerischen Alpen Museums Bern und des Gletschergarten-Museums Luzern vom 09.06.–14.08.1983 (Luzern), 24.08.–16.10.1983 (Bern).*

### 3.5 Appendix 1

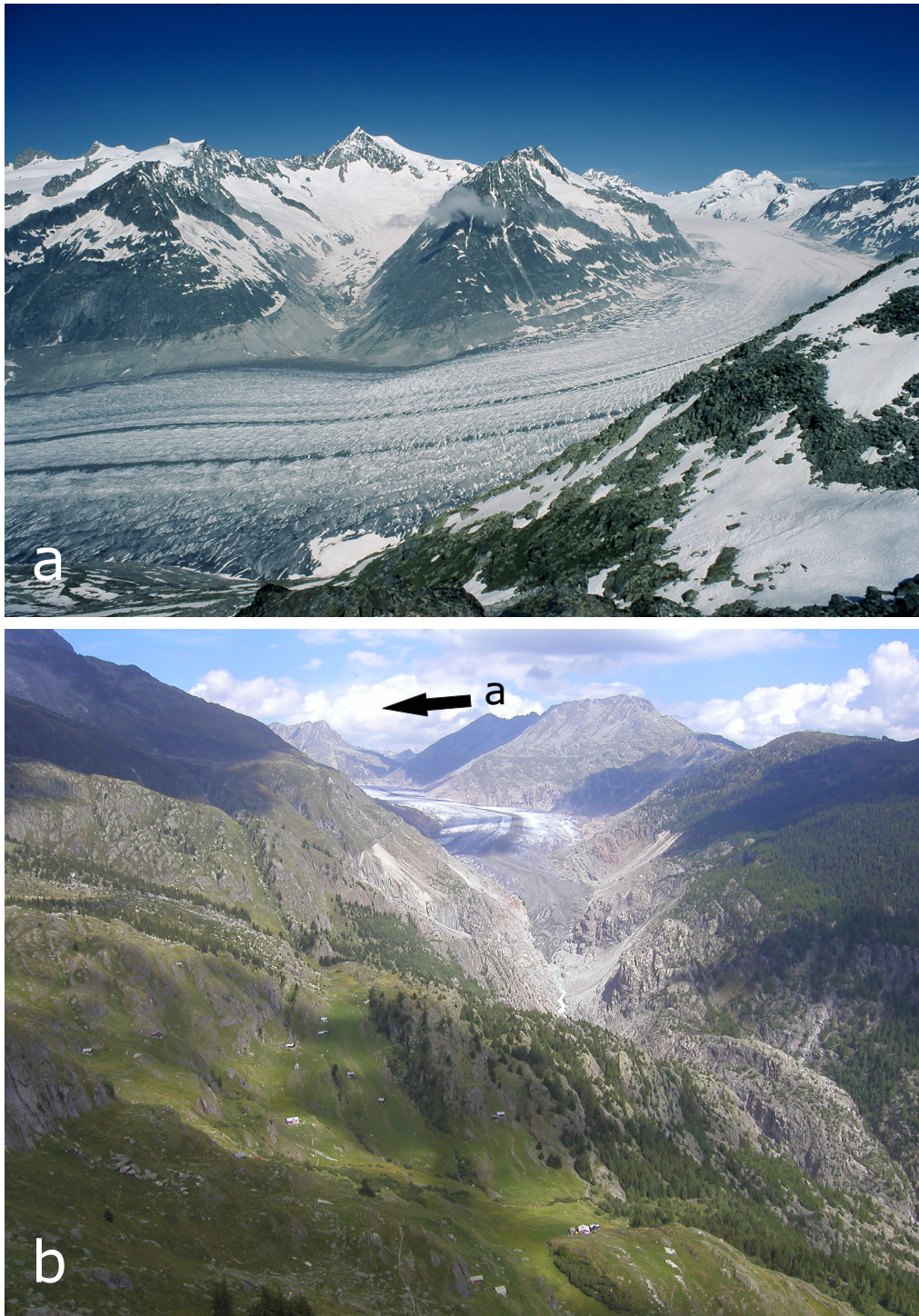


**Figure 3.8:** (a) *The Great Aletsch Glacier, Switzerland, from the Eggishorn. Photograph by Heinz J. Zumbühl, 22.7.1994.*

(b) *The snout of the Great Aletsch Glacier, Switzerland. Photograph by Christian Theler, 3.9.2004.*

## Chapter 4

# Sensitivity of European Glaciers to Precipitation and Temperature – Two case studies

Daniel **Steiner**<sup>1,2</sup>, Andreas **Pauling**<sup>1</sup>, Atle **Nesje**<sup>3</sup>, Jürg **Luterbacher**<sup>1,2</sup>, Heinz **Wanner**<sup>1,2</sup>, Heinz Jürg **Zumbühl**<sup>1</sup>

<sup>1</sup> Meteorology and Climatology, Institute of Geography, University of Bern, Switzerland

<sup>2</sup> NCCR Climate, University of Bern, Switzerland

<sup>3</sup> Department of Earth Science, University of Bergen, Norway

*Climate Dynamics; submitted (July 2005)*

### Abstract

*A nonlinear Backpropagation Neural Network (BPN) has been trained with high-resolution multi-proxy reconstructions of temperature and precipitation (input data) and glacier length variations of the Alpine Lower Grindelwald Glacier, Switzerland (output data). The model was then forced with two regional climate scenarios of temperature and precipitation derived from a probabilistic approach: The first scenario ("no change") assumes no changes in temperature and precipitation for the 2000–50 period compared to the 1970–2000 mean. In the second scenario ("combined forcing") linear warming rates of 0.036–0.054 °C per year and changing precipitation rates between –17% and +8% compared to the 1970–2000 mean have been used for the 2000–50 period. In the first case the Lower Grindelwald Glacier shows a continuous retreat until the 2020s when it reaches an equilibrium followed by a minor advance. For the second scenario a strong and continuous retreat of approximately –30 meters per year since the 1990s has been modelled.*

*By processing the used climate parameters with a sensitivity analysis based on neural networks we investigate the relative importance of different climate configurations for the Lower Grindel-*

*wald Glacier during four well-documented historical advance (1590–1610, 1690–1720, 1760–1780, 1810–1820) and retreat periods (1640–1665, 1780–1810, 1860–1880, 1945–1970). It is shown that different combinations of seasonal temperature and precipitation have led to glacier variations. In a similar manner, we establish the significance of precipitation and temperature for the well-known early 18th century advance and the 20th century retreat of Nigardsbreen, a glacier in western Norway. We show that the maritime Nigardsbreen Glacier is more influenced by winter and/or spring precipitation than the Lower Grindelwald Glacier.*

**Keywords:** sensitivity analysis, climate variability, glacier variations, temperature, precipitation, length simulation, Backpropagation Neural Network

## 4.1 Introduction

Primarily motivated by investigations of climate change, the scientific community has become increasingly aware that mountains and their environments are highly sensitive indicators of climate variability over the decadal to centennial timeframe. Glaciers have become the subject of intensive observation because their fluctuations are an impressive manifestation of varying climatic conditions. Corresponding to global trends in temperature, they have retreated significantly since the mid-19th century (e.g. McCarthy et al., 2001; Houghton et al., 2001; Paul et al., 2004; Oerlemans, 2005).

Many studies have been carried out to investigate the relationship between climatic signals and variations of glaciers. For this purpose, regression techniques have often been used to relate for instance mean mass balance to climatic variables. In these studies the number and type of predictors may differ significantly and depend on what is inferred to influence glacier mass balance (e.g. Oerlemans and Reichert, 2000, and references therein). Direct measurements of mass balance are labour-intensive, expensive to maintain and therefore few in number. Most of these records are short and cover only the late 20th/early 21st centuries (Vincent et al., 2005).

On the other hand some long records of front positions of glaciers in Europe are available. The longest and one of the best-documented record is that of the Lower Grindelwald Glacier which starts in 1535 (Zumbühl, 1980; Zumbühl et al., 1983; Oerlemans, 2005). Change in glacier length is an easily measured but indirect, filtered and delayed response of climate change (Oerlemans, 2001). Nevertheless, it can be used to reconstruct glacier mass balance (Haerberli and Hoelzle, 1995; Hoelzle et al., 2003) as well as large scale temperature changes over the last centuries (Oerlemans, 2005).

However, the complexity of available glacier-climate models is as wide as the possible application of such models. The models range from those using air temperature as a sole index for energy available for melt to those that evaluate the surface energy fluxes to great details (e.g. Reichert et al., 2001; Nesje and Dahl, 2003; Klok and Oerlemans, 2004). Besides these classical methods that commonly use linear assumptions, Neural Network Models (NNMs) have become popular for performing non-linear regression and classification since the late 1980s (e.g. Hsieh, 2004, and references therein). A neural network (NN) is an information processing paradigm that is inspired by the way biological nervous systems, such as the brain, process information.

Thus, NNs, with their remarkable ability to derive meaning from complicated data, can be used to extract patterns and detect trends that are too complex to be noticed by either humans or other computer techniques.

An objective of the present paper is to show the capabilities of nonlinear NNs in a glaciological context. It is also intended to be a follow-up to a first study on this subject (see Section 3; Steiner et al., 2005a), which proposes a NN method to reconstruct the mass balance series of the Great Aletsch

Glacier, Switzerland, back to 1500. That study dealt only with monthly and seasonal temperature and precipitation data as driving factors of the glacier model and on a mass balance record as target variable.

Thus, besides the problem of simulating future glacier front variations of the Lower Grindelwald Glacier, a sensitivity analysis of potential climatic influences on two appropriate glaciers, using a NN approach, is discussed here.

In section 4.2 we give an overview of the data used in this study and the concept of the neural network (NN) approach. As an example for a NN, we discuss the Backpropagation Network (BPN). Furthermore, we perform a sensitivity analysis based on a BPN to measure the time-dependent influence of temperature and precipitation on the Lower Grindelwald Glacier, Switzerland, and Nigardsbreen Glacier, Norway.

Section 4.3 deals with the simulation of future length variations of the Lower Grindelwald glacier, Switzerland, by using neural networks. Furthermore, we analyze the sensitivity of glacier variations to seasonal temperature and precipitation, again based on NNs. For an independent comparison we apply this method to Nigardsbreen Glacier, Norway.

In section 4.4 the results and the performance of the used methods are discussed. In section 4.5 conclusions are provided and further scientific investigations are proposed.

## 4.2 Data and methods

### 4.2.1 The study sites

Figure 4.1 shows the topography and some locations within the greater region of the Lower Grindelwald Glacier, situated in the northern Bernese Alps (western Switzerland) and the location of the Lower Grindelwald Glacier in Switzerland. Table 4.1 gives some characteristics, Figure 4.11 some current impressions of the Lower Grindelwald Glacier.

The Bernese Alps are one of the main European watersheds, separating the catchment area of the Aare (draining into the North Sea via the Rhine) from that of the Rhône (which flows into the Mediterranean Sea). According to their geographic situation between 46° and 47°N, the climate of the Bernese Alps is of temperate character, typical for the southern side of the extratropical westerlies. It constitutes a border between the Mediterranean and the North Atlantic climate zone (Wanner et al., 1997). The northern part of the Bernese Alps, exposed to the westerlies, shows maximum precipitation during summer, with quite low variability. The mean annual temperature at Grindelwald (1040 meters asl.), located approx. 3 kilometers from the glacier front of the Lower Grindelwald Glacier, was 6.7°C during the 1966–89 period. The mean temperature during the accumulation season (October–April) and ablation season (May–September) during the 1966–89 period was 2.3°C and 12.9°C, respectively. The mean annual precipitation during the 1961–90 normal period was 1428 mm. The precipitation during the accumulation season (October–April) and ablation season (May–September) during the 1961–90 normal period was 720 mm and 708 mm, respectively (data from the online database of MeteoSwiss). Mean cloudiness is higher in the north. This results in an increase in the height of the mean glacier elevation from about 2500 meters asl. in the northern part of the Bernese Alps to 2900 meters asl. in the south. Because of the high precipitation (locally exceeding 4000 mm per year), the Bernese Alps show a relative low glacier equilibrium line altitude (ELA) and are the mountain range showing the heaviest glacierization of the Alps. Both the glacier with the lowest front (Lower Grindelwald Glacier; this study) and the largest glacier of the Alps (Great Aletsch Glacier; see Section 3) are situated within this region (Kirchhofer

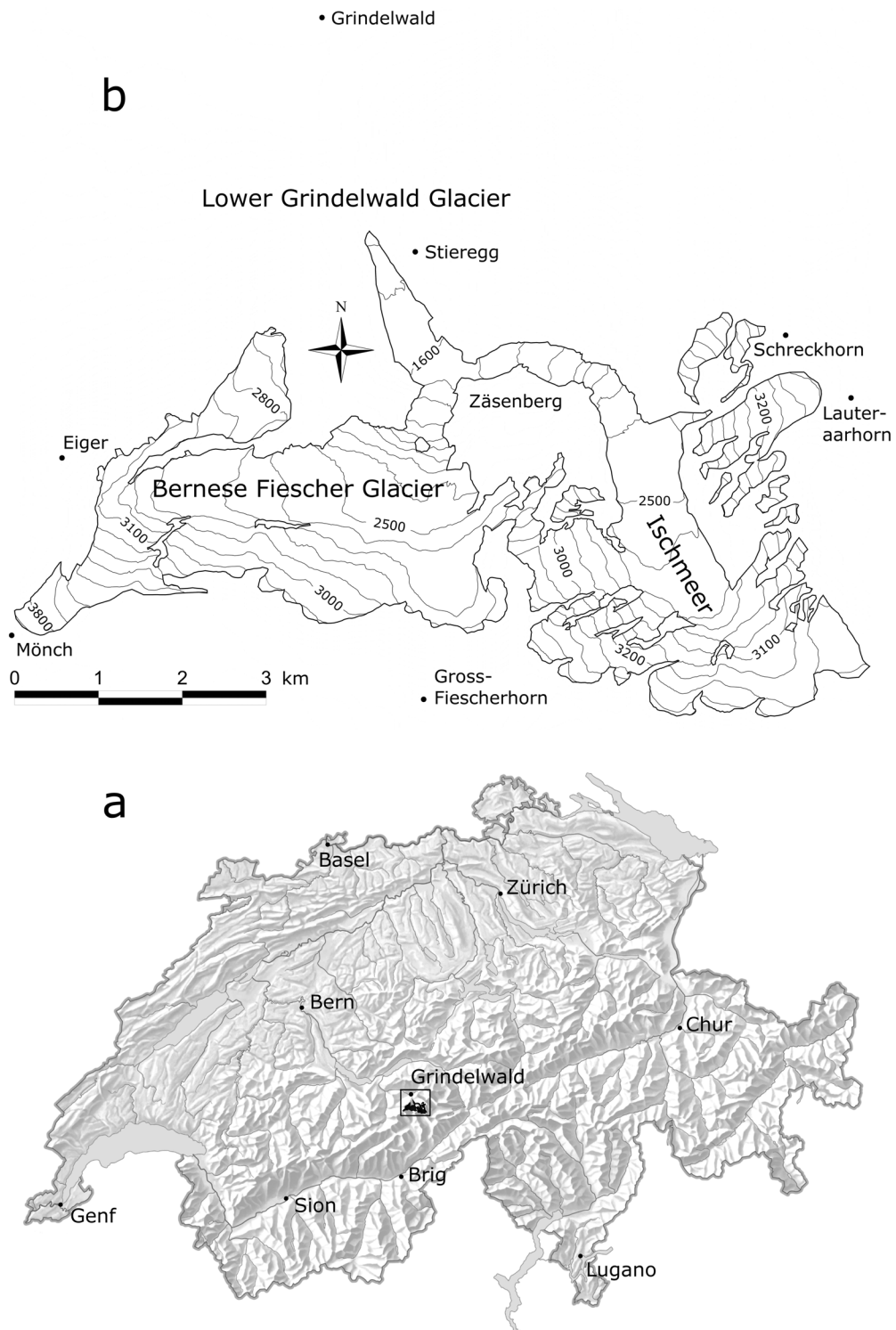


**Figure 4.1:** (a) The Grindelwald region (area with solid outline) within Switzerland.

(b) Map showing some remarkable locations, mountain peaks and the topography of the Lower Grindelwald Glacier with its main branches and tributaries.



and Sevruk, 1992; Imhof, 1998).

The Nigardsbreen Glacier is an outlet from the largest ice cap in Norway, Jostedalsbreen (487 km<sup>2</sup>). Figure 4.2 shows the location of the glacier within western Norway. Shown is also a map of the glacier tongue and its foreland, together with dates of the formation of some of the moraines. Table 4.1 shows some characteristics, Figure 4.10 an impression of the Nigardsbreen Glacier. The mean

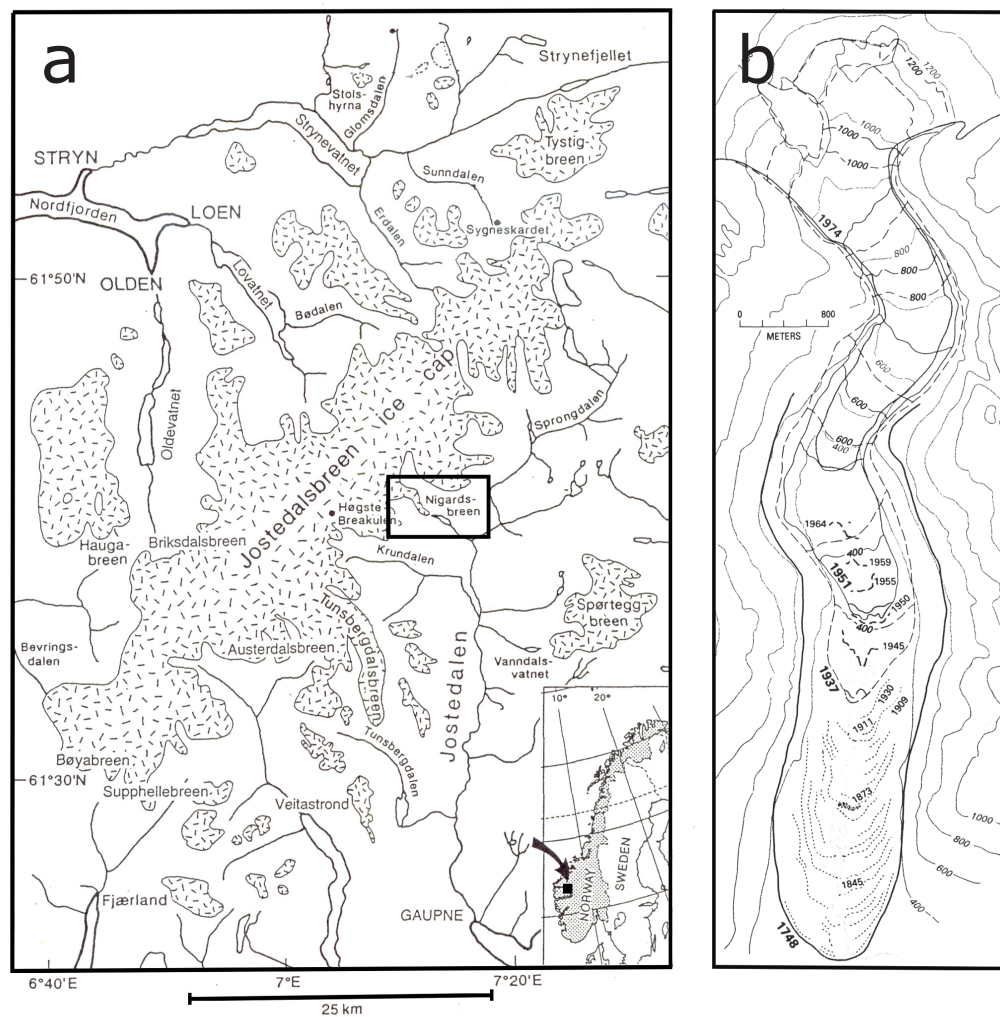


**Figure 4.2:** (a) Map showing the Jostedalsbreen ice cap with its main branches.

(b) The tongue of the Nigardsbreen Glacier and its foreland with dates for the formation of some moraines (Østrem et al., 1977).

annual temperature at Bjørkehaug (324 meters asl.), located approx. 5 kilometers from the glacier front of Nigardsbreen, was 3.7°C during the 1961–90 normal period. The mean temperature during the accumulation season (October–April) and ablation season (May–September) during the 1961–90 normal period was –1.4°C and 10.9°C, respectively. The mean annual precipitation during the 1961–90 normal period was 1380 mm. The precipitation during the accumulation season (October–April) and ablation season (May–September) during the 1961–90 normal period was 920 mm and 460 mm, respectively (data from the Norwegian Meteorological Institute).

	Lower Grindelwald Glacier	Nigardsbreen
Geographical coordinates	46°35'N, 8°05'E	61°45'N, 7°08'E
Length (km)	8.85	9.6
Surface area (km <sup>2</sup> )	20.6	48.2
Elevation of head (m asl.)	4107	1950
Elevation of terminus (m asl.)	1297	355
Average height (m asl.)	2840	1150
Equilibrium line altitude ELA (m asl.)	2640	1560
Exposure	N–NW	E–SE
Average slope (%)	31.8	16.6
Firn fields	Ischmeer Bernese Fiescher Glacier	

**Table 4.1:** *Topographical characteristics of the Lower Grindelwald Glacier, Switzerland (data from 2004: Steiner et al., 2005b), and Nigardsbreen Glacier, Norway (data from 1986: Østrem et al., 1988).*

#### 4.2.2 Multiproxy reconstructions of temperature and precipitation back to 1500

Luterbacher et al. (2004) and Xoplaki et al. (2005) reconstructed monthly European surface air temperature patterns back to 1659 and seasonal estimates from 1500–1658 at  $0.5^\circ \times 0.5^\circ$  resolution. Reconstructions are developed using principal component regression analysis. The leading Empirical Orthogonal Functions (EOFs) of the predictor data variance and the leading EOFs of the total predictand variability (gridded temperature; New et al., 2000; Mitchell and Jones, 2005) are calculated for the 1901–1960 calibration period. A multivariate regression is then performed against each of the grid point EOFs of the calibration period against all the retained EOFs of the predictor data. Applying the multivariate regression model to independent data from the verification period 1961–1995 allows testing the quality of the reconstructions. In a final step, a recalibration over the 1901–1995 period has been done in order to derive the final temperature patterns for the period 1500–1900 for the European land areas (see Luterbacher et al., 2004 for a detailed description of the reconstruction methods, the used predictor data and the reliability of the reconstructions). Due to the changing number of the predictor data over time, several hundreds of nested models for the 1500–1900 period have been developed for the temperature reconstructions. For this application, the winter and summer temperature estimates of Luterbacher et al. (2004) have been reperformed using a few additional predictor data and fitting to the Mitchell and Jones (2005) updated data.

Using the same methods as Luterbacher et al. (2004) and Xoplaki et al. (2005) for their temperature reconstructions, Pauling et al. (2005) reconstructed seasonal precipitation back to 1500. That gridded dataset ( $0.5^\circ \times 0.5^\circ$  resolution) covers all Europe (land area only). It is based on a combination of long instrumental records, indices based on documentary evidence and natural proxies (tree-rings, ice cores, corals and speleothems). Reconstructive skill has been estimated by the Reduction of Error (RE) statistic that was calculated using 1901–56 for calibration and 1957–83 for verification. RE

values of 1 indicate a perfect reconstruction, and reconstructions with any RE value greater than zero are better than climatology. The final models that were used for the reconstructions back to 1500 are based on the 1901–83 period. For details on the precipitation reconstructions see Pauling et al. (2005).

For the sensitivity analysis of the Lower Grindelwald Glacier we selected the nearest grid point 8.25°E/46.75°N of the reconstructions to the glacier location. Regarding precipitation in the Nigardsbreen region, we selected the average over the region 5–7°E/60–62°N (winter) and 17–20°E/63–65°N (spring) as this is the nearest region where reconstructive skill is above zero. For the selected Nigardsbreen area (5–7°E/60–62°N), the reconstructed temperature data can be considered as reliable (Luterbacher et al., 2004).

### 4.2.3 Climate scenarios for the Swiss Alpine region

Climate scenarios are plausible representations of future climate that have been constructed for explicit use in investigating the potential impacts of anthropogenic climate change. Climate scenarios often make use of climate projections (descriptions of the modelled response of the climate system to scenarios of greenhouse gas and aerosol concentrations), by manipulating model outputs and combining them with observed climate data (Houghton et al., 2001).

A main problem of climate scenarios are the large uncertainties associated with these model projections, and that uncertainty estimates are often based on expert judgement rather than objective quantitative methods. In a probabilistic approach such uncertainties can be partially quantified from ensembles of climate change integrations, made using different models starting from different initial conditions (Frei, 2004). For the global mean temperature several probabilistic climate projections have been developed by Wigley and Raper (2001) and Knutti et al. (2002).

Results from regional climate model simulations (Schär et al., 2004; Stott et al., 2004), under the IPCC SRES A2 transient greenhouse-gas scenario ("business-as-usual"), suggest increasing summer temperatures in central and southern Europe within the 21st century with about every second summer that will be as hot or even hotter than 2003 by the end of the 21st century (2071–2100).

Frei (2004) performs regional probabilistic projections of temperature and precipitation for the Swiss Alpine region based on simulations with 16 different climate model chains. The IPCC SRES A2 and IPCC SRES B2 ("dynamics-as-usual") emission scenarios were used as model inputs. Table 4.2 shows the two climate scenarios for the 2000–2050 period used in this study. Scenario 1 represents the "no change" climate, i.e. no changes in temperature and precipitation up to 2050 compared to the 1970–2000 mean. Scenario 2 ("combined forcing") stands for the response of the climate system to expected (anthropogenic) forcings. The two climate scenarios have been used as input data to the NN model to simulate future glacier length variations (see Section 4.3.1).

### 4.2.4 Backpropagation Neural Networks as modelling and analysis tools

Inspired by the structure of the human brain, a neural network (NN) consists of a set of highly interconnected units, which process information as a response to external stimuli. A NN is thus a simplistic mathematical representation of the brain that emulates the signal integration and threshold firing behavior of biological neurons by means of mathematical equations.

There are many types of NN models (NNMs); some are only of interest to neurological researchers, while others are general nonlinear data techniques. The most widely used NNMs are the feedforward neural networks (Rumelhart et al., 1986). Their applications cover a broad field of the environmental

	P_DJF	P_MAM	P_JJA	P_SON	T_DJF	T_MAM	T_JJA	T_SON
<b>scenario 1</b>	No change in climate: 1970–2000 mean							
<b>scenario 2</b>	+8%	0%	–17%	–6%	+1.8°C	+1.8°C	+2.7°C	+2.1°C

**Table 4.2:** Two regional climate scenarios for the northern part of the Swiss Alps. The values refer to the change between the 1970–2000 period and the 2035–2065 period (Frei, 2004). The time series of winter (DJF), spring (MAM), summer (JJA), autumn (SON) precipitation (P) and temperature (T) are abbreviated as "P\_DJF", "T\_DJF", "P\_MAM", "T\_MAM", "P\_JJA", "T\_JJA", "P\_SON" and "T\_SON", respectively.

sciences including meteorology and climatology. Some examples of recent applications using NN include the tropical Pacific sea–surface temperature prediction (Yuval, 2001), efficient radiative transfer computation in atmospheric general circulation models (Chevallier et al., 2000), and the detection of anthropogenic climate change (Walter and Schönwiese, 2002; Walter and Schönwiese, 2003). For a general overview of applications of neural networks in environmental sciences, see Hsieh and Tang (1998).

In this study the standard NNM, the Backpropagation Network (BPN), was applied (Rumelhart et al., 1986). This network architecture is based on a supervised learning algorithm to find a minimum cost function. In contrast to a simulated annealing schedule (Metropolis et al., 1953), the BPN does not guarantee that the global minimum of this cost function will be reached, though it is very likely that a minimum good enough to reproduce responses in the data can be found. Because this approach bears a certain risk of overfitting, the data have to be separated into a training and a validation subset. The actual 'learning' process of the network is performed on the training subset only, whereas the validation subset serves as an independent reference for the simulation quality. This technique is called Cross–Validation (Stone, 1974; Michaelson, 1987). When applying NNMs to a nonstationary time series, as in this approach, the training subset includes the full range of extremes in both predictors and predictands. Otherwise, the algorithm will fail during the validation process if confronted with an extreme value that was not part of the training subset. We used 75% of all data for training and the remaining 25% for validation (Walter and Schönwiese, 2003).

A typical NNM consists of three layers: input, processing and output layers. Figure 4.3 shows an example of a simplified neural network. The input to an NNM is a vector of elements  $x_k$ , where the index  $k$  stands for the number of input units in the network (Input Layer in Figure 4.3). In this study two new gridded ( $0.5^\circ \times 0.5^\circ$  resolution) multiproxy reconstructions (see Section 4.2.2) of seasonal temperature (Luterbacher et al., 2004) and precipitation fields (Pauling et al., 2005) from 1500–2000 for European land areas were used as input data. These inputs are weighted with weights  $w_{jk}$  where  $j$  represents the number of processing units, to give the inputs to the processing units.

Using too few/many processing units can lead to underfitting/overfitting problems because the simulation results are highly sensitive to the number of processing units and learning parameters. Therefore a variety of BPNs must be checked to obtain robust results.

For the simulation of the glacier length variations of the Lower Grindelwald Glacier we used six potential input units as forcings (T\_MAM, T\_JJA, T\_SON, P\_DJF, P\_MAM, P\_SON), each of them have been stepwise shifted so that all lags between 0 and 45 years are considered to account for the uncertain and changing reaction time of this glacier. In this manner the NNM will use those shifted input series that explain the behaviour of the target function.

Hence, there are  $46 \cdot 6 = 276$  input units (climate variables), 138 processing units in 1 processing layer and the length fluctuations as output unit. This NN architecture is abbreviated as 276–138–1.

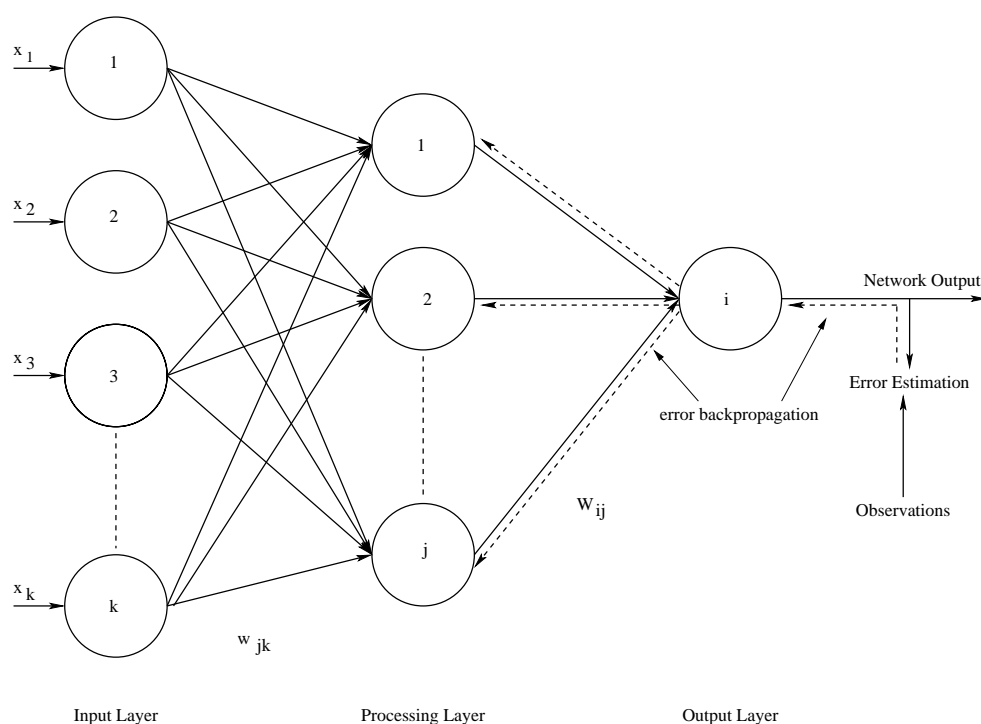


**Figure 4.3:** An example of a simplified three-layer  $k$ - $j$ -1 BPN architecture. Also shown is the concept behind the Backpropagation training algorithm.

In the case of the sensitivity analysis of Nigardsbreen, a 105–53–1 architecture was applied because only five forcing time series (T\_MAM, T\_JJA, T\_SON, P\_DJF, P\_MAM) were available. The number of processing units is half the number of inputs (climate variables). This number has been determined after a time-consuming procedure by repeated simulations with different numbers of processing units and by analyzing the performance on the validation sample.

After weighting and summation of the inputs, the results were passed to nonlinear activation functions (e.g. sigmoid functions) in each processing unit (Processing Layer in Figure 4.3). These functions produced the output of the processing layer. The outputs of the processing units are fed to the output layer where they are again weighted with the weights  $W_{ij}$ . The use of a second activation function will finally produce the output of the network (Output Layer in Figure 4.3).

The purpose of training a NNM is to find a set of coefficients that reduces the error between the model outputs and the given test data  $y(x_k)$ . This is usually done by adjusting the weights  $W_{ij}$  and  $w_{jk}$  to minimize the least square error. One way to adjust these weights is error backpropagation. The backpropagation training consists of two passes of computation: a forward pass and a backward pass. In the forward pass an input vector is applied to the units in the input layer. The signals from the input layer propagate to the units in the processing layer and each unit produces an output. The outputs of these units are propagated to units in subsequent layers. This process continues until the signals reach the output layer where the actual response of the network to the input vector is obtained. During the forward pass the weights of the network are fixed. During the backward pass (see dashed arrows in Figure 4.3), on the other hand, the weights are all adjusted in accordance with an error signal that is propagated backward through the network against the initial direction.

As mentioned above, this network architecture still bears the risk of being stuck in local minima on the error hypersurface. To reduce this risk, conjugate gradient descent was used in this study.

This is an improved version of standard backpropagation with accelerated convergence. A detailed description of this technique can be found in Section 3 (Steiner et al., 2005a).

A second uncertainty in the BPN simulation is related to the fact that the identified minimum is dependent on the starting point on the error hypersurface. To reduce this kind of uncertainty, the BPN was performed 30 times, each time only varying the starting point on the error hypersurface. Finally, the average of the 30 model results has been analyzed.

Sensitivity analysis using neural networks is based on the measurements of the effect that is observed in the output layer due to changes in the input data. A common way to perform this analysis consists of comparing the error made by the network from the original patterns with the error made when restricting the input of interest to the average value. Thus, the greater the increase in the error function upon restricting the input, the greater the importance of this input in the output (e.g. Wang et al., 2000). In this study we kept one seasonal temperature or precipitation input constant while the other inputs were allowed to fluctuate. The observed error of glacier response gave us indications of its sensitivity to the input that was constant.

## 4.3 Results

### 4.3.1 Modelling the response of the Lower Grindelwald Glacier to climate change

A disadvantage of the Lower Grindelwald Glacier is the absence of long-term mass-balance data. Furthermore, most instrumental data series for temperature and precipitation from nearby locations just cover the 20th century. Therefore, we must rely upon indirect evidence to provide information about climate and glacier variability over the past centuries. Due to the extraordinary low position of the terminus and its easy access the Lower Grindelwald Glacier is the best-documented glacier in the Swiss Alps (Holzhauser and Zumbühl, 1996). Zumbühl (1980), Zumbühl et al. (1983), Holzhauser and Zumbühl (1999, 2003) used historic pictures (drawings, paintings, prints, photographs) to derive a detailed length variation curve of Lower Grindelwald Glacier back to 1535 (Figure 4.4).

As independent input data of the NN, precipitation data of Pauling et al. (2005) and temperature data of Luterbacher et al. (2004) at the grid point 8.25°E/46.75°N (nearest gridpoint to the Lower Grindelwald Glacier) have been used. The above mentioned glacier length fluctuations of the Lower Grindelwald Glacier (Zumbühl, 1980; Zumbühl et al., 1983; Holzhauser and Zumbühl, 2003) served as output dataset of the model.

Before feeding the NN, the data are standardized to the 1535–1983 mean and standard deviation (z-transformation) so that the data are in comparable units (for robust NN performance). The data are then filtered with a 20-year low-pass filter. After fitting the BPN with the conjugate gradient descent method, the full model was used to reconstruct a proxy of annual length change of the Lower Grindelwald Glacier from the two regional climate scenarios when no output data were available. In a final step, the data were rescaled by the inverse z-transformation and averaged. Confidence intervals are calculated from Root Mean Square (RMS) errors of the predictions.

Figure 4.5 shows the response of the Lower Grindelwald Glacier to the two regional climate scenarios used in this study (Table 4.2). In both projections the small advance of the glacier in the 1980s is correctly simulated.

Figure 4.5a (scenario 1; see Table 4.2) shows a continuous retreat of the glacier until the year 2025 of about  $-600 \pm 200$  meters (95% confidence interval). From 2025 onwards the model indicates

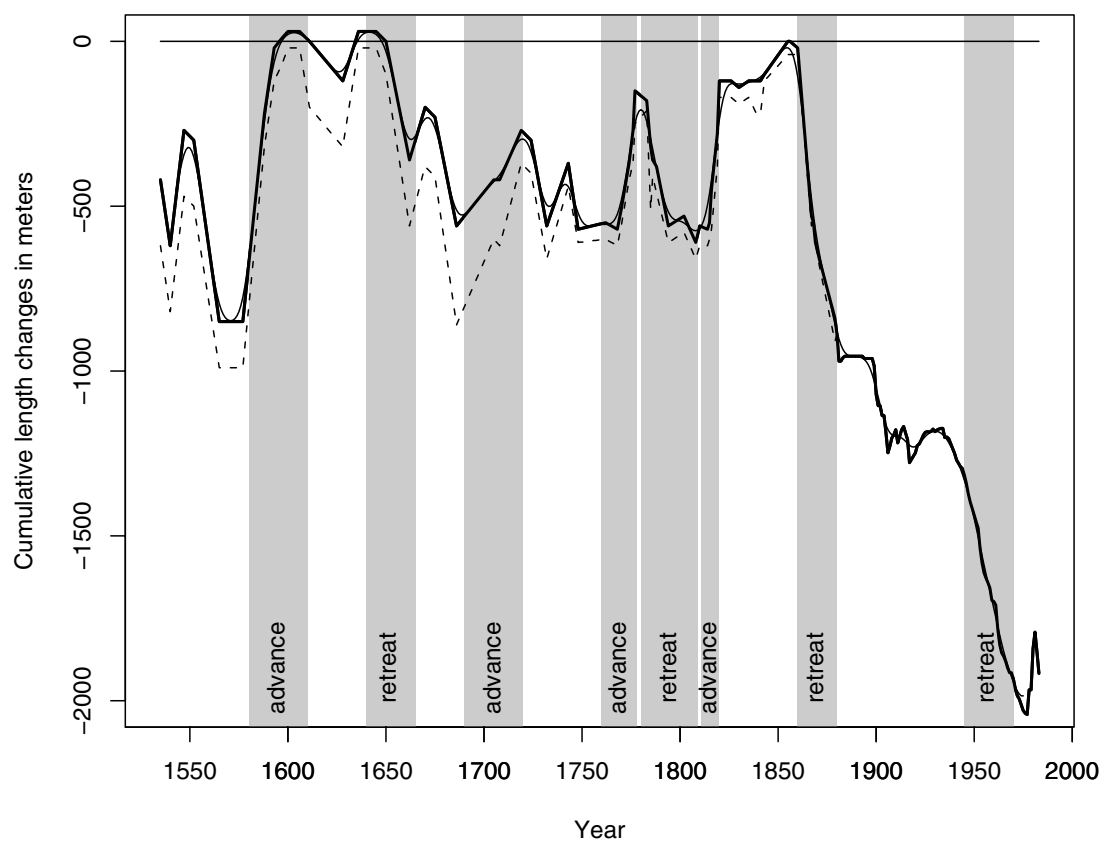


**Figure 4.4:** Cumulative length variations of the Lower Grindelwald Glacier from 1535 to 1983, relative to 1855/56 (= 0). As a consequence of uncertainties in determining an exact front position from documentary data (drawings, paintings), a spread of possible front positions is given.

Maximal extensions of the Lower Grindelwald Glacier are represented by a thick line, maximal extensions (smoothed with a 20-year low-pass filter) by a solid line, and minimal extensions by a dashed line (e.g. Zumbühl, 1980; Zumbühl et al., 1983). Also shown are the advance/retreat periods (grey shaded bands) that are analyzed in Section 4.3.2.

a glacier advance of about  $+400 \pm 400$  meters (95% confidence interval). This result is consistent with Oerlemans et al. (1998) who postulated significant growing for the Lower Grindelwald Glacier in the 21st century. Note that the projections in Oerlemans et al. (1998) have been made with the assumption that climate conditions will be constant and equal to the average climate conditions over the period 1961–1990.

Figure 4.5b (scenario 2; see Table 4.2) represents a possible projection of the glacier length due to anthropogenic forcings. After the minor advance in the 1980s the Lower Grindelwald Glacier shows a strong retreat of around  $-1400 \pm 300$  meters (95% confidence interval) until the 2050s.

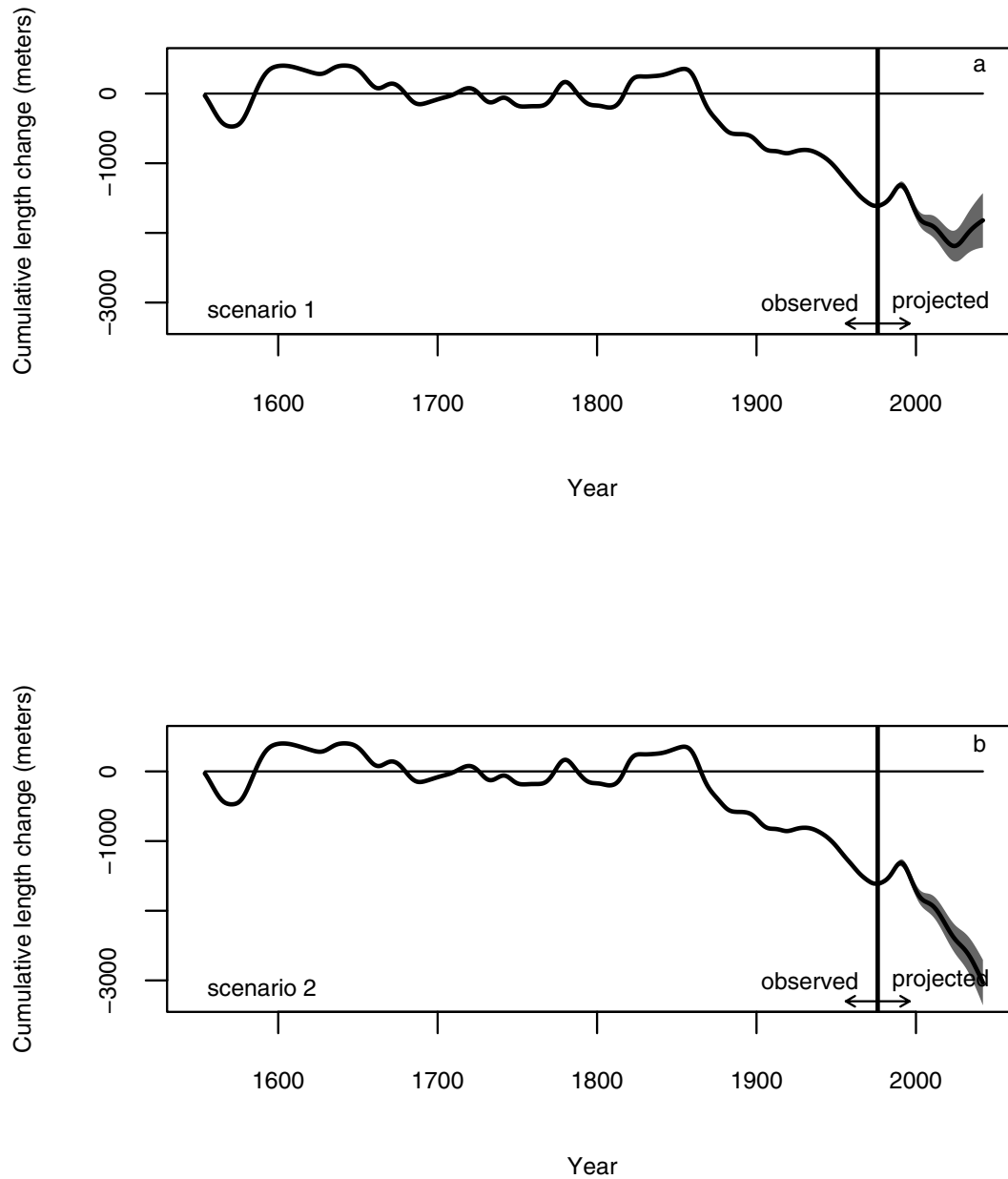


**Figure 4.5:** Filtered cumulative glacier length variations of the Lower Grindelwald Glacier for the 1550–2050 period. For the 1550–1975 period the thick line represents length fluctuations reconstructed from historical evidences, for the 1976–2050 period it is the average of the predictions derived from different initial starting points. Also shown is a 95 % error interval (grey shading) around the predictions of cumulative length variations. The NN was forced with two regional climate scenarios: (a) scenario 1 ("no change scenario"), (b) scenario 2 ("combined forcing scenario")



### 4.3.2 Precipitation and temperature significance for historic glacier variations – a comparison

Glacier mass balance and subsequent frontal response is influenced by climate, mainly temperature during the ablation season (summer) and precipitation during the accumulation season (winter). When calculating the mass-balance on present-day glaciers, the accumulation and ablation seasons are regarded to seven (October–April) and five (May–September) months, respectively. In an attempt to find consistency between glacier advances and both temperature and precipitation reconstructions we compared the Lower Grindelwald Glacier (Switzerland) with precipitation reconstructions by Pauling et al. (2005) and temperature reconstructions by Luterbacher et al. (2004). As mentioned above, historic length variation of this glacier belongs to the world's best-documented ones of its kind thanks to a unique wealth of historic picture sources (Zumbühl, 1980; Zumbühl et al., 1983; Oerlemans, 2005).

To investigate the relative importance of the influencing factors we performed a sensitivity analysis using neural networks based on winter (Prec\_DJF), spring (Prec\_MAM) and autumn precipitation (Prec\_SON) as well as spring (Temp\_MAM: Xoplaki et al., 2005), summer (Temp\_JJA) and autumn temperature (Temp\_SON: Xoplaki et al., 2005) as input variables of the Backpropagation Neural Network (BPN) (see Figures 4.6 and 4.7). An analysis of the Seasonal Sensitivity Characteristics (SSCs) of both the Lower Grindelwald Glacier and Nigardsbreen showed that summer (JJA) precipitation and winter (DJF) temperature do not lead to a strong response in mass balance and therefore glacier length reaction (Figure 4.12). So, these two time series are not used as input variables (Oerlemans and Reichert, 2000; Reichert et al., 2001; personal communication by Johannes Oerlemans, University of Utrecht, 10.8.2005).

Before feeding the BPN, the input data was standardized to their mean and standard deviation over the whole training/verification period 1535–1983 so that temperature and precipitation are comparable (for a robust NN performance). As explained before, each climate input has been stepwise shifted in time so that all lags between zero and 45 years have been used. This was done to account for the varying reaction time of the glacier. Note that Schmeits and Oerlemans (1997) calculated a response time of 34–45 years for the Lower Grindelwald Glacier. Reaction time of glaciers may vary due to different glacier states. For instance, longer periods of cool summers combined with high precipitation during the accumulation season are needed to trigger an advance following an extraordinary warm and dry period than following a period of average climate.

After training the BPN one input has been set to its mean and the rest of the inputs to their real values. The trained model has been fed with this new pattern. By comparing the network error of the original model with the error resulting from the new pattern, we can establish a relative importance of the changed input variable. This procedure is repeated for each input variable.

Figures 4.6 and 4.7 show boxplots describing the relative importance of the input data for four advance and four retreat periods of the Lower Grindelwald Glacier (Zumbühl, 1980; Zumbühl et al., 1983; Holzhauser and Zumbühl, 1999, 2003). Each boxplot is based on the average outputs of 30 model runs with different lags as input to reduce the effect of falling into local minima (Steiner et al., 2005a). This resulted in varying importance of the input variables. In Figures 4.6 and 4.7 this uncertainty is displayed by the boxplots. Please see also Figure 4.13 (precipitation) and Figure 4.14 (temperature) for the used model input time series. Furthermore, Table 4.3 shows the main climatic combinations that led to the glacier advances and retreats.

The 1590–1610 advance (Figure 4.6a) seems to be driven by low summer and low spring temperatures. Autumn precipitation plays a secondary role. It is surprising that the above-average winter precipitation before and during this advance period is not shown as significant. The 1690–1720

advance was likely triggered by low spring temperature and high spring precipitation (Figure 4.6b). High precipitation and low summer temperatures could have been the driving factors of the short, but well pronounced 1760–1780 glacier advance (Wanner et al., 2000). The 1810–1820 advance, which marks the beginning of the mid–19th century maximum glacier extent, was presumably driven by low summer temperatures and high autumn precipitation (Figure 4.6d). Note that in this case the variability of the relative importance is lower compared to the other advance periods. Furthermore, this advance shows specifically the expected pattern of an advancing Alpine glacier: Above normal (autumn) precipitation leads to a positive mass balance in the accumulation area, which is a prerequisite for later advances of the glacier snout. Low summer temperatures during the advance period hinder ablation making glacier advances possible.

It is not surprising that the four retreat periods were mainly driven by high temperatures (Figures 4.7a–4.7d). The 1640–1665 retreat seems to be triggered by high summer temperatures and low spring and autumn precipitation (Figure 4.7a). A typical pattern of retreating glaciers can be seen in the 1780–1810 period (Figure 4.7b): High overall temperatures and low winter precipitation enhance ablation while accumulation during winter season is reduced. High spring temperatures and decreasing autumn precipitation could have been the cause for the 1860–1880 retreat (Figure 4.7c). Finally, the 1945–1970 retreat could have been driven by high spring and autumn temperature and low autumn precipitation (Figure 4.7d). It has to be noted that in this case the variability of the relative importance is higher compared to the other retreat periods.

We performed the same sensitivity study for glacier Nigardsbreen, western Norway (61.7°N/7.1°E). From that area both, temperature (Luterbacher et al., 2004) and precipitation reconstructions (Pauling et al., 2005) are available. Please see Figure 4.15 (precipitation) and Figure 4.16 (temperature) for the used model input time series. However, reconstructive skill of spring precipitation in the Nigardsbreen region is below zero. Hence, we used spring precipitation data from a region in northern Sweden (17–20°E/63–65°N) where reconstructive skill is above zero. All the other time series are taken from the area of Nigardsbreen. The temporal evolution of the RE values is depicted in Figure 4.8. The RE values may change through time as during different periods different predictors are available. Interestingly, very high spring precipitation was reconstructed from 1700 to around 1740 (Figure 4.15b).

This period of extremely high spring precipitation coincides precisely with advances of Nigardsbreen; described by Nesje and Dahl (2003). They report advances of 2800 meters for the 1710–1735 period and another advance of 150 meters between 1735 and the historically documented "Little Ice Age" maximum in 1748 (Nesje and Dahl, 2003). Additionally, Nigardsbreen Glacier retreated only slightly until at least 1790 (Nesje and Dahl, 2003). Given a frontal lag time to net mass-balance perturbations of 20 years (Nesje and Dahl, 2003) this matches rather well our high spring precipitation amounts between 1700 and 1740. Additionally, summer temperature proved to be lower than normal during this period, which may also have promoted glacier advances. A problem may arise from the different locations of Nigardsbreen and the reconstructed spring precipitation time series. However, the correlation between spring precipitation in N–Sweden (average of the area 17–20°E/63–65°N) and W–Norway (5–7°E/60–62°N; location of Nigardsbreen Glacier) is highly significant during the 20th century ( $p$ -value = 0.00013) which suggests that spatial extrapolation over these areas is allowable.

Winter precipitation reconstructions are also rather reliable for the Nigardsbreen region (Figure 4.8). Thus, besides the temperature reconstructions from Luterbacher et al. (2004) we also used the winter precipitation series as input data of the NNM. Summer and autumn precipitation could not be used since they do generally not provide sufficient reconstruction skill (Figure 4.8).

In an analogous procedure as described above the relative importance of climate data have also

	period	climate variables
Advance	1590–1610	P_SON, T_MAM, <b>T_JJA</b>
Advance	1690–1720	P_MAM, <b>T_MAM</b>
Advance	1760–1780	P_DJF, <b>P_MAM</b> , P_SON, T_JJA
Advance	1810–1820	P_SON, <b>T_JJA</b>
Retreat	1640–1665	P_MAM, P_SON, <b>T_JJA</b>
Retreat	1780–1810	P_DJF, <b>T_MAM</b> , T_JJA, T_SON
Retreat	1860–1880	P_SON, <b>T_MAM</b>
Retreat	1945–1970	P_SON, <b>T_MAM</b> , T_SON

**Table 4.3:** Major advance and retreat periods of the Lower Grindelwald Glacier and the combinations of seasonal temperature and precipitation (forcings) which led to the described glacier variations (*bold: most important forcing data series*).

been evaluated for Nigardsbreen (Figure 4.9). The 1710–1748 advance (and the following large extent 1748–1790) seem to be forced by high spring and increasing winter precipitation, low summer and decreasing autumn temperatures (Figure 4.9a). Although we use only two precipitation input variables for sensitivity analysis we found a significant contribution to positive glacier length variations.

The 1945–1970 retreat is mainly driven by low spring precipitation and high autumn temperatures (Figure 4.9b).

## 4.4 Discussion

### 4.4.1 Simulation of future glacier length variations

The simulation of future glacier length variations of the Lower Grindelwald Glacier for scenario 1 and scenario 2 shows a retreating glacier at the beginning of the 21st century (Figure 4.5). For scenario 1 ("no change") the glacier retreat is weaker and is expected to end in 2025. Afterwards, a significant growing period can be seen. This advance could be explained by a memory effect of the glacier: During the 1970–2000 period winter, spring and autumn precipitation were above average so that mass accumulation could have been taken place. Furthermore, in the 2020s the glacier could reach a new equilibrium from which glacier advances are more likely.

As a result of climate scenario 2 ("combined forcing") the Lower Grindelwald Glacier shows a strong continuous retreat. By comparing this model output with climate scenarios in which only temperature or precipitation forcings are used, we can show that the Lower Grindelwald Glacier is mainly driven by temperature (not shown). High precipitation can weaken the retreat of the glacier, but the model outputs do not differ significantly from the outputs of scenario 1 or scenario 2.

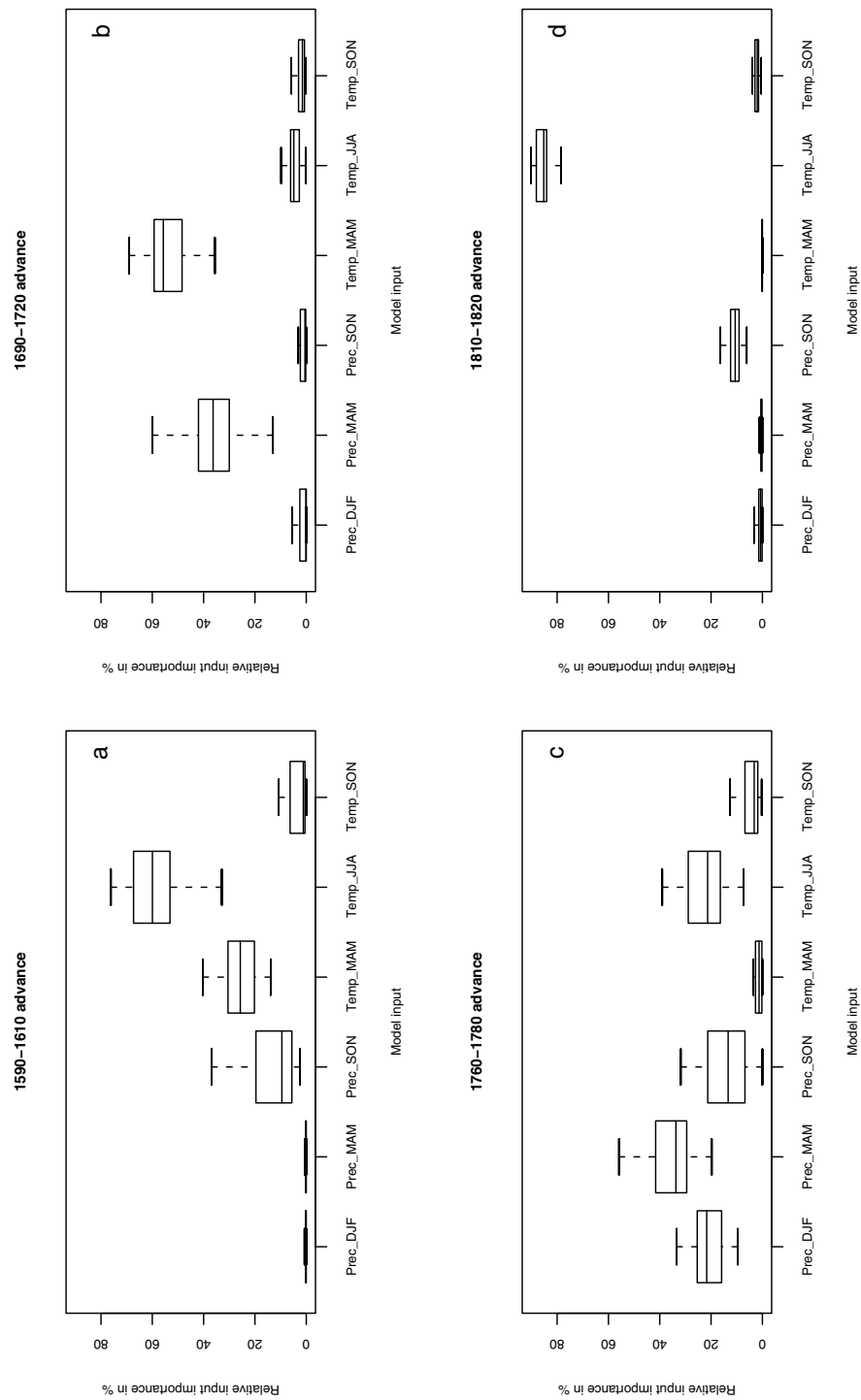


**Figure 4.6:** Relative importance of climate input variables to length fluctuations of the Lower Grindelwald Glacier (Switzerland) for four advance periods: (a) 1590–1610, (b) 1690–1720, (c) 1760–1780 and (d) 1810–1820. For each input variable the median, the first and third quartile (lower/upper hinge) and the 95% confidence interval for the median (lower/upper whisker) of the 30 model runs are given.

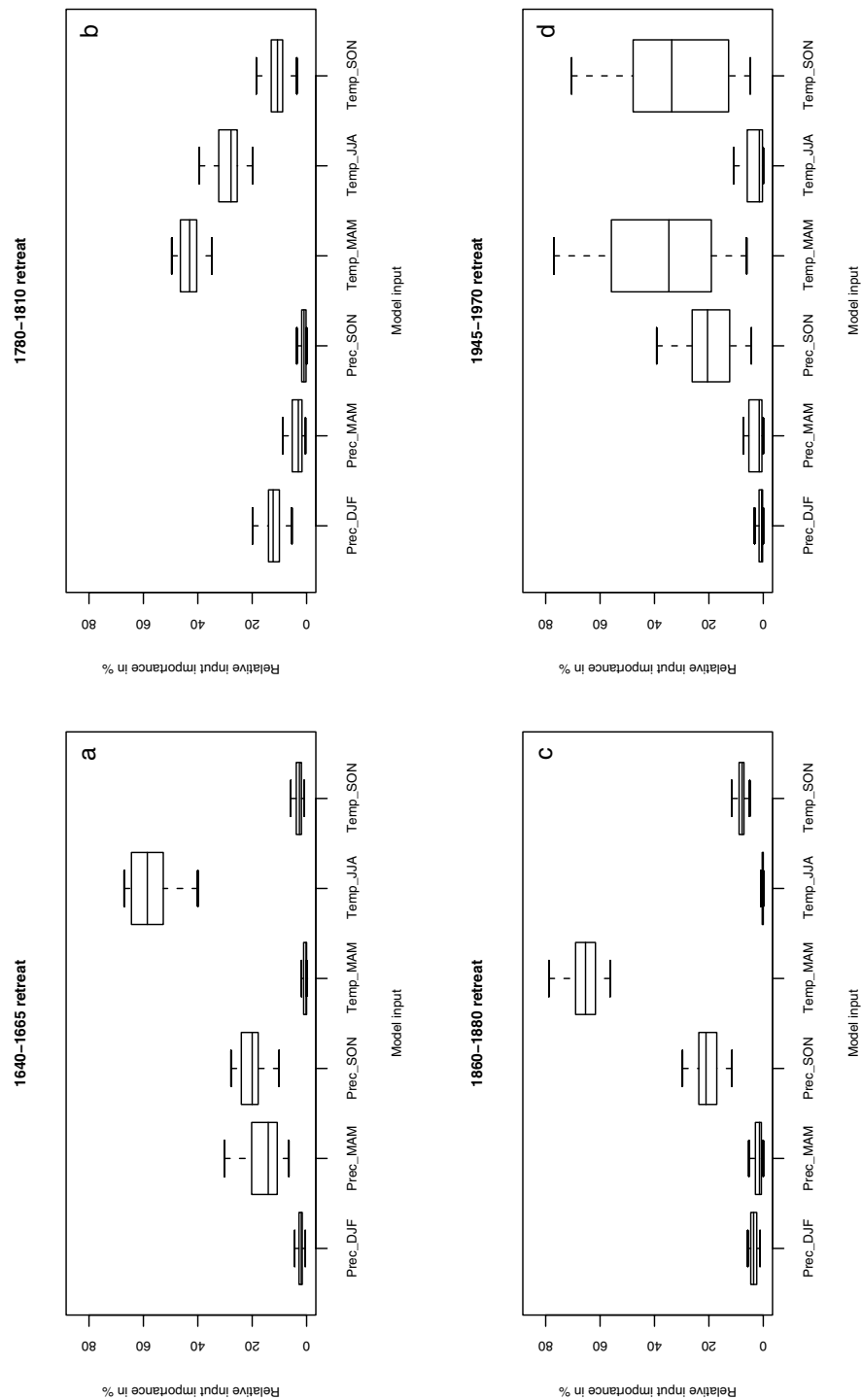


**Figure 4.7:** Relative importance of climate input variables to length fluctuations of the Lower Grindelwald Glacier (Switzerland) for four retreat periods: (a) 1640–1665, (b) 1780–1810, (c) 1860–1880 and (d) 1945–1970. For each input variable to the neural network the median, the first and third quartile (lower/upper hinge) and the 95% confidence interval for the median (lower/upper whisker) of the 30 model runs are given.

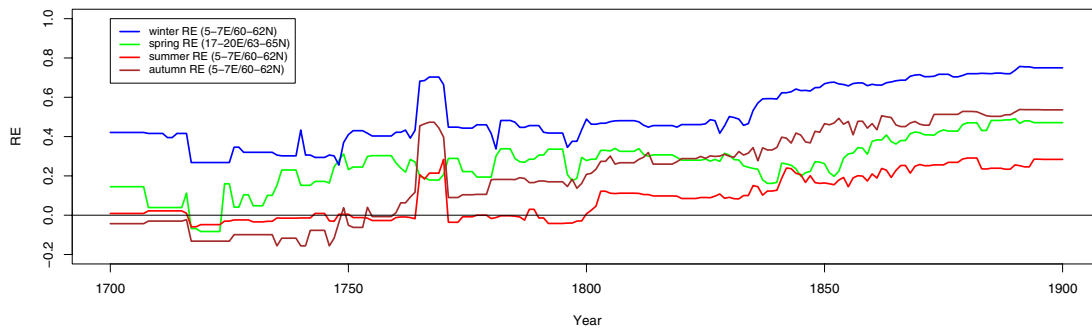


**Figure 4.8:** RE values of the precipitation time series over the Nigardsbreen region (winter, summer, autumn). The RE values of spring precipitation are the average over the region 18–20°E/63–65°N.

#### 4.4.2 Climate parameters and historic glacier variations

The relative importance of climate data to glacier advances shows changing patterns during the last 500 years, i.e. during the "Little Ice Age". There were periods with spring/summer temperatures being the main driving factors of glacier advances. Thus, low temperatures cause a low ablation rate in the spring/summer/autumn months. Nevertheless, in most cases high precipitation during the accumulation season contributes as well to positive mass balance and glacier advances. High winter precipitation rates together with average/low summer temperatures normally cause positive mass balance, a decisive prerequisite for glacier advances.

The clearest results are the sensitivity analyses of the 1810–1820 advance and the 1860–1880 retreat of the Lower Grindelwald Glacier (Figures 4.6d and 4.7c). During the 1810–1820 advance summer temperature seems to be the most important factor and autumn precipitation the second factor of importance. For the 1860–1880 retreat spring temperature and autumn precipitation show a significant influence. The other inputs proved to be negligible.

The 1590–1610 advance gives similar results though spring temperature becomes equally relevant. The importance of precipitation for the 1760–1780 advance is remarkable. The observed differences between the input importance for these two advance events can be attributed to different reasons. First, it is conceivable that different climate configurations may lead to positive mass balances and thus advances of the glacier. However, the uncertainties of the influences are considerable in many cases. This advance was quite short but well marked. One may argue that also glacier dynamics has played a role. Abundant meltwater in combination with high inclination of the lower parts of the glacier may accelerate glacier speed leading to advances that are not exclusively due to climatic conditions. In 1760 the Lower Grindelwald glacier ended above steep rocks (Zumbühl et al., 1983). The subsequent advance may have been amplified by this topographical feature. However, also other Alpine glaciers like the Rhône and the Rosenloui Glacier (Swiss Alps) advanced considerably during that period (Zumbühl and Holzhauser, 1988). Another reason may be the decreasing quality of the reconstructions further back in time (Luterbacher et al., 2004; Xoplaki et al., 2005; Pauling et al., 2005). However, during the late 18th century both temperature and precipitation have been skilfully reconstructed and the pattern of importance is similar in three of four advance periods (Figure 4.6). Hence, we argue that precipitation was the main reason for the 1760–1780 advance.

A striking feature is the importance of autumn precipitation, especially for the 1810–1820 advance. Precipitation in autumn may already fall as snow on large parts of the glacier which increases the

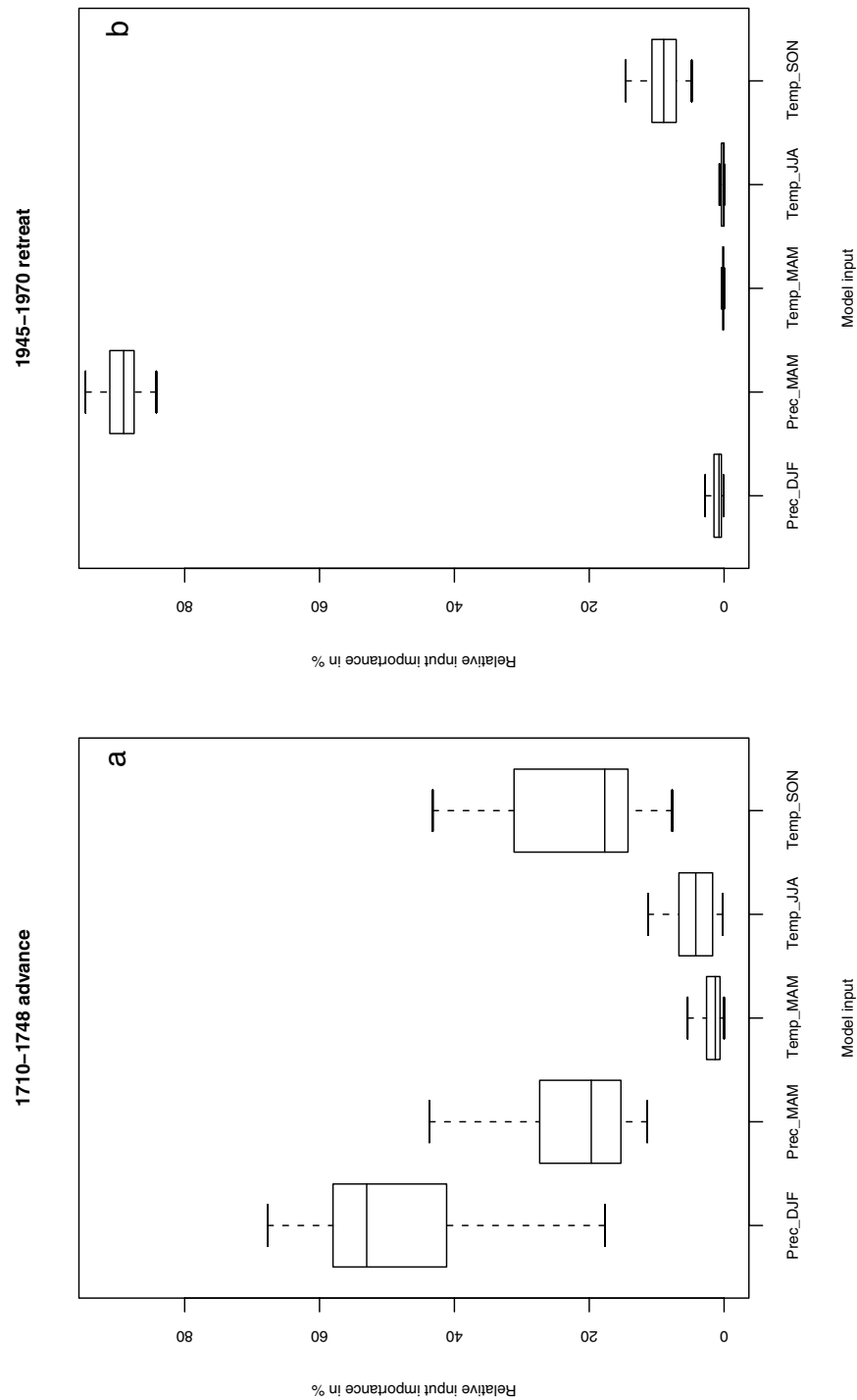


**Figure 4.9:** Relative importance of climate input variables to length fluctuations of the glacier Nigardsbreen for: (a) the advance period 1710–1748 and (b) the retreat period 1945–1970. For each input variable the median, the first and third quartile (lower/upper hinge) and the 95% confidence interval for the median (lower/upper whisker) of the 30 model runs are given.

albedo. This equals to a shortening of the ablation period that promotes positive mass balance.

The 1640–1665 retreat was triggered by decreasing spring and autumn precipitation and increasing summer temperature. This is a typical feature of a retreating glacier: High temperatures lead to strong ablation. Due to the low precipitation amounts insufficient mass accumulation takes place resulting in negative mass balance.

A similar pattern can be seen during the 1780–1810 and 1945–1970 retreat. High temperatures and in second order low precipitation have been producing negative mass balance and thus glacier retreat. It must be noted that the 1780–1810 retreat is situated within the last part of the Little Ice Age, a well-known glacier-friendly period. Vincent et al. (2005) studied the glacier variations at the end of the Little Ice Age (1760–1830) and argue that the advance of glaciers in the Alps during the mentioned period conflicts with the high summer temperature signal. Because Vincent et al. (2005) analyzed the 1760–1830 period as a whole, our results disagree with the previous statement. On the one hand, we found even a glacier retreat within this period (1780–1810), on the other hand summer temperature contributes significantly to this retreat.

Regarding the advance of Nigardsbreen, the most striking feature is the high importance of winter and spring precipitation relative to the other input factors used. Note that spring precipitation is high during the whole advance period whereas winter precipitation is slowly increasing during this period. It is well known that Scandinavian glaciers are sensitive to changes in winter precipitation (winter included the entire accumulation season October–April; Nesje et al., 2000; Nesje and Dahl, 2003), which is largely determined by the state of the North Atlantic Oscillation (NAO) but the importance of spring precipitation is still striking. Regarding the inferred low summer temperatures during that period, the real accumulation season may have been longer than at present. Thus, the accumulation during the entire spring period could have contributed to the observed glacier advance even though winter precipitation is not specifically high. However, the early 18th century is by far the wettest period in that region over the whole reconstruction period.

The 1945–1970 retreat of Nigardsbreen is mainly triggered by low spring precipitation. This time series shows a very similar run of the curve as the length variations of Nigardsbreen, with a lag of about 10 years. The high autumn temperatures imply an extended ablation period.

From a methodological point of view it can be argued that precipitation is possibly underestimated by the sensitivity analysis presented here. As the training data set includes only limited information on past climatic conditions (maximum time lag: 45 or 20 years), it can be supposed that the model does not take into account mass that accumulated more than 45 years/20 years before the beginning of an advance. On the other hand, the melting effect of high summer temperature is immediately visible.

The influence of precipitation on length variations of the Lower Grindelwald Glacier is smaller than in the case of Nigardsbreen. This can be due to the more southerly location of the Alps in the transition zone between maritime and continental regimes, which makes (summer) temperature the dominating factor, whereas Nigardsbreen is more sensitive to precipitation during the accumulation season. Please notice that surprisingly the SSCs of the Lower Grindelwald Glacier (Figure 4.12) and Nigardsbreen Glacier (Oerlemans and Reichert, 2000) are rather similar: Both glaciers show a low sensitivity in summer (JJA) precipitation and winter (DJF) temperature. Besides the expected high sensitivity in summer (JJA) temperature and winter (DJF) precipitation, a rather high sensitivity in "spring" (AM) temperature (Lower Grindelwald Glacier), resp. "autumn" (SO) temperature (Nigardsbreen Glacier) can be seen. However, these results have shown that also high precipitation is needed before the advances to ensure positive mass balance in the accumulation region of the glacier. This precipitation can fall during different seasons. It could be shown that also autumn (from September onwards) may well contribute to glacier advances.



## 4.5 Conclusions and Outlook

Using spatially and temporally highly resolved temperature and precipitation reconstructions we could simulate future glacier length variations of the Lower Grindelwald Glacier, Switzerland, forced by two different climate scenarios. Scenario 1 ("no change scenario") shows a retreat of the glacier until the year 2025 with a little advance from 2025 onwards. Scenario 2 ("combined forcing scenario") shows a strong retreat of the glacier until the 2050s. It must be assumed that scenario 2 likely lies ahead of us (climate change).

It has also been demonstrated that the relative importance of seasonal variations of temperature and precipitation has been variable in historic times and that various combinations of temperature/precipitation characteristics can lead to advances/retreats of a glacier in historic times. In particular, precipitation plays an important role in the behavior of the Nigardsbreen Glacier in western Norway. The Lower Grindelwald Glacier proved to be less sensitive to precipitation and more sensitive to temperature than Nigardsbreen Glacier.

This analysis has been done using NN approaches. The results show that NNs are useful tools for analyzing climate–glacier connections and simulating glacier variations in a nonlinear way. Because the limitations and chances of these techniques are not fully explored, further investigations towards a "neuro–glaciology" should be done, including different glaciers in different climate regions.

## Acknowledgments

This study was supported by the Swiss National Science Foundation (SNSF) through its National Center of Competence in Research on Climate (NCCR Climate), project PALVAREX.

This work is also part of the EU–Project SOAP (Simulations, Observations and Palaeoclimate Data: Climate Variability over the last 500 Years), the Swiss contribution being funded by the Staatssekretariat für Bildung und Forschung (SBF), under contract 01.0560.

The authors also wish to thank the following institutions for access to their data: The Swiss National Weather Service (MeteoSwiss), Zürich; the Norwegian Meteorological Institute (met.no), Oslo; the Climatic Research Unit (CRU), Norwich, and the Tyndall Centre for Climate Change Research, Norwich, UK.

Thanks also go to Johannes Oerlemans, Utrecht University, The Netherlands, for the calculation of the Seasonal Sensitivity Characteristic (SSC) of the Lower Grindelwald Glacier.

## Bibliography

- Chevallier, F., J.-J. Morcrette, F. Chéruy, and N. A. Scott (2000). Use of a neural–network–based long–wave radiative–transfer scheme in the ECMWF atmospheric model. *Quarterly Journal of Royal Meteorological Society* 126(563), 761–776.
- Frei, C. (2004). *Die Klimazukunft der Schweiz – Eine probabilistische Projektion (Working paper for the OcCC project "Switzerland in 2050")*. Organe consultatif sur les changements climatiques (OcCC), Bern.
- Haeberli, W. and M. Hoelzle (1995). Application of inventory data for estimating characteristics of and regional climatic–change effects on mountain glaciers: a pilot study with the European Alps. *Annals of Glaciology* 21, 206–212.

- Hoelzle, M., W. Haeberli, M. Dischl, and W. Peschke (2003). Secular glacier mass balances derived from cumulative glacier length changes. *Global and Planetary Change* 36(4), 295–306, doi:10.1016/S0921–8181(02)00223–0.
- Holzhauser, H. and H. J. Zumbühl (1996). To the history of the Lower Grindelwald Glacier during the last 2800 years – palaeosols, fossil wood and historical pictorial records – new results. *Zeitschrift für Geomorphologie, Neue Folge, Supplementband 104*, 95–127.
- Holzhauser, H. and H. J. Zumbühl (1999). Glacier Fluctuations in the Western Swiss and French Alps in the 16th Century. *Climatic Change* 43(1), 223–237, doi:10.1023/A:1005546300948.
- Holzhauser, H. and H. J. Zumbühl (2003). Nacheiszeitliche Gletscherschwankungen. In R. Weingartner and M. Spreafico (Eds.), *Hydrologischer Atlas der Schweiz*, Bundesamt für Landestopografie, Bern–Wabern, Tafel 3.8.
- Houghton, J. T., Y. Ding, D. J. Griggs, M. Noguer, P. J. van der Linden, X. Dai, K. Maskell, and C. A. Johnson (2001). *Climate Change 2001: The Scientific Basis*. Cambridge University Press, Cambridge, UK, and New York, NY, USA.
- Hsieh, W. W. (2004). Nonlinear multivariate and time series analysis by neural network methods. *Reviews of Geophysics* 42(1), RG1003, doi:10.1029/2002RG000112.
- Hsieh, W. W. and B. Tang (1998). Applying Neural Network Models to Prediction and Data Analysis in Meteorology and Oceanography. *Bulletin of the American Meteorological Society* 79(9), 1855–1870, doi:10.1175/1520–0477(1998)079<1855:ANNMTP>2.0.CO;2.
- Imhof, M. (1998). Rock glaciers, Bernese Alps, western Switzerland. In *International Permafrost Association, Data and Information Working Group*, National Snow and Ice Data Center (NSIDC)/World Data Center for Glaciology, University of Colorado, Boulder, CO, CD-ROM.
- Kirchhofer, W. and B. Sevruc (1992). Mittlere jährliche korrigierte Niederschlagshöhen 1951–1980. In R. Weingartner and M. Spreafico (Eds.), *Hydrologischer Atlas der Schweiz*, Bundesamt für Landestopografie, Bern–Wabern, Tafel 2.2.
- Klok, E. J. and J. Oerlemans (2004). Modelled climate sensitivity of the mass balance of Morteratschgletscher and its dependence on albedo parametrization. *International Journal of Climatology* 24(2), 231–245, doi:10.1002/joc.994.
- Knutti, R., T. F. Stocker, F. Joos, and R. Plattner (2002). Constraints on radiative forcing and future climate change from observations and climate model ensembles. *Nature* 416(6882), 719–723, doi:10.1038/416719a.
- Luterbacher, J., D. Dietrich, E. Xoplaki, M. Grosjean, and H. Wanner (2004). European Seasonal and Annual Temperature Variability, Trends, and Extremes Since 1500. *Science* 303(5663), 1499–1503, doi:10.1126/science.1093877.
- McCarthy, J., O. F. Canziani, N. A. Leary, D. J. Dokken, and K. S. White (2001). *Climate Change 2001: Impacts, Adaptation & Vulnerability*. Cambridge University Press, Cambridge, UK, and New York, NY, USA.
- Metropolis, N., A. W. Rosenbluth, M. N. Rosenbluth, A. H. Teller, and E. Teller (1953). Equations of State Calculations by Fast Computing Machines. *Journal of Chemical Physics* 21(6), 1087–1092.
- Michaelson, J. (1987). Cross-Validation in Statistical Climate Forecast Models. *Journal of Applied Meteorology* 26(11), 1589–1600, doi:10.1175/1520–0450(1987)026<1589:CVISCF>2.0.CO;2.

- Mitchell, T. D. and P. D. Jones (2005). An improved method of constructing a database of monthly climate observations and associated high-resolution grids. *International Journal of Climatology* 25(6), 693–712, doi:10.1002/joc.1181.
- Nesje, A. and S. O. Dahl (2003). The 'Little Ice Age' – only temperature? *The Holocene* 13(1), 139–145, doi:10.1191/0959683603hl603fa.
- Nesje, A., Ø. Lie, and S. O. Dahl (2000). Is the North Atlantic Oscillation reflected in Scandinavian glacier mass balance records? *Journal of Quaternary Science* 15(6), 587–601, doi:10.1002/1099-1417(200009)15:6<587::AID-JQS533>3.0.CO;2-2.
- New, M. E., M. Hulme, and P. D. Jones (2000). Representing Twentieth-Century Space-Time Climate Variability. Part II: Development of 1901–1996 Monthly Grids of Terrestrial Surface Climate. *Journal of Climate* 13(13), 2217–2238, doi:10.1175/1520-0442(2000)013<2217:RTCSTC>2.0.CO;2.
- Oerlemans, J. (2001). *Glaciers and Climate Change*. A. A. Balkema Publishers, Rotterdam, The Netherlands.
- Oerlemans, J. (2005). Extracting a Climate Signal from 169 Glacier Records. *Science* 308(5722), 675–677, doi:10.1126/science.1107046.
- Oerlemans, J., B. Anderson, A. Hubbard, P. Huybrechts, T. Johannesson, W. H. Knap, M. Schmeits, A. P. Stroeven, R. S. W. van de Wal, J. Wallinga, and Z. Zuo (1998). Modelling the response of glaciers to climate warming. *Climate Dynamics* 14(4), 267–274, doi:10.1007/s003820050222.
- Oerlemans, J. and B. K. Reichert (2000). Relating glacier mass balance to meteorological data by using a seasonal sensitivity characteristic. *Journal of Glaciology* 46(152), 1–6.
- Østrem, G., K. Dale Servig, and K. Tandberg (1988). *Atlas of glaciers in South Norway*. Norges vassdrags- og energiverk, vassdragsdirektoratet, Meddelelse No. 61 fra Hydrologisk avdeling.
- Østrem, G., O. Liestøl, and B. Wold (1977). Glaciological investigations at Nigardsbreen, Norway. *Norsk Geografisk Tidsskrift* 30, 187–209.
- Paul, F., A. Kääb, M. Maisch, T. Kellenberger, and W. Haeberli (2004). Rapid disintegration of Alpine glaciers observed with satellite data. *Geophysical Research Letters* 31(21), L21402, doi:10.1029/2004GL020816.
- Pauling, A., J. Luterbacher, C. Casty, and H. Wanner (2005). 500 years of gridded high-resolution precipitation reconstructions over Europe and the connection to large-scale circulation. *Climate Dynamics*, revised.
- Reichert, B. K., L. Bengtsson, and J. Oerlemans (2001). Midlatitude Forcing Mechanisms for Glacier Mass Balance Investigated Using General Circulation Models. *Journal of Climate* 14(17), 3767–3784, doi:10.1175/1520-0442(2001)014<3767:MFMFGM>2.0.CO;2.
- Rumelhart, D. E., G. E. Hinton, and R. J. Williams (1986). Learning Internal Representations by Error Propagation. In D. E. Rumelhart and J. L. McClelland (Eds.), *Parallel Distributed Processing: Explorations in the Microstructure of Cognition*, MIT Press, Cambridge, MA, 318–362.
- Schär, C., P. L. Vidale, D. Lüthi, C. Frei, C. Häberli, M. A. Liniger, and C. Appenzeller (2004). The role of increasing temperature variability in European summer heatwaves. *Nature* 427(6972), 332–336, doi:10.1038/nature02300.
- Schmeits, M. J. and J. Oerlemans (1997). Simulation of the historical variations in length of Unterer Grindelwaldgletscher, Switzerland. *Journal of Glaciology* 43(143), 152–164.

- Steiner, D., A. Walter, and H. J. Zumbühl (2005a). The application of a Nonlinear Backpropagation Neural Network to study the Mass Balance of the Great Aletsch Glacier. *Journal of Glaciology* 51(173), in press.
- Steiner, D., H. J. Zumbühl, and A. Bauder (2005b). Two Alpine glaciers over the last two centuries: a scientific view based on pictorial sources. In B. Orlove, E. Wiegandt, and B. Luckman (Eds.), *The Darkening Peaks: Glacial Retreat in Scientific and Social Context*, University of California Press, Berkeley, CA, USA, revised.
- Stone, M. (1974). Cross-validation choice and the assessment of statistical predictions. *Journal of the Royal Statistical Society B36*(1), 111–147.
- Stott, P. A., D. A. Stone, and M. R. Allen (2004). Human contribution to the European heatwave of 2003. *Nature* 432(7017), 610–614, doi:10.1038/nature03089.
- Vincent, C., E. Le Meur, D. Six, and M. Funk (2005). Solving the paradox of the end of the Little Ice Age in the Alps. *Geophysical Research Letters* 32(9), L09706, doi:10.1029/2005GL022552.
- Walter, A. and C.-D. Schönwiese (2002). Attribution and detection of anthropogenic climate change using a backpropagation neural network. *Meteorologische Zeitschrift* 11(5), 335–343, doi:10.1127/0941–2948/2002/0011–0335.
- Walter, A. and C.-D. Schönwiese (2003). Nonlinear statistical attribution and detection of anthropogenic climate change using simulated annealing algorithm. *Theoretical and Applied Climatology* 76(1–2), 1–12, doi:10.1007/s00704–003–0008–5.
- Wang, W., P. Jones, and D. Partridge (2000). Assessing the Impact of Input Features in a Feedforward Neural Network. *Neural Computing and Applications* 9(2), 101–112.
- Wanner, H., H. Holzhauser, C. Pfister, and H. J. Zumbühl (2000). Interannual to century scale climate variability in the European Alps. *Erdkunde* 54(1), 62–69.
- Wanner, H., R. Rickli, E. Salvisberg, C. Schmutz, and M. Schüepp (1997). Global Climate Change and Variability and its Influence on Alpine Climate – Concepts and Observations. *Theoretical and Applied Climatology* 58, 221–243.
- Wigley, T. M. L. and S. C. B. Raper (2001). Interpretation of High Projections for Global-Mean Warming. *Science* 293(5529), 451–454, doi:10.1126/science.1061604.
- Xoplaki, E., J. Luterbacher, H. Paeth, D. Dietrich, N. Steiner, M. Grosjean, and H. Wanner (2005). European spring and autumn temperature variability and change of extremes over the last half millennium. *Geophysical Research Letters* 32(15), L15713, doi:10.1029/2005GL023424.
- Yuval (2001). Enhancement and Error Estimation of Neural Network Prediction of Niño–3.4 SST anomalies. *Journal of Climate* 14(9), 2150–2163, doi:10.1175/1520–0442(2001)014<2150:EAEEON>2.0.CO;2.
- Zumbühl, H. J. (1980). *Die Schwankungen der Grindelwaldgletscher in den historischen Bild- und Schriftquellen des 12. bis 19. Jahrhunderts. Ein Beitrag zur Gletschergeschichte und Erforschung des Alpenraumes*. Denkschriften der Schweizerischen Naturforschenden Gesellschaft (SNG), Birkhäuser, Basel/Boston/Stuttgart, Band 92.
- Zumbühl, H. J. and H. Holzhauser (1988). Alpengletscher in der Kleinen Eiszeit. Sonderheft zum 125jährigen Jubiläum des SAC. *Die Alpen* 64(3), 129–322.

Zumbühl, H. J., B. Messerli, and C. Pfister (1983). *Die kleine Eiszeit: Gletschergeschichte im Spiegel der Kunst. Katalog zur Sonderausstellung des Schweizerischen Alpen Museums Bern und des Gletschergarten-Museums Luzern vom 09.06.–14.08.1983 (Luzern), 24.08.–16.10.1983 (Bern).*

## 4.6 Appendix 1



**Figure 4.10:** Nigardsbreen Glacier, western south Norway, with the terminal moraines for the 1750s, the 1850s and 1930s, respectively (see also Figure 4.2b). Photograph by Bjørn Wold, 1990.



**Figure 4.11:** (a) The Lower Grindelwald Glacier, Switzerland. Photograph by Martin Funk, 21.7.2004. (b) The snout of the Lower Grindelwald Glacier. Photograph by Andreas Bauder, 7.9.2005.

## 4.7 Appendix 2

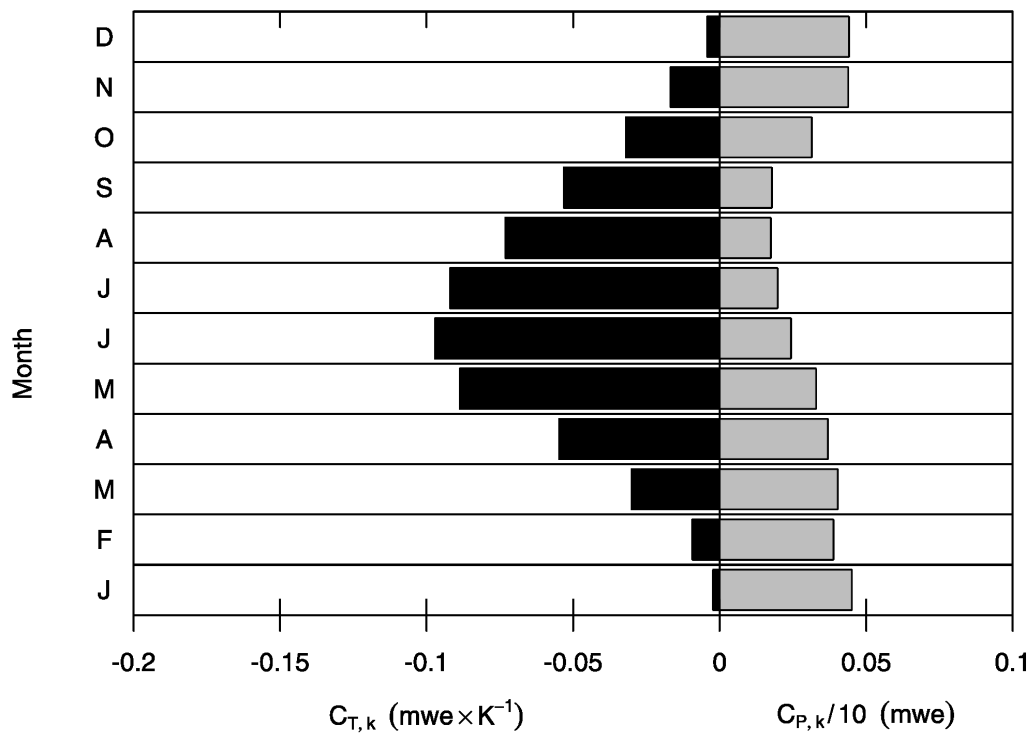


**Figure 4.12:** Seasonal Sensitivity Characteristic (SSC) for the Lower Grindelwald Glacier, Switzerland. The SSC represents the dependence of glacier mass balance on monthly anomalies in temperature (solid bars) and precipitation (shaded bars). The coefficients  $C_{T,k}$  and  $C_{P,k}$  have been determined by a one-dimensional energy-balance model and represent the 24 values of the SSC. They quantify the change in mass balance resulting from a change in monthly temperature and from a relative change in monthly precipitation. For the Lower Grindelwald Glacier, a  $1^{\circ}\text{C}$  increase in summer (JJA) would, for example, roughly have the same effect (0.1 mwe in mass balance) as a 20 % decrease of precipitation in winter (DJF). For a comparison, see the SSCs of Nigardsbreen (Norway) and Rhône Glacier (Switzerland) in Oerlemans and Reichert (2000) and Reichert et al. (2001).

## 4.8 Appendix 3

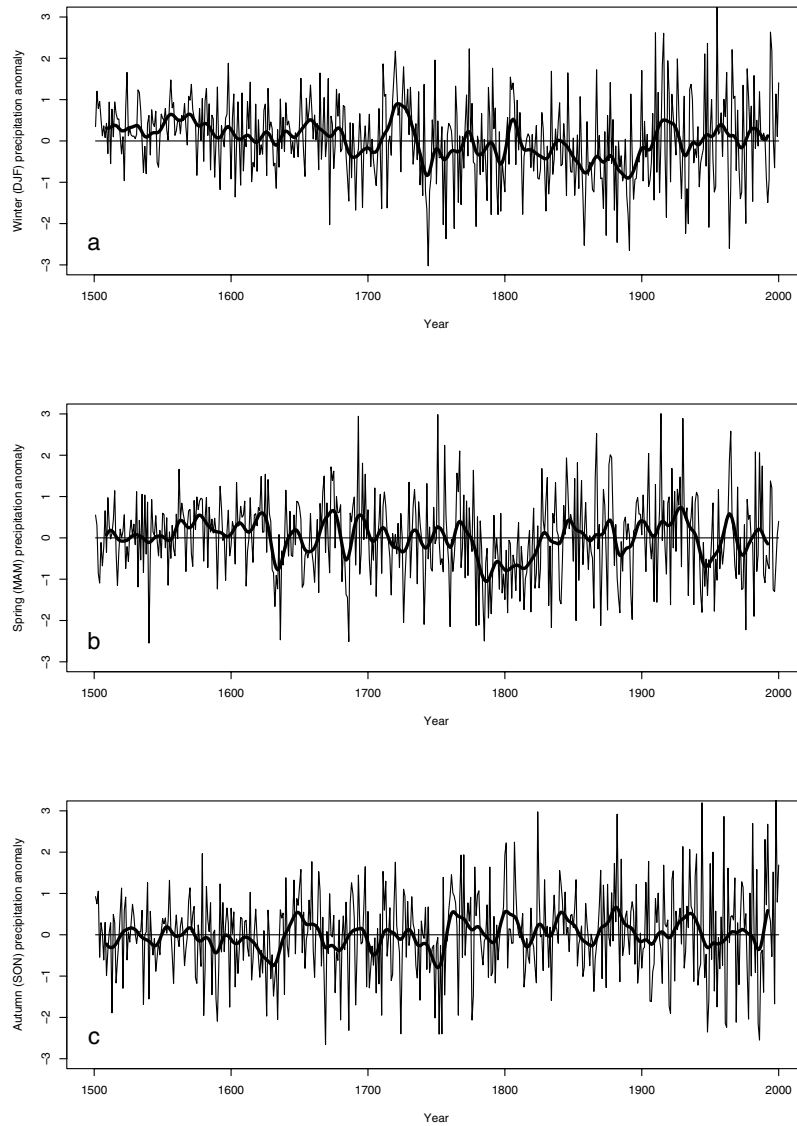


**Figure 4.13:** Precipitation anomalies for the 1500–2000 period (solid lines) at the grid point  $8.25^{\circ}E/46.75^{\circ}N$  (Lower Grindelwald Glacier; after Pauling et al., 2005): (a) Winter (DJF) precipitation anomaly, (b) Spring (MAM) precipitation anomaly, (c) Autumn (SON) precipitation anomaly. Also shown are the 20-year low-pass filtered time series of the precipitation model inputs (thick lines). The time series are z-standardized relative to the 1535–1983 mean and standard deviation.



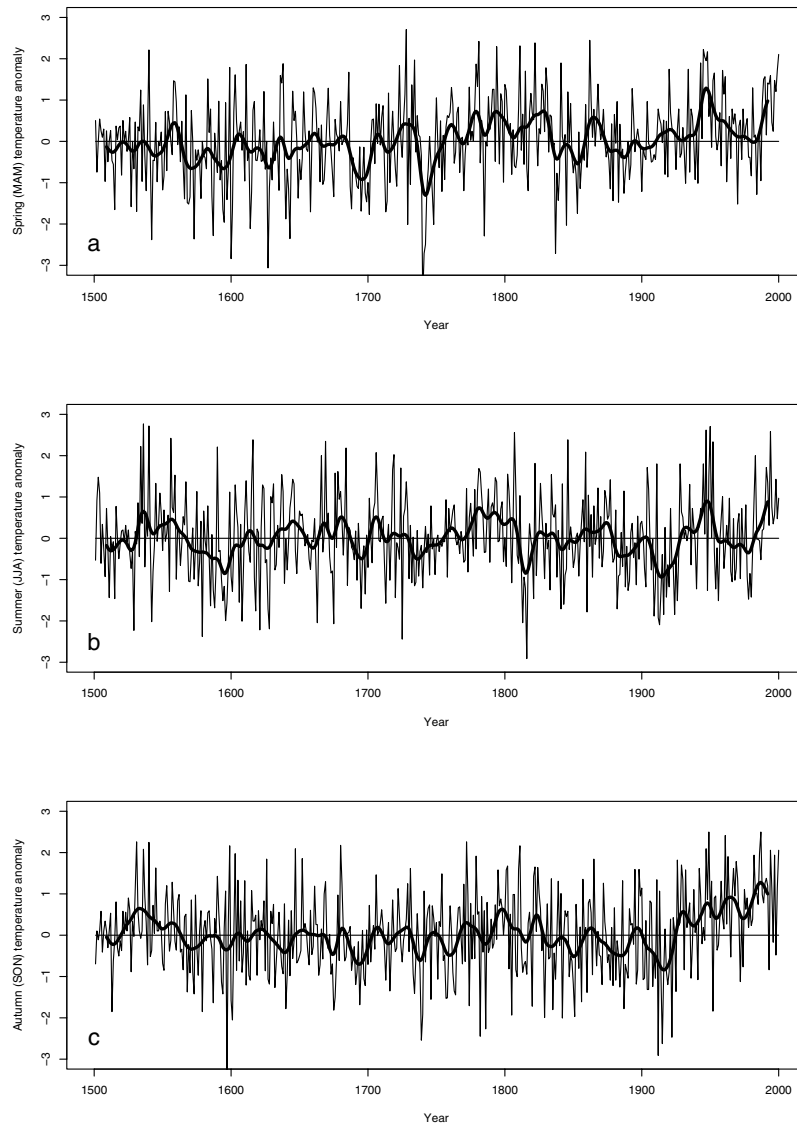


**Figure 4.14:** Temperature anomalies for the 1500–2000 period (solid lines) at the grid point  $8.25^{\circ}E/46.75^{\circ}N$  (Lower Grindelwald Glacier; after Luterbacher et al., 2004): (a) Spring (MAM) temperature anomaly, (b) Summer (JJA) temperature anomaly, (c) Autumn (SON) temperature anomaly. Also shown are the 20-year low-pass filtered time series of the temperature model inputs (thick lines). The time series are z-standardized relative to the 1535–1983 mean and standard deviation.

## 4.9 Appendix 4

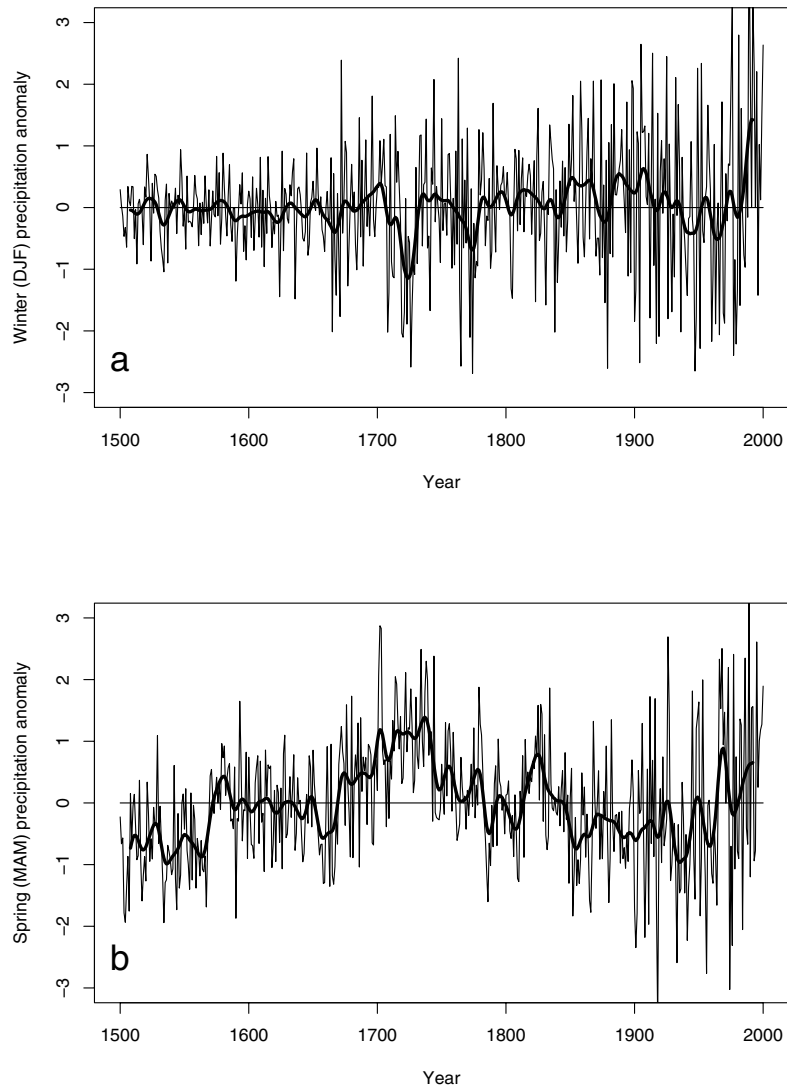


**Figure 4.15:** Precipitation anomalies for the 1500–2000 period (solid lines) over the Nigardsbreen region  $5\text{--}7^\circ\text{E}/60\text{--}62^\circ\text{N}$  (DJF) and a highly correlated region in northern Sweden  $17\text{--}20^\circ\text{E}/63\text{--}65^\circ\text{N}$  (MAM; after Pauling et al., 2005): (a) Winter (DJF) precipitation anomaly, (b) Spring (MAM) precipitation anomaly. Also shown are the 20-year low-pass filtered time series of the precipitation model inputs (thick lines). The time series are z-standardized relative to the 1535–1983 mean and standard deviation.

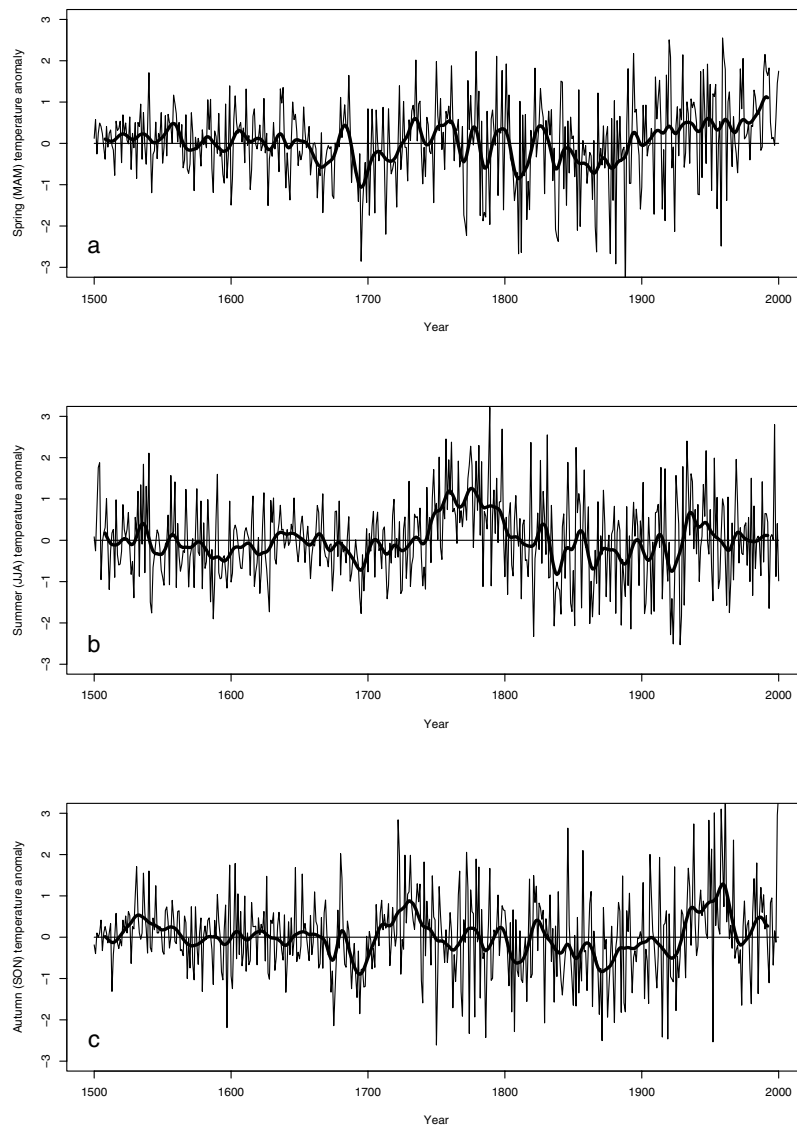


**Figure 4.16:** Temperature anomalies for the 1500–2000 period (solid lines) over the Nigardsbreen region 5–7°E/60–62°N (after Luterbacher et al., 2004): (a) Spring (MAM) temperature anomaly, (b) Summer (JJA) temperature anomaly, (c) Autumn (SON) temperature anomaly. Also shown are the 20-year low-pass filtered time series of the temperature model inputs (thick lines). The time series are z-standardized relative to the 1535–1983 mean and standard deviation.



## Chapter 5

# Concluding remarks

Due to the access to long and highest-quality records of glacier variations and to the highest density of proxy evidence worldwide, there is the unique chance to develop knowledge on past glacier and climate variability for the European Alps with an outstanding precision, currently not possible for any other region in the world.

Based on these data and new highly resolved temperature and precipitation reconstructions, this PhD thesis presents both, new results of glacier changes as well as new methods for studying the complex climate–glacier relationship.

Firstly, an exemplary study of the mid–19th century maximum extent of two Alpine glaciers is presented. A change in glacier representation techniques only within 15 years can be studied against the background of the beginning of experimental glaciology. Moreover, the dramatic retreat of the selected glaciers since the mid–19th century is quantified using different pictorial sources.

Secondly, nonlinear Neural Network Models (NNMs) have been applied to reconstruct and simulate glacier variations (mass balance and length changes) in order to test its capabilities, advantages and limitations in glaciological contexts. Furthermore, with this approach, we are aiming to gain a better understanding the way glaciers react to different climate configurations.

### **Two Alpine glaciers over the last two centuries: a scientific view based on pictorial sources**

The mid–19th century equals not only the last maximum extent of a big number of glaciers worldwide, it is also the time when modern glaciology had been starting. Already in the first half of the 19th century, the Lower Aare Glacier, Switzerland, was object of scientific investigations. This pioneer work contributed substantially to our present understanding of glaciers. Still today, the Lower Aare Glacier is amongst the most comprehensively studied glaciers in the Swiss Alps.

The Lower Grindelwald Glacier, Switzerland, plays a similar important role in terms of scientific glacier research. Its record of length variations back to 1535 has been derived from a wealth of documentary evidence, as a consequence thereof it is one of the best–documented glaciers in the world.

We explored the contemporaneous occurrence in the mid–19th century of the "ice age hypothesis", the beginning of modern glaciology, the change in glacier representation techniques and the maximum extent of many Alpine glaciers.

Over a period of only 15 years, from the 1840s to the late 1850s, glacier drawings were complemented by topographic surveys and finally by scientific photographs. We show that the development of modern glaciology has been accelerated by the scientific debate on the "ice age theory". Furthermore, an increasing public interest in glaciers as well as first natural scientists investigating glacier phenomena motivated new glacier representations (e.g. topographic maps and photographs) by taking new available techniques into account.

Volume, area and length changes in both the Lower Aare and the Lower Grindelwald Glacier since the end of the "Little Ice Age" were determined by digital interpretation of the high-quality pictorial sources (e.g. topographic maps, original plane table sheets, aerial photographs). On the one hand, we show an accelerated and asymmetric retreat of the Lower Grindelwald Glacier in the period 1860/61–70. On the other hand, the well-known enormous retreat of the Lower Aare and Lower Grindelwald Glacier since their last maximum extent around the mid-19th century could be quantified as follows: Both glaciers show a similar average thickness change of  $-0.42$  meters per year (Lower Grindelwald Glacier) and  $-0.48$  meters per year (Lower Aare Glacier). Finally, an analysis of the spatial thickness changes of the Lower Grindelwald Glacier since the 1860s could possibly indicate an extraordinary dynamical behavior of the glacier.

## **The application of a nonlinear Backpropagation Neural Network to study the mass balance of Great Aletsch Glacier, Switzerland**

A Neural Network (NN) is an information processing paradigm which originates from biological nervous systems (e.g. brain). NNs provide a methodology for extracting patterns from noisy data. They have been applied to a wide variety of problems, also in meteorological and climatological contexts.

In this thesis a Neural Network Model (NNM) has been applied to a glacier for the first time. We used a hydrologically based long-term mass balance series of the Great Aletsch Glacier, Switzerland, as target series to the NNM. As forcing variables to the NNM, we applied monthly resolved instrumental series of temperature and precipitation (20th century), respectively seasonally resolved reconstructions of temperature and precipitation (1500–1999 period).

In general, the resulting reconstructed proxy of annual mass balance of the Great Aletsch Glacier going back to AD 1500, shows a reliable developing of glacier advance and retreat periods. It also confirms that the mass balance of the Great Aletsch Glacier is rather driven by summer (JJA) temperature than by winter (DJF) precipitation.

In the case of the climate–mass balance relation mentioned above, we show that NNMs are very powerful tools. As they capture nonlinear dependencies in data, we are able to study the climate–mass balance relationship in a more comprehensive way.

## **Sensitivity of European Glaciers to Precipitation and Temperature – Two case studies**

As a consequential follow-up of the previous study, we strongly advice to apply NNMs for studying glacier length variations of the Lower Grindelwald Glacier, Switzerland, and Nigardsbreen Glacier, Norway. Length variations are the most comprehensive data of glaciers. But in contrast to glacier

mass balance, fluctuations in glacier length are rather indirect, delayed, filtered and strongly enhanced responses to climate change.

From this perspective, a potential use of glacier length variations as target series to NNMs is more difficult. In two case studies we investigate potential capabilities of the suggested NNM which also incorporates the varying reaction times of the selected glaciers.

Firstly, for both the Lower Grindelwald and the Nigardsbreen Glacier, we demonstrate a sensitivity analysis based on NNs which analyses the relative importance of seasonal variations of temperature and precipitation to glacier advances and retreats. We show that different combinations of temperature and/or precipitation can lead to a certain glacier behavior.

Secondly, future glacier length variations of the Lower Grindelwald Glacier until the year 2050 are simulated by using two regional climate scenarios for the Swiss Alps.

Finally, it is to be noticed that serious glacier studies using NNMs are only reliable if both, high-quality glacier data as well as high-quality climate series are available. Probably better than elsewhere in the world, this is the case for the Swiss Alps. Nevertheless, to test the power and limitations of NNMs in the field of glaciology, further investigations towards a "neuro-glaciology" using other glaciers in different climate regions will have to be done.





# Acknowledgments

I would like to thank all the people, which made this PhD thesis possible. I do appreciate everyone who have helped me with advice, comments, critics, feedback and suggestions.

First of all, I would like to thankfully acknowledge PD Dr. Heinz J. Zumbühl, my doctoral advisor. He was the initiator of this "glacier project" and gave me the opportunity to write this dissertation. He was a great motivator, an inspiring and often challenging scientific partner. Thanks go also to Prof. Dr. Heinz Wanner. He always gave me fruitful ideas and impulses and the needed (financial) support on my work. Many thanks also to Dr. Jürg Luterbacher for contributions on various aspects of this thesis. Hereby, also the Swiss National Science Foundation (SNSF) through its National Center of Competence in Research on Climate (NCCR Climate; project PALVAREX) and Sebastiana S.A., Pully, are kindly acknowledged.

Big thanks go to Hermann Bösch, Laboratory of Hydraulics, Hydrology and Glaciology (VAW) of the Swiss Federal Institute of Technology, Zürich (ETHZ). He helped me in many photogrammetric problems. Dr. Andreas Bauder (VAW ETHZ) is addressed for fruitful discussions on glacier variability and for providing data on glacier variations. I thank Pierre Gerber and Martin Rickenbacher, Federal Office of Topography (swisstopo), Wabern–Bern. They assisted me with discussing and solving problems in historical cartography.

Thanks also to all members of the KLIMET research group at the Institute of Geography, University of Bern, for the enjoyable years that I have spent on the 5th floor. Isabella Geissbühler–Greco and Marlis Röthlisberger are acknowledged for their administrative work, Basilio Ferrante and Hubert Gerhardinger for the IT-support.

Furthermore, I thank all my co-authors and everybody that contributed to my work, especially Andreas Pauling (University of Bern, Switzerland), Dr. Andreas Walter (Deutscher Wetterdienst (DWD), Offenbach am Main, Germany) and Prof. Dr. Atle Nesje (Bjerknes Centre for Climate Research and University of Bergen, Norway).

Oliver Berger, Andreas Pauling, Dr. Theodore Wachs and Jean Charlton White are kindly acknowledged for English corrections of the manuscripts.

Last, but not least, I would like to dedicate this PhD thesis to my family, my wife Maria Steiner–Brütsch, my daughter Tabitha Maria and my son Raphael Mattia, for their love, patience and understanding. They allowed me to spend a lot of time on this thesis. Thank you very much.



# Curriculum Vitae

## Personal

Born 16 April 1973 in Sumiswald, Switzerland  
Son of Hans and Elisabeth Steiner-Bieri, one brother and four sisters  
married to Maria Steiner-Brütsch, two children

---

## Education

1980–1984 Primary School, Oeschenbach  
1984–1989 Secondary School, Kleindietwil  
1989–1994 Teacher's Training College, Langenthal  
30.06.1994 Degree as Primary School Teacher  
1994–1999 Student of Mathematics, Geography and Computer Science,  
University of Bern  
04.11.1999 Diploma in Mathematics, Diploma Thesis on  
"Maximale Unterverbände endlicher distributiver Verbände"  
1999–2000 Höheres Lehramt, University of Bern  
04.07.2000 Degree as Grammar School Teacher of Mathematics and Geography  
2002–2005 Doctoral Student, Institute of Geography, University of Bern

---

## Professional

### Experience

1994–1997 Teacher, Primary School, Schwanden near Sigriswil  
1997–1999 Research Assistant, Mathematical Institute, University of Bern  
1998 Teacher for Mathematics, Business School, Langenthal  
1999–2005 Teacher for Mathematics and Computer Science,  
Teacher's Training College and Gymnasium, Langenthal  
2005– Lecturer for Didactics of Mathematics,  
Pädagogische Hochschule, Zürich

---